The Earth Observer. November - December 2012. Volume 24, Issue 6.

the earth observer

Editor's Corner

Steve Platnick
EOS Senior Project Scientist

In a previous Editorial, we highlighted the tenth anniversary of the launch of Aqua and described a number of activities that took place at NASA's Goddard Space Flight Center (GSFC) on May 4 to commemorate the mission's decade in space[1]. On **page 4** of this issue we are pleased to feature an article written by **Claire Parkinson** [GSFC—*Aqua Project Scientist*] that elaborates on the science achievements of the first ten years of Aqua.

As Parkinson mentions in her article, there are now over 2000 published scientific papers using Aqua data. This is a tremendous testament to the value of the individual Aqua datasets as well as the synergy Aqua provides with other Afternoon constellation (A-Train) observations. Parkinson's article highlights the variety of Aqua data being used for science and practical applications. Further information can be found at *aqua.nasa.gov* and the many links provided therein. We look forward to continued success from the Aqua team and its user community.

Meanwhile, the Tropical Rainfall Measuring Mission (TRMM) celebrates its fifteenth anniversary on November 27. TRMM—a joint NASA–Japan Aerospace Exploration Agency (JAXA) mission—provides measurements of the tropical and subtropical regions (**Figure 1**). Its observations of precipitation, clouds, and water vapor have greatly increased our understanding of the water cycle and the movement of heat that powers tropical cyclones

[1] See the Editorial of the May–June 2012 issue of *The Earth Observer* [**Volume 24**, **Issue 3**, pp. 1-2].

continued on page 2

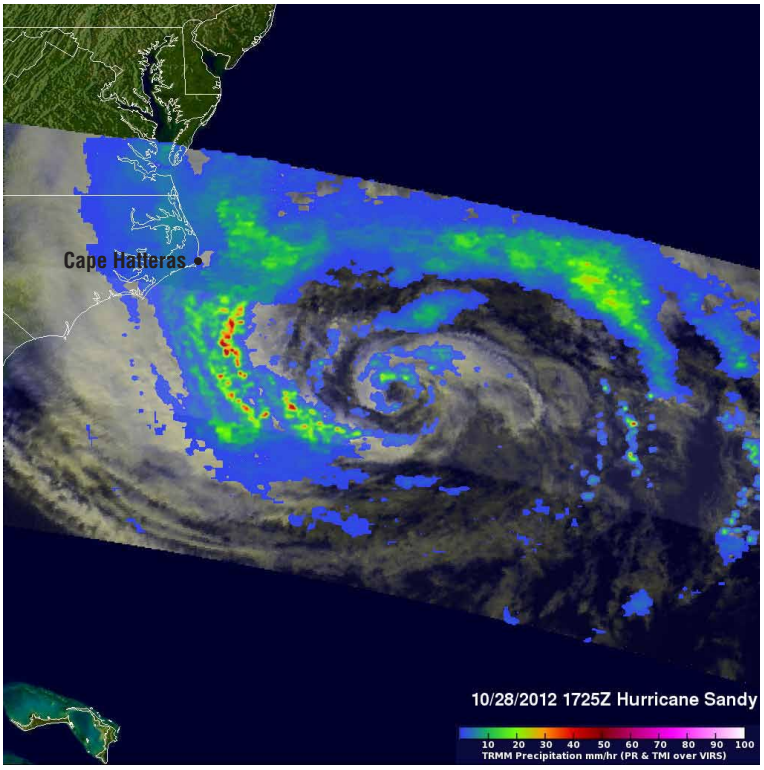

Figure 1. November 27 marked the 15th anniversary of the launch of the Tropical Rainfall Measuring Mission (TRMM). Positioned in low Earth orbit, TRMM has an ideal vantage point to observe precipitation, clouds, and water vapor over Earth's tropical and subtropical regions. The data returned from TRMM have helped to improve our knowledge of the water cycle and the movement of heat that powers tropical cyclones and hurricanes.

On October 28, at 1725 UTC (1:25 PM EDT) TRMM flew over Hurricane Sandy as she churned in the Atlantic. An analysis of rainfall from TRMM's Microwave Imager (TMI) and Precipitation Radar (PR) is shown here. The highest rainfall amounts are southeast of Cape Hatteras, NC. For high resolution image go to: *trmm.gsfc.nasa.gov/trmm_rain/Events/sandy_28_october_2012_1725_utc.jpg*. **Credit:** NASA

editor's corner

eos.nasa.gov

In This Issue

Reminder: To view newsletter images in color, visit: *eospso.gsfc.nasa.gov/eos_homepage/for_scientists/earth_observer.php*

and hurricanes. TRMM carries five instruments; among these five, the Precipitation Radar was the first spaceborne radar designed to show the three-dimensional structure of storms. Data from TRMM have also provided a new benchmark climatology of rainfall across the tropics; allowed a quantification of the diurnal cycle of rainfall and climatology of profiles of latent heating that, before TRMM, was impossible; and demonstrated impacts of humans on rainfall in terms of the effects of urban areas, deforestation, and aerosols (pollution, smoke); among many other achievements. Rainfall data from TRMM have also led to the development of better flood warning systems around the world.

TRMM has paved the way for collaboration among international satellite missions monitoring rainfall with microwave radiometers. Continuing and improving on TRMM's measurements, the upcoming Global Precipitation Measurement (GPM) mission is designed to incorporate data from nine partner satellites with radiometer and radar data from the GPM "Core Satellite" into a global precipitation dataset every three hours. GPM is the first mission designed to detect light rain and snow.

GPM Core is currently on track to launch on a Japanese H-IIA rocket from Tanegashima Space Center in Japan, February 2014. Last March, the GPM Microwave Imager (GMI) built by Ball Aerospace, and the Dual-frequency Precipitation Radar (DPR) built by JAXA, were delivered to GSFC. In May engineers integrated them onto the spacecraft bus, and last month, GPM had a successful comprehensive performance test in advance of its environmental testing program. As of this writing, the spacecraft is in *thermal vacuum*[2] testing.

While engineers work to complete testing of the GPM Core spacecraft and instruments, the science team continues to conduct field experiments to help further refine the planned algorithms. The most recent of these efforts was a six-week joint NASA–Environment Canada (EC) airborne validation campaign called the GPM Cold Season Precipitation Experiment (GCPEx) that took place between January 16 and February 29, 2012. The primary objectives of the campaign focused on conducting a complete study of snowfall physics (i.e., sampling from the ground through all levels of the atmosphere) using ground-based precipitation instruments, *in situ* aircraft observations, and high-altitude airborne instruments, which simulated the microwave measurements that DPR and GMI will obtain[3]. Most flights took place in and around the EC Centre for Atmospheric Research Experiments (CARE) near Egbert, Ontario, while a few of the flights extended as far as Lake Huron and Georgian Bay (to observe lake effect precipitation). Please see the article on **page 26** of this issue to learn more about the experiment.

NASA has selected the Tropospheric Emissions: Monitoring of Pollution (TEMPO) instrument from among 14 proposals submitted in response to its

[2] This simulates the environment that the spacecraft and instruments will encounter in orbit.
[3] As of November 2012, GPM At-Launch retrieval algorithms to convert GPM satellite instrument observations (radar, radiometer, and radar + radiometer) to uniform rain and snow estimates globally every three hours are being delivered to the Precipitation Processing System (PPS) for integration and testing within the data system environment.

Earth Venture Instrument (EVI-1) Announcement of Opportunity[4]. As the first EVI selection, the TEMPO instrument will be completed by 2017. Total investigation costs, which include algorithm development and data processing, have a cap of $90 million (excluding launch vehicle and platform integration). The instrument will share a ride on a commercial satellite to a geostationary orbit with a view of North America. TEMPO's ultraviolet and visible observations will determine concentrations of many key atmospheric pollutants. The advantage of a geostationary orbit is that it allows for observations that can track the temporal evolution of pollution as opposed to infrequent snaphots provided from *low-Earth orbit*. Other space agencies are planning similar observations over Europe and Asia after TEMPO is in orbit, allowing the opportunity to create a global constellation of geostationary air quality satellites. Congratulations to Principal Investigator **Kelly Chance** [Smithsonian Astrophysical Observatory in Cambridge, MA] and the entire TEMPO team, which includes partners at Ball Aerospace and Technologies Corporation, NASA's Langley Research Center (LaRC), GSFC, the U.S. Environmental Protection Agency, and several university and research institutions.

[4] The TEMPO instrument joins five sub-orbital *Venture* class missions [selected through EV-1 in 2010] and a complete satellite mission, the Cyclone Global Navigation Satellite System (CYGNSS), [selected through EV-2 in 2012]. Two more Venture calls are anticipated in 2013, with additional calls planned in the coming years. The EV missions are part of the Earth System Science Pathfinder program at LaRC (see *go.nasa.gov/MKvgJO*).

We would be remiss if we did not mention our concern for the millions of people impacted by *Superstorm Sandy*—particularly those who live in the areas hardest hit along the coasts of New Jersey and New York. NASA's Earth-observing satellite fleet, together with other U.S. and international satellites, are highly effective at tracking the progress of storms and other natural disasters (**Figure 2**). Satellite observations feed into model forecasts and help raise awareness of the impending danger far enough in advance to allow adequate time for preparations and evacuations that mitigate even worse consequences. The data collected during this superstorm will no doubt be analyzed for years to come.

On **page 18** of this issue, we present a visual chronology of how NASA's Earth-observing satellites observed the progress of Sandy from its inception in the Caribbean, to its final landfall along the U.S. East Coast, and beyond.

Once again, I find it difficult to believe that another year (and six issues of *The Earth Observer*) has seemed to pass by so quickly. Hopefully, this is merely an indication that we are busily engaged in interesting science, measurements, and education and outreach activities. On behalf of *The Earth Observer* staff, I wish everyone a productive and enjoyable year as we continue to seek a better understanding of our home planet. Best wishes to you and yours in 2013! ■

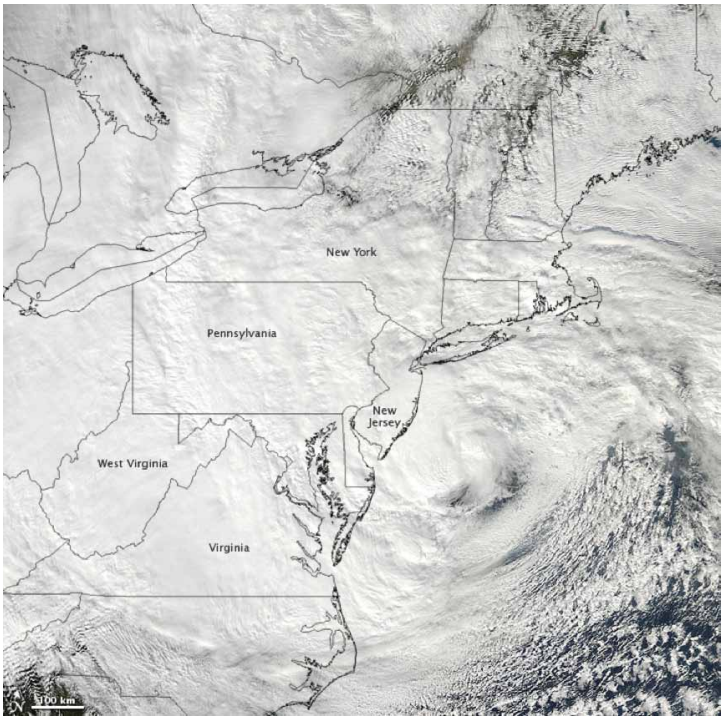

Figure 2. The Moderate Resolution Imaging Spectroradiometer (MODIS) on NASA's Aqua satellite acquired this image of Hurricane Sandy at 1820 UTC (2:20 PM EDT) on October 29, 2012.

At 2:00 PM EDT, the U.S. National Hurricane Center reported that the storm was located at 38.3° N and 73.1° W, about 180 km (110 mi) southeast of Atlantic City, NJ, and 285 km (175 mi) south-southeast of New York City, NY. Maximum sustained winds were 150 km/hr (90 mi/hr), and the central pressure was 940 hPa (27.76 in). For high resolution image go to: *earthobservatory.nasa.gov/NaturalHazards/view.php?id=79561*. **Credit:** NASA's Earth Observatory/ LANCE MODIS Rapid Response Team

feature articles

Aqua 10 Years After Launch

Claire L. Parkinson/Aqua Project Scientist, NASA's Goddard Space Flight Center, claire.l.parkinson@nasa.gov

A little over ten years ago, in the early morning hours of May 4, 2002, crowds of spectators stood anxiously watching as the Delta II rocket carrying NASA's Aqua spacecraft lifted off from its launch pad at Vandenberg Air Force Base in California at 2:55 AM.

Introduction

A little over ten years ago, in the early morning hours of May 4, 2002, crowds of spectators stood anxiously watching as the Delta II rocket carrying NASA's Aqua spacecraft lifted off from its launch pad at Vandenberg Air Force Base in California at 2:55 AM—see photograph. The rocket quickly went through a low-lying cloud cover, after which the main portion of the rocket fell to the waters below and the rocket's second stage proceeded to carry Aqua south across the Pacific, onward over Antarctica, and north to Africa, where the spacecraft separated from the rocket 59.5 minutes after launch. Then, 12.5 minutes later, the solar array unfurled over Europe, and Aqua was on its way in the first of what by now have become over 50,000 successful orbits of the Earth.

Following a sequence of six ascent burns, all planned long before, Aqua reached its operational orbit on June 17, 2002. That near-polar, sun-synchronous orbit has Aqua at an altitude of 705 km (~438 mi), orbiting the Earth once every 98.8 minutes and crossing the equator going north at 1:30 PM and south at 1:30 AM, local time. Before reaching that operational orbit, four of Aqua's six Earth-observing instruments had been turned on and tested out, and by June 25, 2002, the remaining two instruments had also been turned on and tested out. Ten years later, these Aqua instruments have provided the world with a wealth of information about the Earth system and the interactions within it. Four of the Earth-observing instruments and the spacecraft continue to work well, four years beyond the planned six-year prime mission. This article provides a brief summary of the Aqua mission and what it has accomplished so far.

The Delta II rocket carrying the Aqua spacecraft lifts off from its launch pad at Vandenberg Air Force Base in California at 2:55 AM, May 4, 2002. **Image credit**: **Bill Ingalls**, courtesy of NASA.

The Aqua Earth-Observing Instruments

Aqua's six Earth-observing instruments are the Atmospheric Infrared Sounder (AIRS), the Advanced Microwave Sounding Unit (AMSU), the Humidity Sounder for Brazil (HSB), the Advanced Microwave Scanning Radiometer for the Earth Observing System (AMSR-E), the Moderate Resolution Imaging Spectroradiometer (MODIS), and the Clouds and the Earth's Radiant Energy System (CERES). The Brazilian Institute for Space Research provided HSB; the Japan Aerospace Exploration Agency (JAXA) provided AMSR-E; and NASA provided the remaining instruments and the spacecraft.

The three sounders on Aqua—AIRS, AMSU, and HSB—work together as a unified sounding system, and as a result there is one science team covering the three instruments. With AIRS the centerpiece of the threesome, the science team is generally referred to as the AIRS Science Team, although sometimes as the AIRS/AMSU/HSB Science Team. AIRS was a major technological advance developed for the Aqua mission. It has 2382 channels, 2378 of them measuring in infrared (IR) wavelengths and the remaining four measuring in visible wavelengths. In contrast, the 15-channel AMSU and four-channel HSB both measure in microwave wavelengths. While AIRS is unique to Aqua, AMSU and HSB

are near-copies of instruments that have flown on various satellites of the National Oceanic and Atmospheric Administration (NOAA).

HSB collected valuable information about atmospheric humidity and cloud liquid water for the first nine months of the Aqua mission but ceased operations in February 2003. AIRS and AMSU continue to transmit high-quality data, and the AIRS Science Team, centered at the NASA/Jet Propulsion Laboratory (JPL), is using these data to determine vertical profiles of atmospheric temperature, moisture, and key trace gases in the atmosphere, as well as cloud and surface parameters.

"During the last ten years no other satellite instrument has been more essential to improve global weather forecasts than AIRS."
***—Joao Teixeira** [JPL—AIRS Science Team Leader]*

The CERES instrument (of which Aqua has two identical copies) has only three channels, but these three channels are geared specifically at the highly important issue of the Earth's overall radiation budget. The three channels measure reflected shortwave radiation at the top of the atmosphere, total outgoing radiation at the top of the atmosphere, and the outgoing radiation in the 8-12 μm atmospheric window. The CERES Science Team, centered at NASA's Langley Research Center (LaRC), can easily obtain outgoing longwave radiation by subtracting the reflected shortwave radiation from the total outgoing radiation and is using the CERES data in conjunction with MODIS and other data for extensive studies on clouds and the Earth's radiation budget.

MODIS is a multipurpose, 36-band radiometer measuring numerous atmosphere, land, and ocean variables at visible and infrared wavelengths. Among the many variables measured are cloud cover, aerosols, water vapor, ocean color, sea surface temperature, surface reflectance, vegetation indices, net primary productivity, leaf-area index, snow cover, and sea ice. MODIS has the finest spatial resolution of any of the Aqua instruments, providing data at resolutions between 250 m (~820 ft) and 1 km (~3280 ft). The MODIS Science Team is centered at NASA's Goddard Space Flight Center and at the University of Colorado.

"CERES Aqua is providing unprecedented detail on how reflected solar and emitted thermal radiation from Earth vary over a range of time-space scales. Furthermore, synergistic use of CERES and other Aqua and A-Train instruments such as AIRS, MODIS, and the instruments on CALIPSO and Cloudsat has led to a significantly revised estimate of the energy budget at the surface and a new understanding of how clouds and aerosols influence the vertical distribution of radiative heating within the atmosphere."
***—Norman Loeb** [LaRC—CERES Science Team Leader]*

The CERES and MODIS instruments launched on Aqua were preceded by CERES and MODIS instruments launched earlier on other satellites. The first CERES was launched on the Tropical Rainfall Measuring Mission (TRMM) in November 1997 and is no longer operational. The next two CERES and the first MODIS were all launched on the Terra satellite in December 1999 and still continue to operate. Having MODIS and CERES on both Aqua and Terra has been of substantial added value, as it has allowed more complete data coverage, including additional information on the daily cycle of variables measured by those two instruments, as Terra crosses the equator at approximately 10:30 AM and 10:30 PM, complementing the 1:30 AM and 1:30 PM equatorial crossings of Aqua. The MODIS Science Team covers both MODIS instruments (on Aqua and Terra), and the CERES Science Team covers all CERES instruments, which by now include not only those on TRMM, Terra, and Aqua, but also one launched on the Suomi National Polar-orbiting Partnership (NPP) in October 2011 and one planned for eventual launch on the first Joint Polar Satellite System (JPSS).

Like MODIS, AMSR-E is a multipurpose instrument. However, AMSR-E's measurements are done at microwave wavelengths. AMSR-E has 12 channels and measures such atmospheric and surface variables as rainfall rates, surface wind speeds over the oceans, vertically integrated water vapor and cloud water amounts, sea surface temperatures, sea ice coverage, snow water content, and soil surface wetness. AMSR-E data have much coarser spatial resolution than MODIS data, but by measuring at microwave wavelengths they have the wonderful advantage of being able routinely to obtain information about surface variables under cloudy as well as cloud-free conditions and during darkness as well

as daylight. The U.S. AMSR-E Science Team is centered at NASA's Marshall Space Flight Center and the University of Alabama in Huntsville (UAH); the Japanese AMSR-E Science Team is centered at JAXA and the Japan Meteorological Research Institute.

AMSR-E collected high-quality data for over nine years—well beyond its design lifetime—but experienced a major anomaly on October 4, 2011. The instrument was turned back on in early February 2012, but without rotation of the antenna, which is needed for high-quality AMSR-E data. In September 2012, initial tests were carried out to restart the rotation, although only for brief periods and at a much lower rotation rate than during the prime mission. These tests are now being analyzed, and the hope is that the instrument will be able to operate, while rotating at least slowly, for a sufficient time to obtain enough data overlapping with a recently launched AMSR2 instrument to provide intercalibration between the AMSR-E and AMSR2. AMSR2 was launched by JAXA on its Global Change Observation Mission - Water (GCOM-W) satellite, named "Shizuku," in May 2012.

"AMSR-E has allowed unprecedented monitoring of historic sea ice changes in the Arctic and Antarctic, as well as of sea surface temperature changes on a worldwide basis. Its ability to observe surface characteristics through most types of cloud cover provides valuable synergy with the other Aqua instruments."
*—**Roy Spencer** [University of Alabama, Huntsville—U.S. AMSR-E Science Team Leader]*

Pre-Launch Changes to the Aqua Name and Instruments

The mission that eventually became "Aqua" began early in the planning for the Earth Observing System (EOS) and was originally named "EOS PM" for its early-afternoon equatorial crossing times. Correspondingly, the satellite that eventually became "Terra" was originally named "EOS AM" for its mid-morning equatorial crossing times. The first name to change was "EOS AM", after the EOS AM team ran a contest for renaming the satellite, with "Terra" being the winning entry. Once EOS AM was renamed, it was time to reconsider the name "EOS PM." At the suggestion of NASA Headquarters, the renaming of EOS PM was done internal to the EOS PM program, with 17 nominations submitted, followed by voting by each of the science teams, project management, and the project science leadership. The winning name—nominated by the long-time AIRS Science Team leader Mous Chahine—was "Aqua," Latin for 'water' and selected for the wealth of information that the satellite would provide about water in all its forms (solid, liquid, and vapor) and about the water cycle. NASA Headquarters approved the new name, and "Aqua" replaced "EOS PM" in October 1999. Interestingly, the strong second-place finisher in the voting was "Suomi," in honor of the University of Wisconsin meteorologist Verner Suomi, after whom the Suomi NPP satellite is now named following the NPP launch in October 2011.

The name wasn't the only feature to change in the development stage of the Aqua program[1]. Notable among the other changes, the spacecraft had to be downsized in the 1990s to fit into a Delta II launch vehicle, and two early international partners pulled out from providing instruments due to financial considerations. Two new partners, however, stepped in to provide instruments: Japan in the case of the passive-microwave imager that was to become AMSR-E, and Brazil in the case of the microwave sounder that was to become HSB. Both Japan and Brazil have proven to be valued partners in the Aqua program.

Aqua Mission Success Criteria

Prior to launch, the Project Scientist and Aqua Science Teams were given the task of working with NASA Headquarters to develop a set of criteria that would constitute success for the Aqua mission. The result was the following list of ten Aqua Mission Success Criteria:

1. Produce the first high-spectral-resolution global infrared spectra of the Earth.
2. Obtain a highly accurate temperature profile of the troposphere.

[1] **Ghassem Asrar's** article in the May–June 2011 issue of *The Earth Observer* [**Volume 23**, **Issue 3**, pp. 4-7] summarizes the original plans for EOS and how those plans evolved over time into the observing system we have today.

3. Extend the improved TRMM rainfall characterization to the extra tropics.
4. Produce the first global sea surface temperature daily maps under nearly all sky conditions for a minimum of one year.
5. Produce large-scale global soil moisture maps for regions with low vegetation.
6. Produce calibrated global observations of the Earth's continents and ocean surfaces.
7. Capture and document two seasonal cycles of terrestrial and marine ecosystems and atmospheric and cloud properties.
8. Produce two seasonal/annual Earth radiation budget records.
9. Produce improved measurements of the diurnal cycle of radiation by combining Aqua and Terra measurements.
10. Produce combined cloud property and radiation balance data to allow improved studies of the role of clouds in the climate system.

In late 2008, at the Aqua End-of-Prime-Mission Review, following the completion of the six-year prime mission for the spacecraft, the Aqua Project Scientist was pleased to report to NASA Headquarters that each of the ten Success Criteria had indeed been accomplished. The AIRS Science Team had produced the first high-spectral-resolution global infrared spectra of the Earth back in 2002 and had obtained and validated highly accurate temperature profiles of the troposphere by the end of 2004. The AMSR-E Science Team had extended the TRMM rainfall characterization to the extra tropics by the end of 2002 (see **Figure 1**), had produced the first global sea surface temperature daily maps under nearly all sky conditions for a full year by the end of 2003, and had generated global soil moisture maps for regions with low vegetation

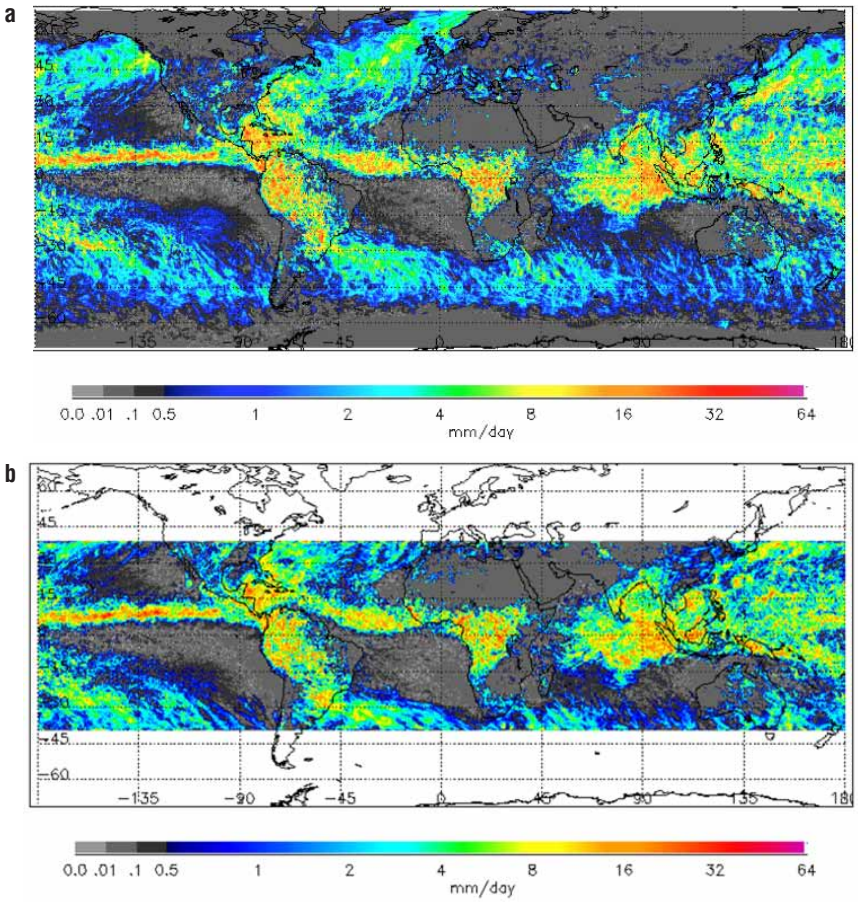

Figure 1. October 2005 rainfall rates as derived from (a) the Aqua AMSR-E and (b) the TRMM Microwave Imager (TMI). The TRMM satellite focuses on tropical measurements and hence has an orbit that is restricted to low- and mid-latitudes. Aqua's near-polar orbit allows AMSR-E to collect data at high latitudes as well. Note in particular the close match of the AMSR-E and TRMM data in the latitudes of the TRMM measurements. **Image credit**: **Chris Kummerow**, **Ralph Ferraro**, and **Elena Lobl** of the AMSR-E Science Team.

by the end of 2002. The MODIS Science Team produced calibrated global observations of the Earth's continents and ocean surfaces by mid-2004 and had documented two seasonal cycles of terrestrial and marine ecosystems and atmospheric and cloud properties by the end of 2004. The CERES Science Team produced the required Earth radiation budget records, combined Aqua and Terra data to produce improved measurements of the diurnal cycle of radiation, and combined Aqua CERES top-of-the-atmosphere and surface flux estimates with a range of data from other sources to produce the required cloud property and radiation balance data for improved studies of the role of clouds in the climate system.

Highlights From the First Ten Years of Aqua Data

As Aqua begins its second decade of on-orbit operations, this is an appropriate time to reflect on its contributions to date and to look toward the future. The Aqua data have provided such a wealth of new information about the Earth system that they have been used in over 2000 scientific publications, making a thorough listing of results quite impractical. Even a mere listing of the approximately 100 core Aqua data products would be cumbersome, and so presented here is instead a small, representative sampling of the Aqua results. These range from large-scale features of the global energy budget down to mapped details of such occurrences as individual oil spills and phytoplankton blooms, beginning with the energy budget.

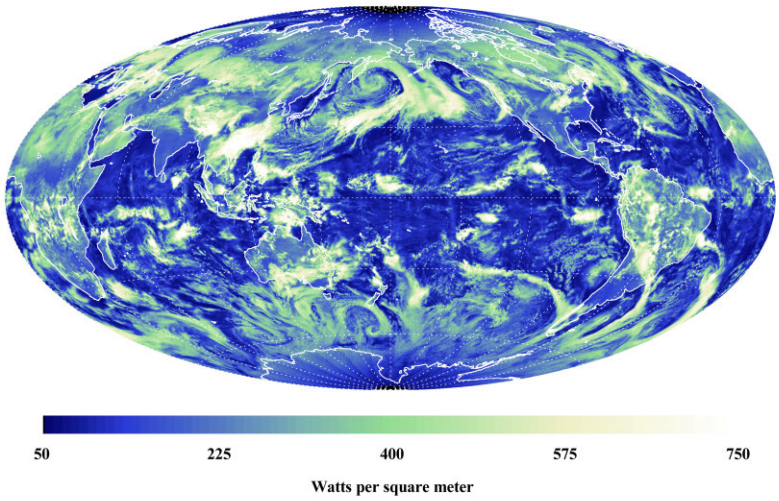

Figure 2. Global map of reflected shortwave radiation, March 18, 2011, as derived from Aqua CERES data. **Image credit**: **Tak Wong** of the CERES Science Team.

Top-of-the-Atmosphere Global Energy Budget

The large-scale global energy budget, involving both the energy entering the Earth system and the energy exiting the system, is fundamental to whether the Earth overall is warming, cooling, or neither warming nor cooling. Aqua does not have instruments measuring the energy entering the Earth system—which is overwhelmingly from the Sun—but it does have the CERES instrument measuring the energy exiting the system, both as the total outgoing radiation and as the shortwave outgoing radiation (which is predominantly reflected solar radiation)—see **Figure 2**.

Furthermore, the CERES Science Team combines the outgoing radiation measurements from the Aqua and Terra CERES instruments with incoming solar radiation measurements obtained from the Total Irradiance Monitor (TIM) on the Solar Radiation and Climate Experiment (SORCE) to obtain the global energy budget. Doing so, they have calculated a slight imbalance at the top of the atmosphere, finding that in recent years more energy has been entering than leaving the Earth system and quantifying the amount of the imbalance. The results are in line with the overall global warming that has received much discussion and concern among both the general public and scientists.

While the CERES measurements obtain information about the energy budget as a whole, other Aqua instruments obtain information about many of the forcing factors affecting that energy budget. Key among these are greenhouse gases, which hinder terrestrial radiation from leaving the Earth system and hence promote warming, and particulate matter, much of which has the opposite effect of cooling the Earth system by reflecting sunlight away.

Greenhouse and Other Atmospheric Trace Gases

Greenhouse gases have a warming effect on the Earth system because they tend to allow solar radiation to enter the system easily but hinder some of the Earth's radiation from exiting. The most abundant greenhouse gas is water vapor; but the second most abundant, carbon dioxide, has received much of the attention when it comes to greenhouse gas effects on recent global warming. This is because there is a solid record of carbon dioxide increases in the atmosphere and a widespread recognition that these increases are in substantial part due to industrial and other human activities.

Both the AIRS/AMSU and MODIS datasets have been used to derive global records of water vapor, and the AMSR-E dataset has been used to derive water vapor over the oceans. Furthermore, AIRS/AMSU data are additionally used to derive global records of carbon dioxide (see **Figure 3**), and in fact the first global maps of mid-tropospheric carbon dioxide concentrations from satellite data were from the AIRS/AMSU data. The AIRS/AMSU record shows that atmospheric carbon dioxide distributions are strongly influenced by such factors as the mid-latitude jet streams and synoptic weather systems.

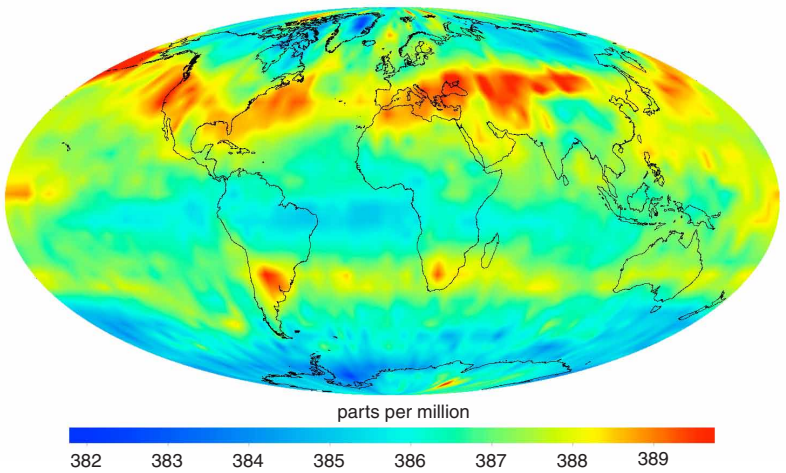

Figure 3. Global carbon dioxide concentrations in the mid-troposphere in July 2009, as derived from AIRS/AMSU data. **Image credit**: **Mous Chahine** and the AIRS Science Team.

However, they also clearly show: (1) a strong seasonal cycle, with atmospheric carbon dioxide increasing during the Northern Hemisphere winter and decreasing during the Northern Hemisphere summer, when vegetation removes carbon dioxide from the atmosphere and uses it for photosynthesis; and (2) an overall upward trend. Through the innovative and persistent efforts of Charles David Keeling and his successors, the seasonal cycle and upward trend of atmospheric carbon dioxide have been carefully monitored since the late 1950s for the location of Mauna Loa, HI; but the AIRS/AMSU data now show these features globally. The long Mauna Loa record and the much shorter but global AIRS/AMSU record nicely complement each other.

In addition to water vapor and carbon dioxide, the AIRS/AMSU data are also used to derive records of several other atmospheric trace gases, including methane, sulfur dioxide, carbon monoxide, and ozone. Methane is a greenhouse gas that could become increasingly important—as its presence in the atmosphere is anticipated to increase with continued decay of high-latitude permafrost. Sulfur dioxide is an important constituent of many volcanic eruptions, allowing the AIRS/AMSU sulfur dioxide product to track volcanic emissions. Carbon monoxide is a common constituent in fires, allowing the AIRS/AMSU carbon monoxide product to track the spread of smoke

from major fires around the globe. Ozone in the upper atmosphere helps protect life at the surface from excessive ultraviolet radiation, while ozone at ground level is a pollutant. The AIRS/AMSU ozone record is a welcome complement to the well-established, longer records of ozone from ultraviolet measurements, as the AIRS/AMSU records—in contrast to the ultraviolet ones—include periods of darkness as well as daylight.

Aerosols and Other Particulate Matter in the Atmosphere

At ground level, particles in the atmosphere tend to be irritants, and abundant amounts tend to be quite unpleasant for humans, especially for people with asthma or other breathing difficulties. However, particles in the atmosphere have many additional effects, some of which are crucial for such processes as the transport of nutrients from one region to another.

"What is really rewarding is the large variety of practical uses to which MODIS data are applied, including fires, oil spills, volcanic eruptions, weather forecasting, and floods, as well as the expected climate observables."

*—**Michael King** [University of Colorado—MODIS Science Team Leader]*

In terms of the global energy budget, particulate matter has the strong reputation of providing a countereffect to the warming promoted by greenhouse gases. It is not the case, however, that all particulate matter has a cooling effect, as some particle types actually promote warming, one prominent example being black carbon.

Particles get into the atmosphere through both natural means and human activities, and the AIRS/AMSU and MODIS instruments make a variety of measurements of particles from both these sources. AIRS/AMSU and MODIS imagery show volcanic emissions clearly, with the AIRS/AMSU sulfur dioxide product also highlighting that particular emission from volcanoes. MODIS imagery further gives clear depictions of large dust storms and fires; and the AIRS/AMSU data have contributed to an improved understanding of how hurricane formation and intensification have been impacted by the dust in the Saharan Air Layer.

The MODIS aerosol calculations have expanded over time in their regions of applicability, with the early algorithms appropriate only for aerosols above dense vegetation and oceans. The *deep-blue algorithm* in particular has enhanced the MODIS calculations by also allowing calculations for aerosols over bright reflecting surfaces, such as deserts. The MODIS aerosol products include aerosol optical thickness, aerosol size distribution, and even a distinction between fine and coarse particles. The latter is particularly noteworthy because the emissions from anthropogenic sources tend to be weighted far more toward fine particles than do the emissions from natural sources.

Aqua measurements include water in the atmosphere (water vapor, clouds, precipitation), water on land (soil moisture, lakes, rivers, land ice, snow cover), and water in the oceans (surface waters, sea ice), fully justifying the "Aqua" name.

Water in the Earth System

Among the extremely important factors in the Earth's energy budget and in the Earth system as a whole, especially in all forms of Earth-based life, is the water cycle. In the water cycle, water evaporates from the surface, taking in energy as it does so, enters the atmosphere as water vapor, moves from place to place in the atmosphere, transporting the energy that it absorbed during evaporation, and releases the energy when it condenses into liquid droplets or solid ice particles. The droplets or particles eventually fall to the surface, often as precipitation. This is one important way in which the water cycle affects the energy transports and budgets within the Earth system. Another way is through the previously mentioned fact that water vapor is the most abundant greenhouse gas, hindering the Earth's radiation from escaping from the Earth system. Water in its solid form is also critically important to the energy budget, as it reflects solar radiation back to space.

Aqua measurements include water in the atmosphere (water vapor, clouds, precipitation), water on land (soil moisture, lakes, rivers, land ice, snow cover), and water in the oceans (surface waters, sea ice), fully justifying the "Aqua" name. Aqua standard products regarding water in the Earth system are listed in **Table 1** (next page).

Table 1. Aqua standard products of water in the Earth system.

Standard Product	Instruments Involved
Evapotranspiration	MODIS
Atmospheric Water Vapor	AIRS/AMSU, AMSR-E, and MODIS
Precipitable Water	AIRS/AMSU and MODIS
Cloud Products	AIRS/AMSU, AMSR-E, CERES, and MODIS
Rainfall	AMSR-E
Sea Ice Concentration and/or Extent	AMSR-E and MODIS
Sea Ice Drift	AMSR-E
Snow Depth on Sea Ice	AMSR-E
Snow Depth on Land and Snow Water Equivalent	AMSR-E
Fractional Snow Cover and Snow Albedo	MODIS
Surface Soil Moisture	AMSR-E

Although water vapor in the lower atmosphere had been derived from satellite measurements for decades prior to the Aqua launch, Aqua's AIRS/AMSU water vapor measurements provide increased accuracies and include upper-atmosphere water vapor as well as the lower-atmosphere product. Somewhat similarly, although the TRMM satellite had already provided impressive rainfall measurements for low latitudes, the AMSR-E instrument has extended these rainfall measurements to high latitudes.

Cloud measurements from the Aqua and Terra MODIS instruments have yielded fundamental new information about the Earth's cloud cover, including that average global cloud coverage is about 67% and that this is true both for the early afternoon measurements collected by Aqua and for the mid-morning (about 10:30 AM) measurements collected by Terra. As expected, cloud coverage is greater over oceans, at about 72%, than over land, at about 55%. Additionally, the Terra mid-morning ocean cloud cover values are slightly higher than the corresponding Aqua early afternoon values, whereas land cloud-cover values are slightly higher from Aqua than from Terra.

Cloud measurements from the Aqua and Terra MODIS instruments have yielded fundamental new information about the Earth's cloud cover, including that average global cloud coverage is about 67% and that this is true both for the early afternoon measurements collected by Aqua and for the mid-morning (about 10:30 AM) measurements collected by Terra.

AMSR-E and MODIS both provide measurements of sea ice and snow cover, with the AMSR-E measurements particularly useful for climate studies because they provide data throughout the year, irrespective of sunlight conditions and cloud coverage. MODIS, on the other hand, has the advantage of finer resolution, providing greater spatial detail for the times when cloud cover is not an issue. The AMSR-E measurements follow a long tradition of passive-microwave instrumentation but with finer spatial resolution than previous passive-microwave imagers, making them particularly valuable, for instance, in depicting a record minimum Arctic sea ice extent that occurred in 2007—see **Figure 4** (next page)—and held until 2012, when yet another new record was reached. In fact, in contrast to the data from previous passive-microwave imagers, the AMSR-E data have sufficient resolution to resolve *leads*—narrow stretches of open water between ice floes—in the sea ice, allowing satellite-based, all-weather studies of heat fluxes in sea-ice fields.

Temperature in the Atmosphere and at the Surface

A net result of all the various energy sources, sinks, and flows to, from, and within the Earth system is the temperature structure within the system, along with its continual changes. AIRS/AMSU measurements are particularly important for obtaining vertical temperature profiles throughout the atmosphere, whether in the presence of clouds or cloud-free. Improved temperature profiles for weather forecasting was one of the primary goals of the AIRS/AMSU efforts, with the very specific goal of 1-K accuracies in 1-km (~3280 ft) layers in the atmosphere, a goal that was met early in the Aqua mission. In fact, the AIRS/AMSU data get near-radiosonde accuracies

Figure 4. Arctic sea ice coverage on September 14, 2007, as derived from AMSR-E data. Until 2012, this was the date of the record minimum sea ice coverage over the period of the satellite record since late 1978. Note in particular the easy Northwest Passage through the Canadian Archipelago. Greenland is prominent in the center of the upper portion of the image; Siberia, the Bering Strait, and Alaska are at the bottom of the image. **Image credit**: NASA Scientific Visualization Studio (SVS), employing AMSR-E data courtesy of JAXA.

(see **Figure 5**), despite the fact that radiosondes measure temperature *in situ* whereas AIRS and AMSU measure from quite a considerable distance, at Aqua's altitude of 705 km (~438 mi).

Both AMSR-E and MODIS data are used to derive global sea surface temperatures (SSTs), but, as with sea ice and other surface measurements obtained by both instruments, the two sets of measurements are nicely complementary. MODIS obtains higher spatial resolution, thereby providing more geographic detail, but AMSR-E data can be used to obtain SSTs under almost all weather conditions, thereby providing much more thorough coverage than the MODIS SST data, which are largely restricted to cloud-free conditions. MODIS additionally gets land surface temperatures, and gets them both for daytime and nighttime, using thermal infrared measurements. An annual identification of the "hottest place on Earth" as obtained from the MODIS data has generated some public interest in recent years, with the "winner" of this unenviable status often being the Lut Desert of Iran.

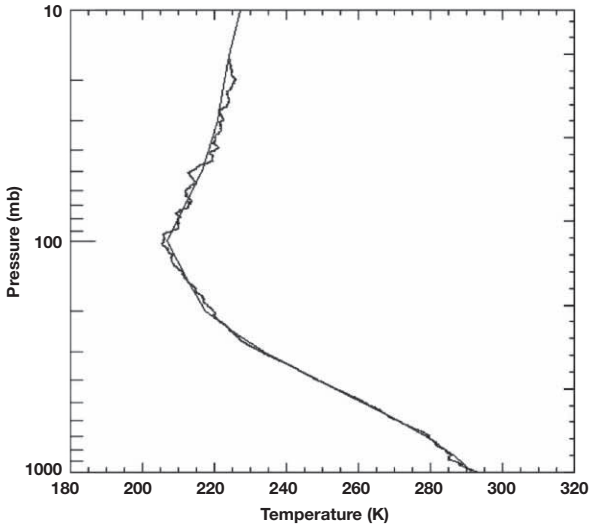

Figure 5. AIRS temperature profile over Chesapeake Bay (smooth curve) overlaid with a radiosonde profile (more-jagged curve) over Chesapeake Bay for the same date, September 13, 2002. Despite the fact that AIRS collects data from an altitude of 705 kilometers (~438 mi), the temperatures derived from the AIRS data match closely with the *in situ* measurements of the radiosonde. **Image credit**: **Wallace McMillan** and the AIRS Science Team, with relabeling.

Land Vegetation and Marine Life

In addition to the wealth of information the Aqua data are providing about the non-biological aspects of the Earth system, Aqua data, especially from the MODIS instrument, are providing information about land vegetation and multiple measures of marine life. In terms of land vegetation, MODIS-derived variables include leaf area index, photosynthetically active radiation, evapotranspiration, the well-established Normalized Difference Vegetation Index (NDVI) that has been used for decades with data from NOAA's Advanced Very High Resolution Radiometer (AVHRR) sensors, and the MODIS Enhanced Vegetation Index (EVI). The EVI has enhanced sensitivity over the NDVI, particularly in areas of dense vegetation, and also reduces the effects of soil variations on the calculations. The MODIS land-vegetation data are used to create global images that show clearly the major deserts and forested areas of the Earth [see **Figure 6** (next page)], but they are also used for local and regional studies—e.g., for examining the drought sensitivity of the Amazon rainforest.

MODIS-derived marine-life datasets include such variables as particulate organic carbon (POC), chlorophyll-*a* concentration, and fluorescence. The MODIS POC product gives the near-surface concentration of organic particles in the water. The MODIS chlorophyll-*a* measurement is an indicator of phytoplankton biomass, chlorophyll-*a* being the main plant pigment involved in photosynthesis. The MODIS measurements

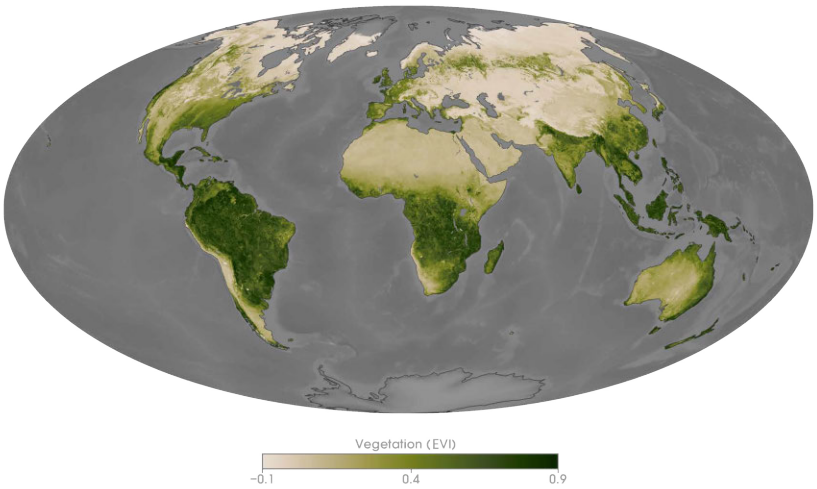

Figure 6. Global image of the MODIS Enhanced Vegetation Index (EVI), averaged over the 16-day period February 10-25, 2012, as derived from Aqua MODIS data. Deep greens highlight the rainforests of the Amazon, equatorial Africa, Indonesia, and Central America; and browns highlight such desert areas as the Sahara Desert in northern Africa, the Gobi Desert in central Asia, the Great Victoria and Great Sandy Deserts of Australia, the Atacama Desert along the west coast of South America, and the Sonoran and Mojave Deserts in the southwestern United States. **Image credit**: **Marit Jentoft-Nilsen**, with data provided by **Kamel Didan** and the MODIS Science Team.

continue the chlorophyll-*a* record from the Sea-viewing Wide-Field-of-view Sensor (SeaWiFS), launched in 1997 on the Orbview-2 satellite. In contrast, the fluorescence measurements are new with the Aqua MODIS and provide the first satellite-derived large-scale view of the physiological stress undergone by ocean phytoplankton. This is an exciting new capability of the Aqua MODIS, providing information about the health of phytoplankton to complement the earlier and continuing information about the phytoplankton biomass. Phytoplankton account for approximately half of the photosynthetic activity on the planet, and they consume carbon dioxide as they do so.

Practical Applications

Although the Aqua mission was developed largely for its many anticipated scientific contributions, from the beginning it was also hoped and expected that the mission would have value in the realm of practical applications. Well before launch, researchers recognized that the high accuracy of the AIRS/AMSU temperature and water vapor measurements would have value in weather forecasting, and indeed since launch the measurements from AIRS/AMSU have been used in many weather forecasting models around the world, with resulting measurable improvements in forecast skill.

Others of the Aqua instruments have also contributed to improved forecasts. In particular, the AMSR-E sea surface temperature, water vapor, and precipitation data have been used by hurricane prediction centers; and incorporation of MODIS polar wind data in computer models has resulted in measurably improved weather forecasts in the polar regions and beyond. Also of importance for forecasting is the large-scale view that satellites provide of hurricanes and typhoons as they form, develop, and approach land—e.g., see **Figure 7**.

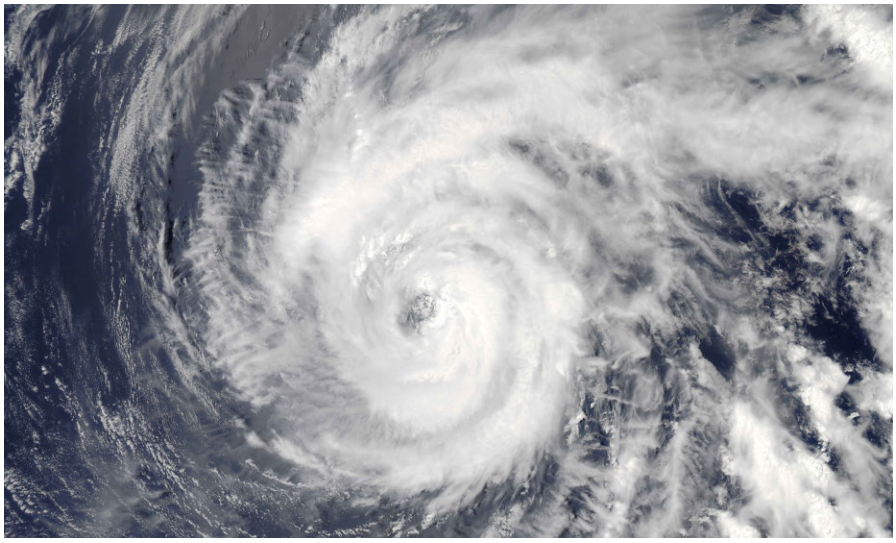

Figure 7. Typhoon Sanvu over the western Pacific, roughly 185 km (~115 miles) southwest of Iwo Jima, Japan, on May 25, 2012, as imaged by the Aqua MODIS. Sanvu had gusts of up to 185 km/hr (~115 mi/hr) and sustained winds of 150 km/hr (~93 mi/hr). **Image credit**: **Jeff Schmaltz** of the MODIS Rapid Response Team at NASA's Goddard Space Flight Center.

"Launched in May 2002 as a six-year mission, Aqua is still an excellent performer. It has met the challenges imposed on it by the science community with distinction and has contributed to the development of climate data records of unprecedented quality. Operational agencies around the world are using Aqua data to improve weather prediction. The six Aqua instruments were carefully selected to make measurements for the improved characterization and understanding of atmospheric temperature and humidity profiles, clouds, global precipitation, and Earth's thermal radiation balance; terrestrial snow and sea ice; sea surface temperature and ocean productivity; and soil moisture. The Aqua sounding instruments and imaging radiometers have considerably higher volume resolution (vertical resolution X footprint area) than the corresponding predecessor instruments. The synergy generated by the Aqua instruments along with other A-train components is allowing us to make extraordinary space-based measurements to study complex and interrelated systems of land surface, biosphere, atmosphere, and oceans. To keep pace with the improved spatial and temporal resolution of the global models, the satellite instruments of the future will continue to improve the volume resolution and find innovative ways to tackle the time resolution horizon. However, the performance provided by the Aqua satellite will be a tough act to follow."

*—**Ramesh Kakar** [NASA Headquarters—Aqua Program Scientist]*

In addition to their value in weather forecasting, Aqua data are proving of practical value in numerous other arenas. Data from the MODIS instruments on both Aqua and Terra show forest fires with great clarity, allowing the U.S. Forest Service and other forest services around the world to see the locations and expanse of forest fires, thereby helping them in their very practical determination of where best to deploy firefighters.

In a different realm, the AIRS/AMSU and MODIS data are used to track and monitor volcanic emissions. Because airborne volcanic ash can pose significant dangers to airplanes, monitoring volcanic emissions has been of great value to airplane pilots and aviation administrations, helping them to steer planes clear of the volcanic ash.

In addition to their value in weather forecasting, Aqua data are proving of practical value in numerous other arenas.

Other practical uses of Aqua data include the use of:

- AIRS/AMSU and MODIS data in air-quality analyses;
- CERES data by utility companies for energy management;
- MODIS data by the U.S. Department of Agriculture for monitoring crop yields and drought;
- CERES data by the Department of Agriculture in its analyses of the factors affecting crop yields;
- AMSR-E SST data by the Japanese fishing industry to help analyze local and regional fishing conditions;
- AMSR-E and MODIS data for monitoring floods and their aftermath;
- MODIS data for monitoring oil spills and dust storms, both of great relevance for people in the path of the oil and dust;
- MODIS data for monitoring phytoplankton blooms and hence identifying ocean regions that abound with life; and
- AMSR-E and MODIS data for sea ice monitoring, helping crews of ships maneuvering in polar oceans to be aware of hazardous conditions.

When Aqua launched in May 2002, it was unclear how much value the Aqua data would have for immediate practical applications beyond weather forecasting. However, in part because of Aqua's direct broadcast capability, whereby the spacecraft routinely broadcasts its real-time data, the value of the Aqua mission for practical applications has exceeded almost all initial expectations.

Ten Singled-Out Achievements (a qualified 'Top Ten' List)

The many and varied contributions made so far with Aqua data make it difficult to identify which contributions are the most important. However, with the help of **Joao Teixeira** [JPL— *AIRS Science Team Leader*], **Roy Spencer** [UAH—*U.S. AMSR-E Science Team Leader*], **Norman Loeb** [LaRC—*CERES Science Team Leader*], **Bruce Wielicki** [LaRC—*Former CERES Science Team Leader*], **Michael King** [University of Colorado—*MODIS Science Team Leader*], **Vince Salomonson** [University of Utah—*Former MODIS Science Team Leader*], other members of the science teams, and **Ramesh Kakar** [NASA Headquarters—*Aqua Program Scientist*], the Aqua Project Scientist has compiled a list of ten contributions singled out as Ten Top Achievements of Aqua's First 10 Years of Observations. These are not presented as necessarily the "Top Ten," but rather as ten that are near the top, fully recognizing that there are other major achievements as well. With that qualification, here is the list of Ten Top Achievements (not ordered by importance):

1. Aqua and Terra data from CERES, in conjunction with incoming solar radiation data from the Solar Radiation and Climate Experiment (SORCE), have been used to quantify changes in the energy imbalance at the top of the atmosphere, determining that the Earth system has been accumulating energy at an overall rate of 0.5 W/m^2.

2. Aqua data from AIRS/AMSU have been used to produce the first global maps from space of mid-troposphere carbon dioxide concentrations and have revealed the influence of large-scale dynamics on carbon dioxide distributions.

3. Aqua radiance data from AIRS provide an unprecedented accuracy and stability that makes them ideal for climate studies, leading to the confirmation of previous estimates of the sign and magnitude of the water vapor feedback and to the creation of novel ways of evaluating climate models.

4. Aqua data from CERES and MODIS have been used to quantify the direct radiative effect of atmospheric aerosols on top-of-the-atmosphere, within-the-atmosphere, and surface radiative fluxes.

5. Aqua data from AMSR-E have been used to extend to high latitudes the high-quality precipitation retrievals from the Tropical Rainfall Measuring Mission (TRMM).

6. Aqua data from AMSR-E have provided near-all-weather global monitoring of a variety of surface variables, including sea surface temperature and sea ice, allowing the observation and analysis of such occurrences as the August 2005 sea surface cold wake following the passage of Hurricane Katrina and the September 2007 then-record minimum (later surpassed) in Arctic sea ice coverage.

7. Aqua data from MODIS have included the first global observations of ocean chlorophyll fluorescence, providing a synoptic view of phytoplankton physiological stress.

8. Aqua data from MODIS have provided the first global annual measure of ecosystem disturbance, a key component for quantifying deforestation and desertification.

9. Aqua and Terra data from MODIS have provided the first decade-long dataset of global evapotranspiration, a key variable in drought monitoring.

10. Aqua data from AIRS/AMSU, MODIS, and AMSR-E have all helped in weather forecasting, and AIRS in particular has been found in several sensitivity studies to be the single most important satellite instrument in improving global weather forecasts during the last 10 years.

The variety of instruments on the A-Train satellites greatly enhances the science that can be done with the A-Train data, and indeed the Aqua science teams are working with science teams from the other A-Train missions to make effective use of the complementary datasets.

The A-Train Constellation of Satellites

Aqua is not alone in its orbital track around the Earth. Instead, it was the first in what became a sequence of satellites launched into a line-up popularly known as the "A-Train" and more formally known as the "Afternoon Constellation." The second satellite into the A-Train was NASA's Aura satellite, launched on July 15, 2004, and placed well behind Aqua. A few months later, on December 18, 2004, the French Centre National d'Etudes Spatiales (CNES) launched a satellite with the acronym PARASOL (standing for Polarization and Anisotropy of Reflectances for Atmospheric Sciences coupled with Observations from a Lidar) and then maneuvered it into position between Aqua and Aura. Next came NASA's CloudSat and the joint NASA/CNES Cloud-Aerosol Lidar and Infrared Pathfinder Satellite Observations (CALIPSO), launched together on April 28, 2006, and placed between Aqua and PARASOL.

The Orbiting Carbon Observatory (OCO) and Glory were both intended for the A-Train, but in both cases the launch sadly failed, OCO on February 24, 2009, and Glory on March 4, 2011. These major disappointments were followed on May 18, 2012 by JAXA's successful launch of the Global Change Observation Mission–Water (GCOM-W), or "Shizuku," and its successful maneuvering into place in the A-Train in front of Aqua on June 29, 2012. Shizuku carries on board an AMSR2 follow-on to Aqua's AMSR-E instrument.

PARASOL was shifted to a lower orbit on December 2, 2009, and is no longer orbiting in the A-Train. CloudSat was temporarily outside of the A-Train but was repositioned back into the A-Train behind CALIPSO on May 15, 2012. The result is that the A-Train is now led by GCOM-W, followed by Aqua, then CALIPSO, CloudSat, and Aura—see **Figure 8**.

The variety of instruments on the A-Train satellites greatly enhances the science that can be done with the A-Train data, and indeed the Aqua science teams are working with science teams from the other A-Train missions to make effective use of the complementary datasets.

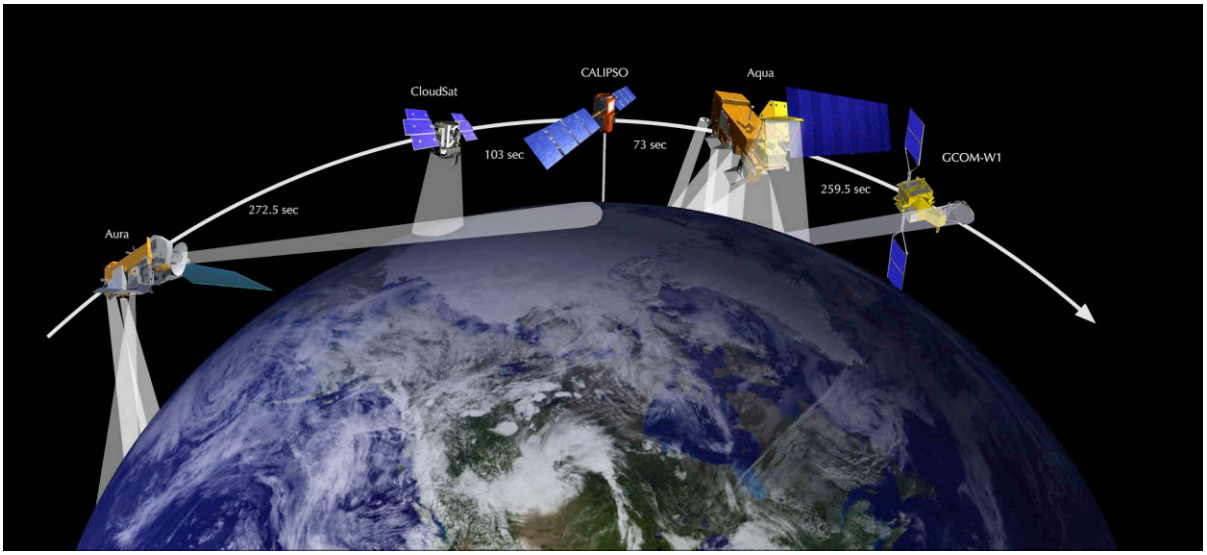

Figure 8. Configuration of the A-Train constellation of satellites as of mid-2012, with GCOM-W in the lead, followed by Aqua, CALIPSO, CloudSat, and Aura. **Image credit**: **Ed Hanka**, **Angie Kelly**, and the A-Train Mission Operations Working Group.

Summary and a Look Toward the Future

Aqua has now exceeded 10 years of on-orbit operations—well beyond its six-year prime mission. The Aqua instruments have gathered information on numerous aspects of the Earth's water cycle, the Earth's energy budget, and such additional components of the Earth system as the vegetative life both on land and in the oceans. These data have enabled the Aqua science teams to successfully accomplish each of the Aqua Mission Success Criteria and proceed far beyond those initial criteria.

With well over 2000 scientific papers now published using Aqua data, any short summary can include only a small sampling of the wealth of scientific output resulting from the Aqua mission. The items highlighted in this article are meant to illustrate the range and value of the Aqua data for science and for practical applications, but much more information can be found on the internet, at *aqua.nasa.gov* and the many links provided there, including to websites for each of the Aqua science teams.

The Aqua spacecraft has enough fuel remaining to last into the early 2020s. At this point, four of Aqua's Earth-observing instruments are still going strong—AIRS, AMSU, CERES, and MODIS—and the hope is that some or even all of them will continue to operate successfully into the next decade.

The hope is also that many of the Aqua datasets will be extended into the future by instruments on other satellites even after the Aqua instruments are no longer operational. For AMSR-E, dataset extensions should come from the Shizuku AMSR2, launched in May 2012. For CERES, dataset extensions can come from the CERES on Suomi NPP, launched in October 2011, and from the CERES planned for eventual launch on JPSS. Many of the MODIS datasets can be extended with data from the Visible Infrared Imaging Radiometer Suite (VIIRS) on Suomi NPP and the VIIRS planned for JPSS; and many of the AIRS/AMSU datasets can be extended with data from the Cross-track Infrared Sounder (CrIS) and Advanced Technology Microwave Sounder (ATMS) on Suomi NPP and the CrIS and ATMS planned for JPSS.

As the currently operating Aqua instruments continue to collect data and instruments on other satellites extend Aqua datasets, the highly successful Aqua mission should continue to have valuable contributions to the advance of Earth system science and practical applications far into the future. ■

As the currently operating Aqua instruments continue to collect data and instruments on other satellites extend Aqua datasets, the highly successful Aqua mission should continue to have valuable contributions to the advance of Earth system science and practical applications far into the future.

feature articles

Tracking Superstorm Sandy from Space

Heather Hanson, NASA's Goddard Space Flight Center/Wyle, heather.h.hanson@nasa.gov

With its fleet of Earth-observing satellites, NASA had an excellent—and unique—vantage point from which to track the progression of what was to become a harrowing storm.

Twenty-four hours a day, seven days a week, NASA's Earth-observing satellite fleet monitors the continuously changing weather on our planet from space. But never in the history of satellite observations has there been a storm so large and intense to make landfall north of Cape Hatteras, NC: *Superstorm Sandy* stretched over 1800 km (1100 mi) and had a minimum pressure of 940 hPa, similarly a record for its landfall location. The rare combination of environmental conditions present during Hurricane Sandy's life cycle led to the development of the storm's unforgettable magnitude—hence, the nickname, "Superstorm Sandy." At landfall, the storm's spiraling bands of rain and wind reached nearly every state in the Mid-Atlantic and Southern New England region. Heavy rains pelted states as far inland as Wisconsin; surging seawater washed away beaches, flooded streets, businesses, homes, even portions of the New York City (NYC) subway system; and raging fires, fueled by tropical storm-force winds, destroyed a significant portion of the Breezy Point neighborhood in Queens, NY. *ABC News* reported that NYC subway officials called this storm the biggest disaster of the subway's 108 years of existence—joining other officials who called this storm the "worst ever."

Even before Sandy reached hurricane strength in the Caribbean, there was a "buzz" on blogs and various weather outlets in the meteorological community that this storm might be "special," and that it might have significant effects on the East Coast of the U.S. as it developed further. The *ensemble* of early models used to forecast Sandy's track varied widely in their projections, so more time would be needed to home in on the details of if, when, and where the storm might hit. Still, forecasters warned that interests from Florida to Maine needed to watch Sandy closely. And NASA scientists were among those watching.

With its fleet of Earth-observing satellites, NASA had an excellent—and unique—vantage point from which to track the progression of what was to become a harrowing storm. We present here a visual chronology of the storm's development and path from its genesis in the Caribbean, to landfall along the U.S. East Coast and beyond.

[Some of the content hereafter has been modified from NASA's Earth Observatory[1] and the NASA Hurricanes/Tropical Cyclones page[2].]

A Storm is Born

Late on Sunday, October 21, 2012, the Tropical Rainfall Measuring Mission (TRMM) spacecraft imaged a cluster of thunderstorms over the warm tropical waters in the western Caribbean Sea—see **Figure 1** (next page). On Monday, October 22, a tropical wave[3] developed a closed circulation, causing the National Oceanic and Atmospheric Administration's (NOAA's) National Hurricane Center (NHC) to issue the first public advisory for what was then called Tropical Depression 18—located approximately 640 km (395 mi) south-southwest of Kingston, Jamaica—at 1100 UTC (7:00 AM EDT). By 2100 UTC (5:00 PM EDT), fed by warm waters and low wind shear, the depression had strengthened into a proper tropical storm. From the start, this storm stood out from the ordinary: Whereas climatology suggests that, on average, two tropical storms develop in the Atlantic basin during October, Tropical Storm Sandy was the fifth.

[1] Extensive coverage of Sandy is available from NASA's Earth Observatory at *go.nasa.gov/XWNqCh*.
[2] NASA's Hurricanes/Tropical Cyclones page can be found at *www.nasa.gov/mission_pages/hurricanes/main*.
[3] The National Hurricane Center defines a tropical wave as a trough or cyclonic curvature maximum in the trade-wind easterlies. The wave may reach maximum amplitude in the lower-middle troposphere.

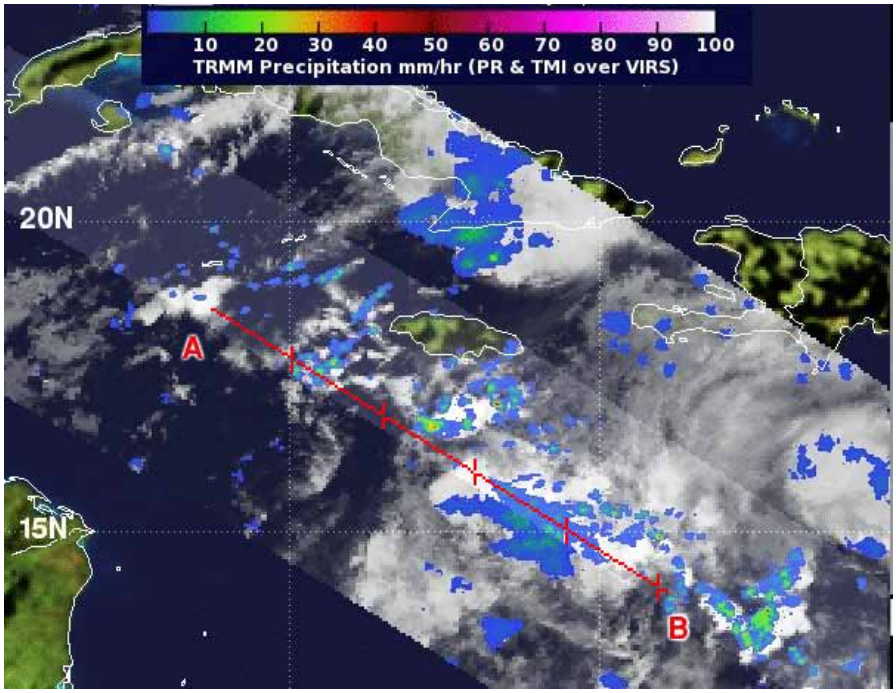

Figure 1. NASA's Tropical Rainfall Measuring Mission (TRMM) satellite flew over the developing storm late on October 21 [*satellite path overlaid on image*] at 0040 UTC (8:40 PM EDT). Measurements from TRMM showed a thunderstorm over 15 km (9.3 mi) high, with regions of heavy rainfall within the low-pressure area. For high resolution image go to: *www.nasa.gov/mission_pages/hurricanes/archives/2012/h2012_Sandy.html#1.* **Credit**: NASA/Science Systems and Applications, Inc. (SSAI)/ **Hal Pierce**

Churning in the Caribbean

On Tuesday, October 23 Tropical Storm Sandy was still hovering over the Caribbean—see **Figure 2**. The NHC reported that Sandy had maximum sustained winds of 85 km/h (50 mi/h), and that the storm was expected to strengthen into a hurricane, making landfall in Jamaica by Wednesday.

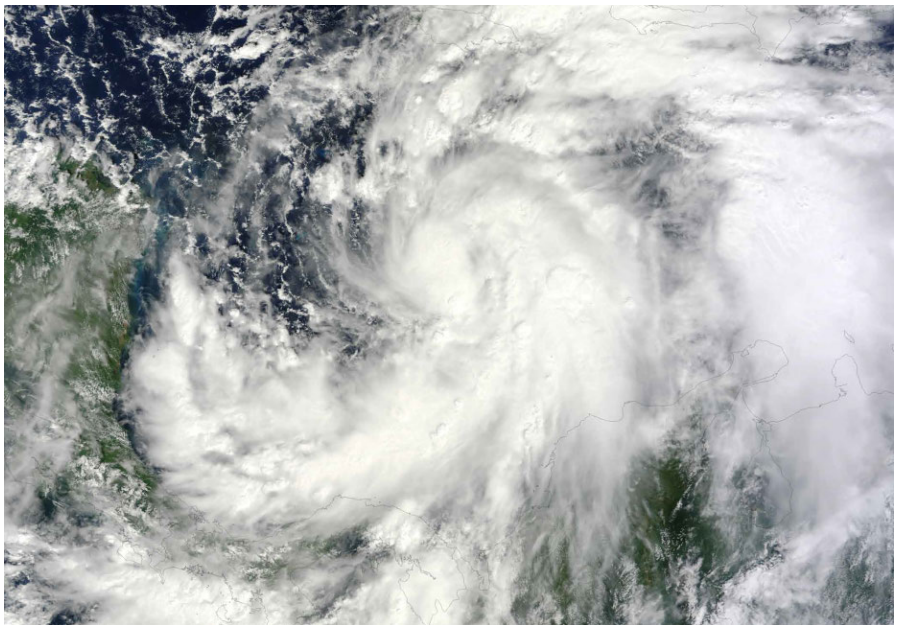

Figure 2. The Moderate Resolution Imaging Spectroradiometer (MODIS) onboard NASA's Terra satellite captured this visible image of Tropical Storm Sandy over the Caribbean Sea on Tuesday, October 23. At that time, Sandy's cloud cover extended outward up to 220 km (140 mi) from the center. For high resolution image go to: *earthobservatory.nasa.gov/NaturalHazards/view.php?id=79503.* **Credit**: NASA's Earth Observatory

Landfall in Jamaica

On Wednesday, October 24 at 1100 UTC (7:00 AM EDT), the NHC reported that Sandy had reached hurricane strength (a Category 1 hurricane on the Saffir-Simpson scale), with maximum sustained winds of 130 km/h (80 mi/h). According to the NHC, Sandy made its first landfall in Southeastern Jamaica at approximately 1900 UTC (3:00 PM EDT), before re-entering the Caribbean and then rapidly intensifying just south of Cuba.

A Growing Threat to the U.S. East Coast

By Thursday, October 25, Sandy had strengthened into a Category 2 hurricane, with maximum sustained winds of 185 km/h (115 mi/h), making landfall just west of Santiago de Cuba at around 0525 UTC (1:25 AM EDT). The storm was moving northward, approaching the central Bahamas—see **Figure 3**. As often happens with tropical systems in the Atlantic, mid-latitude, large-scale weather features would influence its future course.

Figure 3. NASA's Terra MODIS captured this visible image of Hurricane Sandy over the Bahamas on October 25 at 1530 UTC (11:30 AM EDT). Sandy stretched from south Florida to the Bahamas, eastern Cuba, Hispaniola, and western Puerto Rico. For high resolution image go to: *www.nasa.gov/mission_pages/hurricanes/archives/2012/h2012_Sandy.html#5.* **Credit:** NASA/Goddard Space Flight Center/MODIS Rapid Response Team

Specifically, a deepening trough over the Eastern U.S. and a blocking high over the Atlantic, appeared to be narrowing the possibilities for Sandy's movement, and forecasters became increasingly confident that the storm had the potential to become very destructive for the U.S. East Coast. The NHC's five-day forecast showed the storm veering northeastward over the Atlantic Ocean before *retrograding*—making an unusual turn back toward the north-northwest—potentially making landfall around October 30 near the Delmarva Peninsula[4] and the state of New Jersey.

From Tractable Hurricane to Superstorm

After leaving the Bahamas, Sandy weakened to a Category 1 hurricane on Friday, October 26; however, the extent of Sandy's wind field continued to expand, and heavy rains continued to pound the Bahamas and the east coast of Florida—see **Figure 4** (next page). Farther up the coast, the possibility of a dangerous storm surge and tides significantly higher than usual due to a full moon combined to create concerns about potentially devastating impacts leading communities up and down the East Coast to make preparations for Sandy's arrival. By late Friday evening, as the models had consistently predicted, the NHC reported that the storm began to show characteristics of the transition to a *hybrid cyclone*—essentially, becoming a *Nor'easter,* with a hurricane at its core. When the already-powerful storm, loaded with tropical moisture, began to interact with upper-level jet stream energy moving in from the west, the stage was set for explosive storm development.

Speeding Up the Coast

This potential aside, after Sandy transitioned to a hybrid storm on Friday, it was briefly downgraded to a tropical storm. Sandy strengthened into a hurricane again early on Saturday, October 27. Sandy's track speed had doubled over the day[5], and the storm continued to *deepen*—its barometric pressure rapidly dropping—and it became

[4] Parts of Delaware, Maryland, and Virginia make up the Delmarva Peninsula.
[5] The NHC reported that Sandy was moving north-northeast at 11 km/h (7 mi/h) at 0600 UTC (2:00 AM EDT), and by 0300 UTC (11:00 PM EDT), Sandy was moving northeast at 22 km/h (14 mi/h).

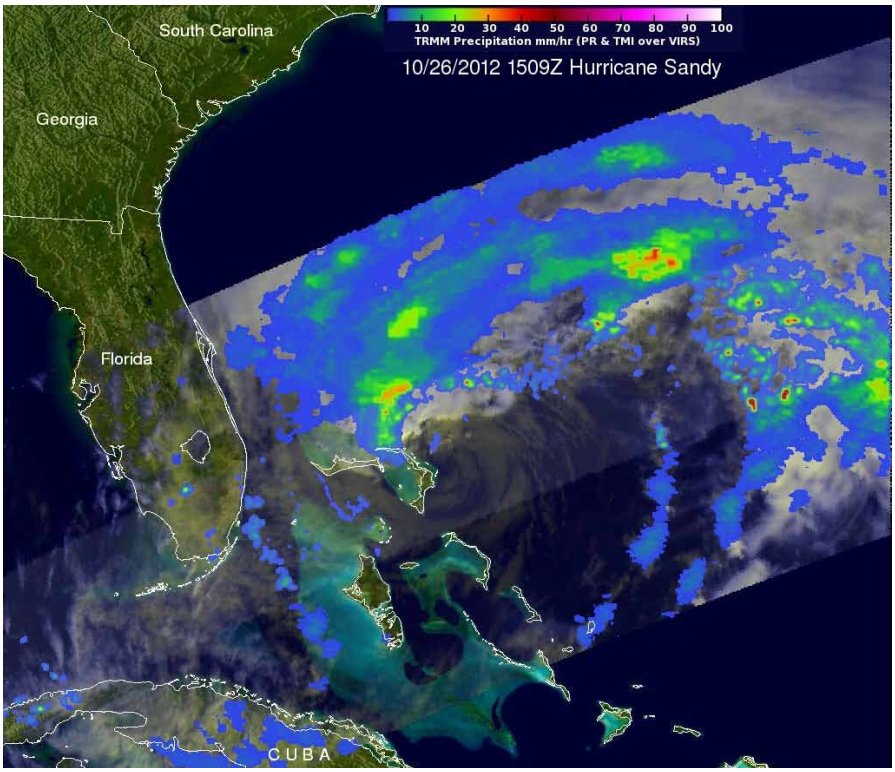

Figure 4. On October 26, at 1509 UTC (11:09 AM EDT), NASA's TRMM satellite saw that rain associated with Hurricane Sandy's storm center was moderate (in green and blue) and falling at a rate of 20–40 mm/h (~0.7–1.5 in/h). The heaviest rainfall at the time of this image was falling northeast of the center at more than 50 mm/h (~2 in/h) (red). For high resolution image go to: *www.nasa.gov/images/content/701077main_20121027_Sandy2-TRMM_full.jpg*. **Credit**: NASA/Science Systems and Applications, Inc. (SSAI)/ **Hal Pierce**

increasingly apparent that significant storm surge, heavy rains, coastal flooding, and tropical-storm-force winds would soon impact Mid-Atlantic states and Southern New England. Components of the Afternoon Constellation[6], or "A-Train"—including CloudSat and Aqua—observed Sandy as they passed over the storm at around 1800 UTC (2:00 PM EDT)—see **Figure 5**.

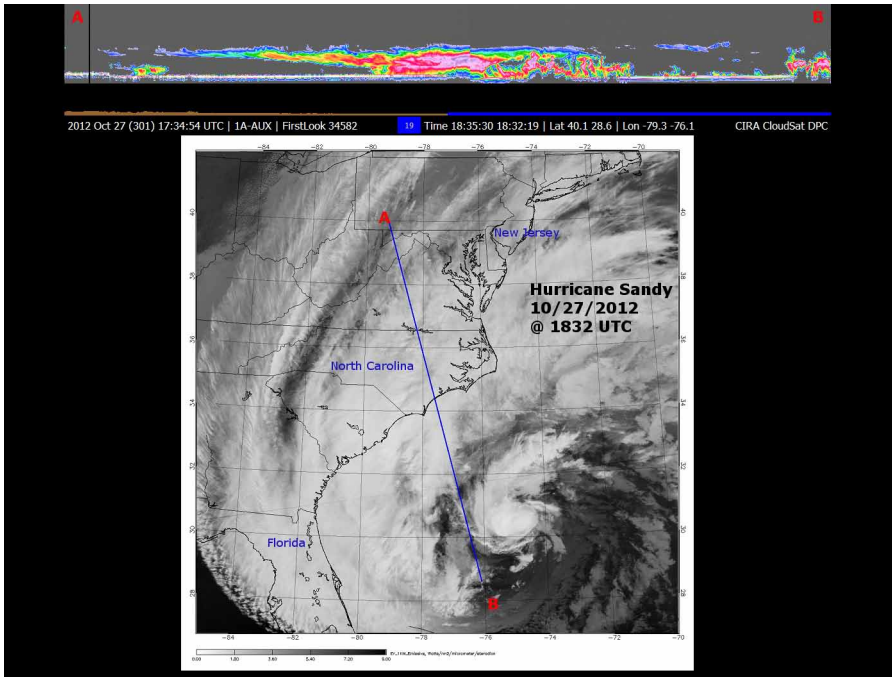

Figure 5. CloudSat [*top image*] observed Hurricane Sandy as it moved up the U.S. East Coast on October 27 and crossed over the warm waters of the Gulf Stream. The image shows a three-dimensional cross section of the storm over the path traveled, from point A to point B [*CloudSat track overlaid on bottom image*]. The brightest white clouds have the coldest cloud tops. The bottom image, from MODIS onboard NASA's Aqua spacecraft, shows an aerial perspective of the storm and the CloudSat overpass. For high resolution image go to: *www.jpl.nasa.gov/news/news.php?release=2012-340#5*. **Credit:** NASA/Jet Propulsion Laboratory-California Institute of Technology

[6] NASA and its international partners operate several Earth-observing satellites that closely follow one after another along the same orbital "track." This coordinated group of satellites, constituting a significant subset of NASA's currently operating major satellite missions, is called the Afternoon Constellation, or the A-Train, for short. For more information about the A-Train, see page 16 of this issue and/or visit: *atrain.nasa.gov*.

Sandy was now a massive storm, with a wind field stretching approximately 800-1125 km (500-700 mi) and projected to affect an area from South Carolina to Maine, and as far inland as the Great Lakes.

Closing In On the Northeast

By Sunday, October 28, Hurricane Sandy's forecast track was coming more and more into focus. Forecasters were unwavering in their prediction that the storm would continue heading north-northeast until the morning of October 29, and then take a hard turn to the northwest, to head into the coastline of Delaware, New Jersey, or New York. Sandy was now a massive storm, with a wind field stretching approximately 800-1125 km (500-700 mi) and projected to affect an area from South Carolina to Maine, and as far inland as the Great Lakes—see **Figures 6-7**. At 1200 UTC (8:00 AM EDT) the NHC reported that Sandy was expected to bring life-threatening storm-surge flooding to the Mid-Atlantic coast, including Long Island Sound and New York Harbor.

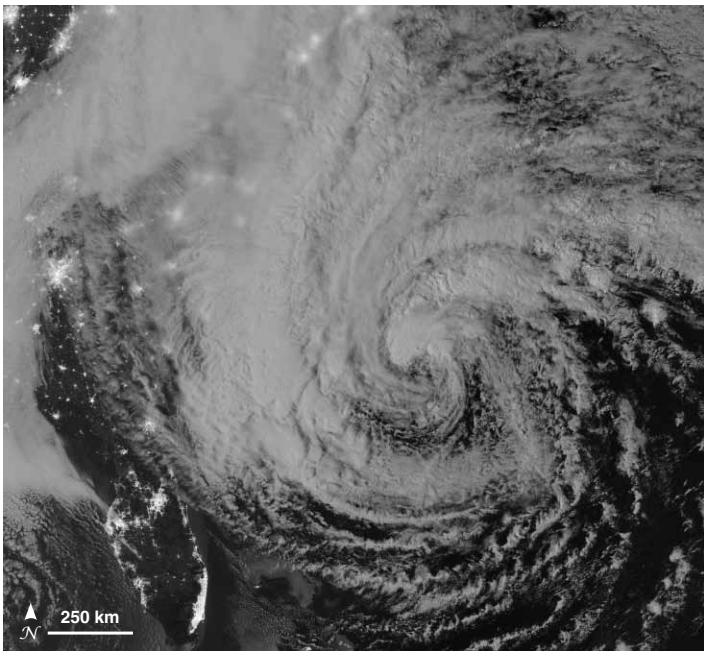

Figure 6. This image of Sandy was acquired by the Suomi NPP Visible Infrared Imager Radiometer Suite (VIIRS) at 0642 UTC (2:42 AM EDT) on October 28. The storm was captured by a special "day-night band," which detects light in a range of wavelengths from green to near infrared. Cloud tops were lit by the nearly full moon, which occurred on October 29. Some city lights in Florida and Georgia are visible through the clouds. At the time this image was acquired, the NHC estimated Sandy's location to be 31.5° N and 73.7° W, 445 km (275 mi) south-southeast of Cape Hatteras, NC, and moving northeast at 22 km/h (14 mi/h). Maximum sustained winds were 120 km/h (75 mi/h), and the minimum central barometric pressure was 960 hPa. For high resolution image go to: *earthobservatory.nasa.gov/NaturalHazards/view.php?id=79545*. **Credit:** NASA's Earth Observatory

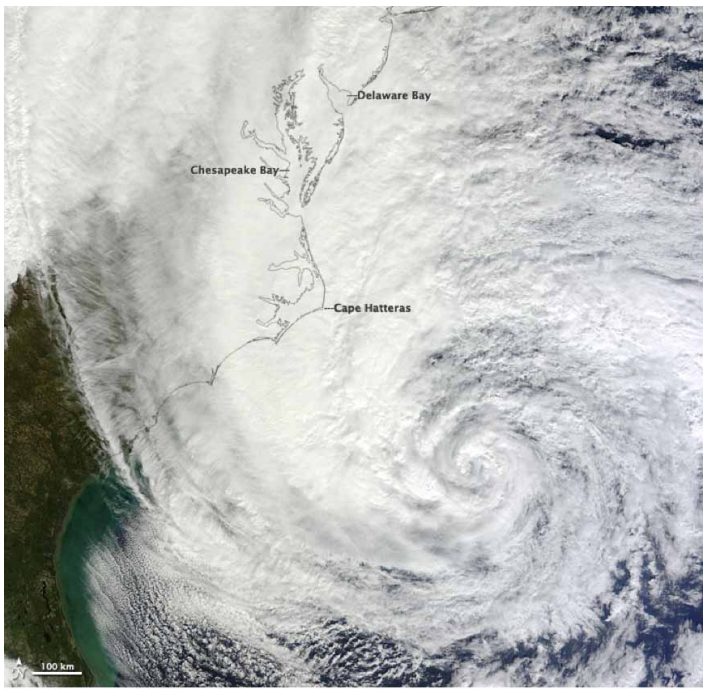

Figure 7. At 1600 UTC (12:00 PM EDT) on October 28, NASA's Terra MODIS acquired this image of Hurricane Sandy off the southeastern U.S. At 11:00 AM local time (one hour before the image was captured), the NHC reported that the storm was located at 32.5° N and 72.6° W, about 400 km (250 mi) southeast of Cape Hatteras, NC, and 930 km (575 mi) south of New York City, NY. Maximum sustained winds were 120 km/h (75 mi/h), and the central pressure was 951 hPa. For high resolution image go to: *earthobservatory.nasa.gov/NaturalHazards/view.php?id=79548*. **Credit**: NASA's Earth Observatory

Landfall in New Jersey

On Monday, October 29, Hurricane Sandy approached the densely populated U.S. East Coast—see **Figures 8-10**. An estimated 60 million Americans were expected to be affected by rain, wind, snow, or ocean surges from the storm. At 1800 UTC (2:00 PM EDT), the NHC reported that Sandy was located about 180 km (110 mi) southeast of

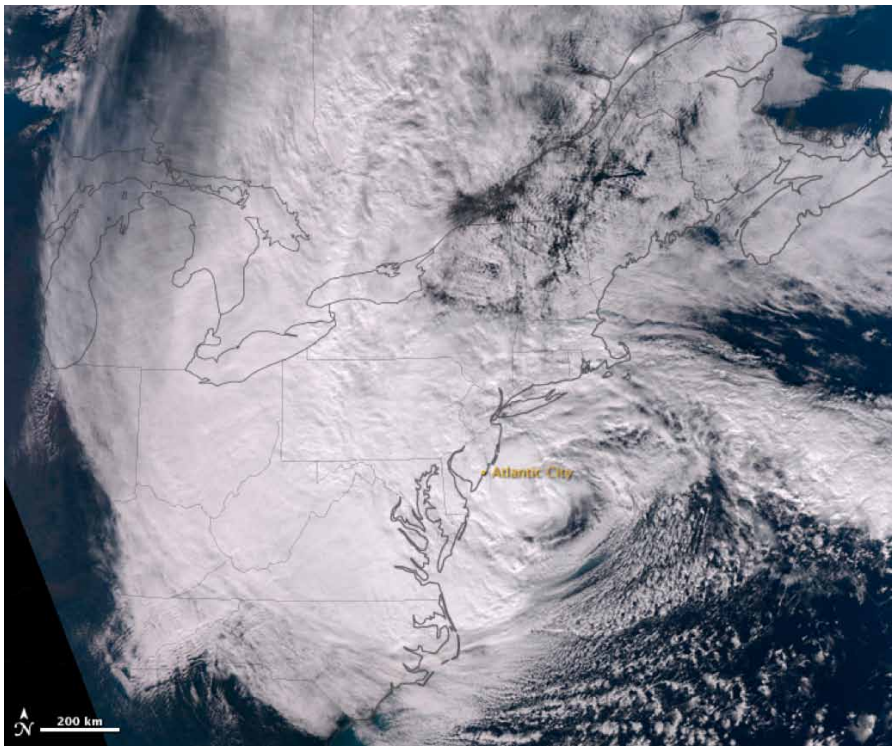

Figure 8. VIIRS onboard Suomi NPP acquired this natural-color image of Sandy at 1735 UTC (1:35 PM EDT) on October 29 as it approached the New Jersey coast. Note the massive cloud shield stretching almost the length of the East Coast, north into Canada, and west to the Great Lakes. For high resolution image go to: *earthobservatory.nasa.gov/NaturalHazards/view.php?id=79556*. **Credit**: NASA's Earth Observatory

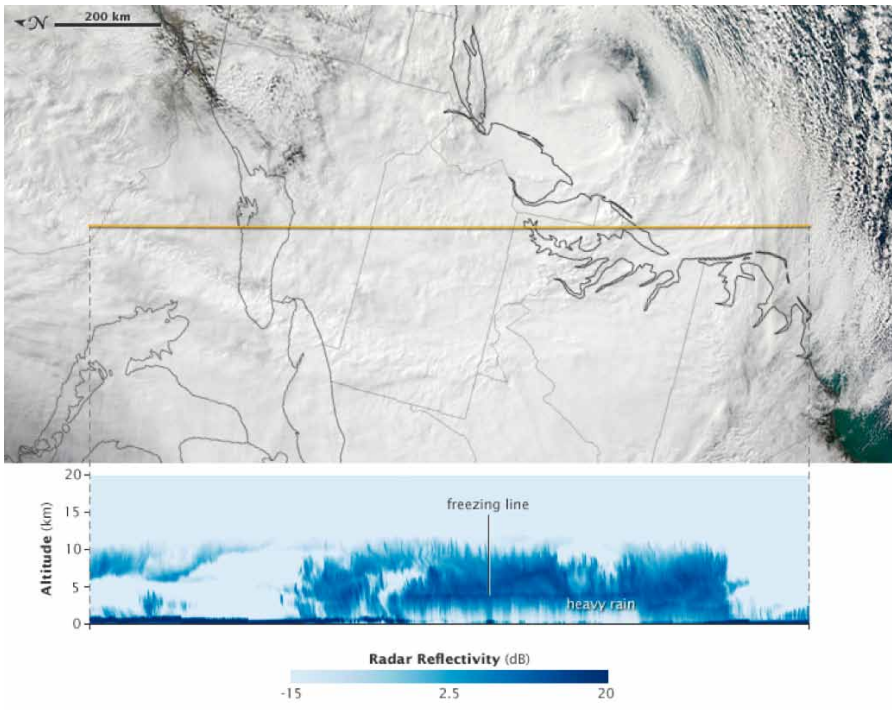

Figure 9. On Monday October 29 at around 1800 UTC (2:00 PM EDT), the Cloud Profiling Radar onboard NASA's CloudSat spacecraft peered inside the storm and observed its vertical structure [*bottom image*]. The image shows a cross section of the storm as viewed from the side. The top image was acquired the same day by the Aqua MODIS. Note that the yellow line is the north-to-south track that CloudSat took over the storm. In the CloudSat data, the darkest blues represent areas where clouds and raindrops reflected the strongest signal back to the satellite radar; these areas had the heaviest precipitation and the largest water droplets. The dark blue line in the center of the bottom image is the freezing line; ice particles formed above it, raindrops below it. Though they look similar from above, the thin clouds on the far left of the image at an altitude between about 6-10 km (4-6 mi) are cirrus clouds, which produced little or no precipitation. For high resolution image go to: *earthobservatory.nasa.gov/NaturalHazards/view.php?id=79577*. **Credit**: NASA's Earth Observatory

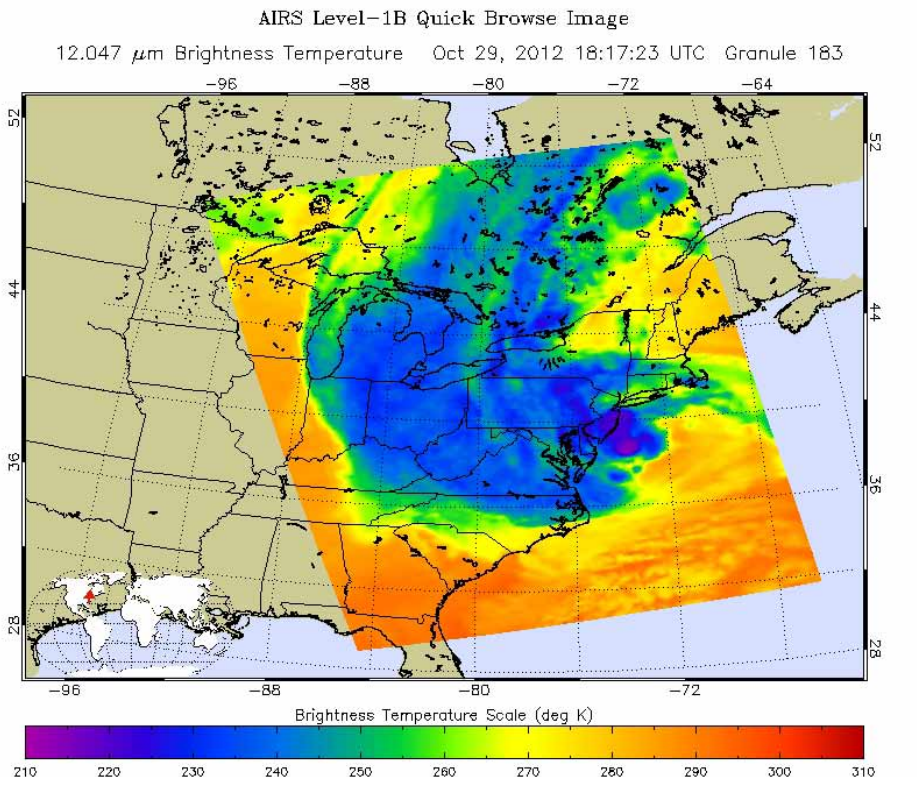

Figure 10. The Atmospheric Infrared Sounder (AIRS) onboard the Aqua spacecraft captured this infrared image of the three elements that converged to form a Superstorm over the East Coat. As Hurricane Sandy approached the coast, another weather front moved in from the west, and cold air was coming down from Canada. The center of the hurricane is the darkest purple area in the Atlantic, just to the east of the New Jersey coast, reflecting areas of Sandy's heaviest rainfall. For high resolution image go to: *www.jpl.nasa.gov/news/news.php?release=2012-340#4.* **Credit:** NASA/Jet Propulsion Laboratory-California Institute of Technology

Atlantic City, NJ, and about 285 km (175 mi) south-southeast of New York City. The storm had maximum sustained winds of 150 km/h (90 mi/h). The storm was moving toward the northwest at about 44 km/h (28 mi/h). At 2300 UTC (7:00 PM EDT), the NHC announced that Sandy had transitioned into a post-tropical cyclone, but cautioned that this would not weaken the storm prior to landfall.

Post-Tropical Cyclone Sandy made landfall near Atlantic City, NJ, at around 0000 UTC (8:00 PM EDT), with maximum sustained winds of 130 km/h (80 mi/h). As the storm came ashore, it continued to pack hurricane-force wind gusts. According to the NHC, the storm surge, combined with astronomical high tides (caused by the full moon), caused storm tide heights of 13.3 ft (~4 m) at Kings Point, NY; 13.8 ft (~4 m) at the Battery in New York; and 13.3 ft (~4 m) at Sandy Hook, NJ. By this time, Sandy had already dropped approximately 20 cm (8 in) of rain, and the mountains of Appalachia were expected to receive up to 1 m (3 ft) of snow.

Aftermath

In the days following landfall, the remnants of Sandy moved inland over Northern New England and Canada before finally dissipating. However, the storm's impacts continued to mount. According to CNN, nearly eight million businesses and homes in 15 states and the District of Columbia were without power by the morning of Tuesday, October 30; the death toll has risen to 175, including at least 106 people in the U.S., 2 in Canada, and 67 in the Caribbean; and initial damage reports were estimated to be upwards of 50 billion dollars.

Sandy's near-hurricane-force winds and powerful storm surge, combined with the full moon, caused most of the damaging floods. Some flooding was also caused by long periods of heavy rainfall that made ditches, rivers, streams, and other water channels and reservoirs overflow their banks. NASA's TRMM satellite gathered data that have now been mapped to show how much rain the storm dropped along the U.S. Eastern

Seaboard. Hurricane Sandy rainfall totals over the Eastern U.S. were calculated[7] for the period from October 24-31. As shown in **Figure 11**, the rainfall analysis indicated that the heaviest rainfall totals were over the open waters of the Atlantic Ocean.

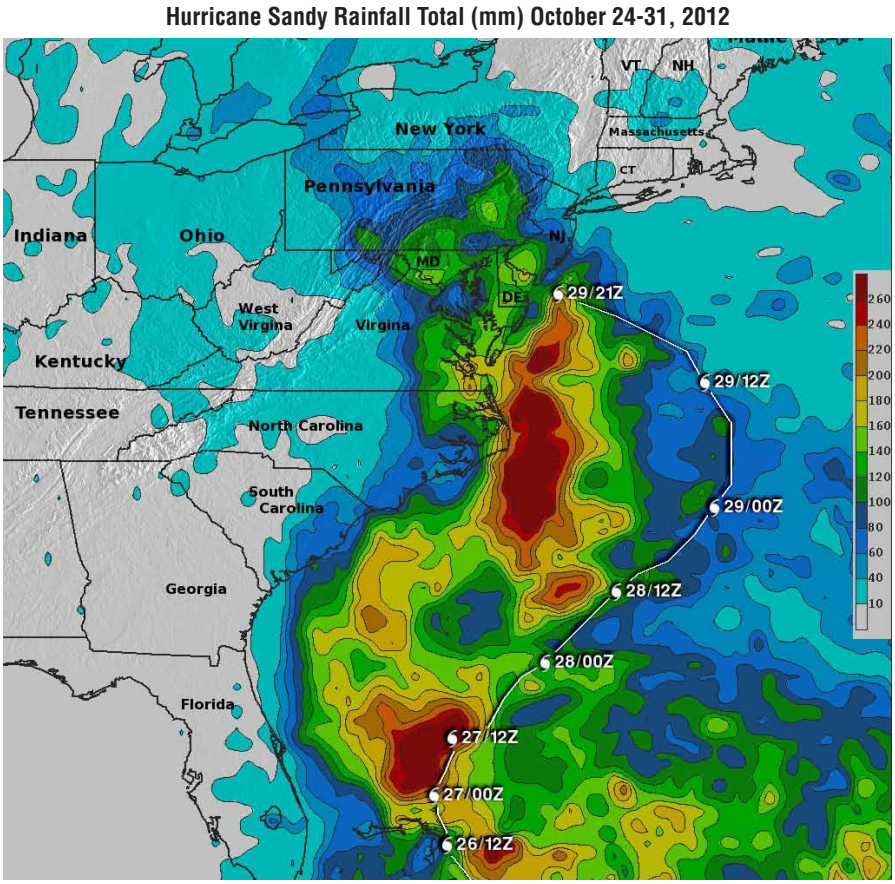

Figure 11. This TRMM rainfall analysis indicates that the heaviest rainfall totals of greater than 260 mm (10.2 in) were over the open waters of the Atlantic Ocean. Rainfall totals of over 180 mm (~ 7 in) are also shown over land in many areas near the Atlantic Coast from New Jersey to South Carolina. Hurricane Sandy's track over the Atlantic Ocean is shown overlaid in white with hurricane symbols on this analysis. For high resolution image go to: *www.nasa.gov/images/content/703387main_20121101_Sandy-TRMMMap_full.jpg* **Credit**: NASA/Science Systems and Applications, Inc. (SSAI)/ **Hal Pierce**

Conclusions

It will take a long time to return to normalcy in the regions hardest hit, but most have already begun their recovery efforts. However, the analysis of this record-breaking "superstorm" will no doubt continue long after the physical damage is repaired. This event was uncharted territory for meteorologists, and the operational forecasting, research, and modeling communities no doubt will learn from this event, and apply that new knowledge to detecting and characterizing future storms. Meanwhile, NASA's current and planned Earth-observing satellites will continue their detailed observation of our home planet, collecting data and transmitting it back for analysis, giving scientists and emergency management personnel the tools to be ready when—not if—the next "big one" hits. ■

[7] Specifically, the TRMM-based, near-real-time Multi-satellite Precipitation Analysis (MPA) monitored rainfall over the area. MPA monitors rainfall from 60° N to 60° S latitude.

feature articles

The NASA-GPM Cold Season Precipitation Experiment (GCPEx)

Walter Petersen, NASA's Goddard Space Flight Center, Wallops Flight Facility, walt.petersen@nasa.gov
Gail Skofronick-Jackson, NASA's Goddard Space Flight Center, gail.s.jackson@nasa.gov
David Hudak, Environment Canada King City, david.hudak@ec.gc.ca

To test and improve GPM snowfall retrieval algorithms, the GPM Cold Season Precipitation Experiment (GCPEx) field campaign was developed as a joint effort between NASA and Environment Canada (EC).

Introduction

Precipitation falling in the form of snow[1] represents a primary contribution to regional atmospheric and terrestrial water budgets, particularly at high latitudes. While often overlooked, falling snow is critically important for society as well as for Earth's climate, geology, and ecosystems. *Snowpacks*—formed from layers of snow that accumulate in a geographic region—store freshwater, and reflect incoming solar radiation, i.e., energy. Snowfall can also have adverse impacts, especially when it occurs in excess over heavily populated areas. For example, blizzards and heavy snow events can cause disruptions in transportation, commerce, and power supply, and virtually paralyze society. As in the case of rainfall, it is not possible or even feasible using only ground-based techniques to adequately quantify the total amount of frozen precipitation occurring at any given time over the entire surface of the Earth. To begin to make this task more tractable, we must rely on spaceborne instrumentation.

Accordingly, NASA and the Japan Aerospace Exploration Agency (JAXA) have initiated the Global Precipitation Measurement (GPM) mission. The GPM mission will expand upon the highly successful Tropical Rainfall Measuring Mission (TRMM) and will provide the next generation of global rain and snow observations every three hours. The GPM concept centers on deploying a *core observatory*, or satellite, that will carry two instruments that improve upon two of those carried by TRMM[2]: the GPM Microwave Imager (GMI) and the Dual-frequency Precipitation Radar (DPR). These instruments will set a new reference standard for precipitation measurement from space. Algorithms applied for precipitation retrievals from these instruments will transform the brightness temperatures (T_B) and radar reflectivities (Z) into three-dimensional precipitation information. The combined radiometer/radar data from the GPM Core Observatory will then serve as a transfer standard to unify precipitation measurements made by an international network of partner satellites to provide near-real-time observations of rain and snow, worldwide. The GPM Core Observatory is scheduled for launch in February 2014.

Improving GPM Algorithms

The GPM radar and radiometer algorithms rely upon ground *validation*—taking measurements on the ground and comparing them with measurements made from the satellite—to develop, improve, and verify the instrument retrievals. With regard to measurements of frozen precipitation, these datasets are required to characterize the ability of multifrequency active and passive microwave sensors to detect and estimate the amount and rate of snowfall.

To test and improve GPM snowfall retrieval algorithms, the GPM Cold Season Precipitation Experiment (GCPEx) field campaign was developed as a joint effort between NASA and Environment Canada (EC). It took place between January 16 and February 29, 2012 (Northern Hemisphere winter), to collect microphysical properties, associated remote sensing observations, and coordinated model simulations of precipitating snow. The GCPEx experiment used an instrumented aircraft—the NASA *DC-8*—for flights over heavily instrumented ground sites located in and

[1] Hereinafter, *falling snow* and *snowfall* will be used interchangeably in reference to precipitating snow.
[2] The instruments on TRMM include the TRMM Microwave Imager (TMI), and Precipitation Radar (PR).

around the EC Centre for Atmospheric Research Experiments (CARE), near Egbert, Ontario in Canada—see **Figure 1**.

The specific science questions addressed by GCPEx were:

- What are the minimum snow rates that can be detected and/or estimated by current satellite precipitation sensors (e.g., TRMM) and the future GPM Core Observatory?
- How well can these sensors discriminate falling snow from rain or clear air?
- Can we develop and/or constrain parameterizations between the physical properties of falling snow particles and their microwave radiative properties?
- What is the impact of variability in these microphysical assumptions and/or parameterizations and those related to macrophysical assumptions (e.g., vertical structure and spatial inhomogeneity) on snow detectability or random errors of retrieved snow rate?
- How do ancillary data—such as surface emissivity, surface temperature, and profiles of temperature, water vapor, and cloud water—help improve detection and estimation performance?
- Do operational model estimates of tropospheric water vapor and temperature fields provide enough fidelity to satisfy GPM snowfall retrieval algorithm needs?
- Can we improve cloud resolving model (CRM) simulations of falling-snow events?

Science Objectives

The GCPEx field campaign expanded upon the successful Canadian CloudSat/Cloud-Aerosol Lidar and Infrared Pathfinder Satellite Observation (CALIPSO) Validation Programme (C3VP), which took place during the 2006-2007 Northern Hemisphere winter season[3]. The primary objectives of GCPEx focused on conducting a complete study of snowfall physics (i.e., sampling from the ground through all levels of the atmosphere) using high-altitude airborne instruments to replicate microwave measurements from the DPR and GMI onboard the GPM Core Observatory. GCPEx

The primary objectives of GCPEx focused on conducting a complete study of snowfall physics (i.e., sampling from the ground through all levels of the atmosphere) using high-altitude airborne instruments to replicate microwave measurements from the DPR and GMI onboard the GPM Core Observatory.

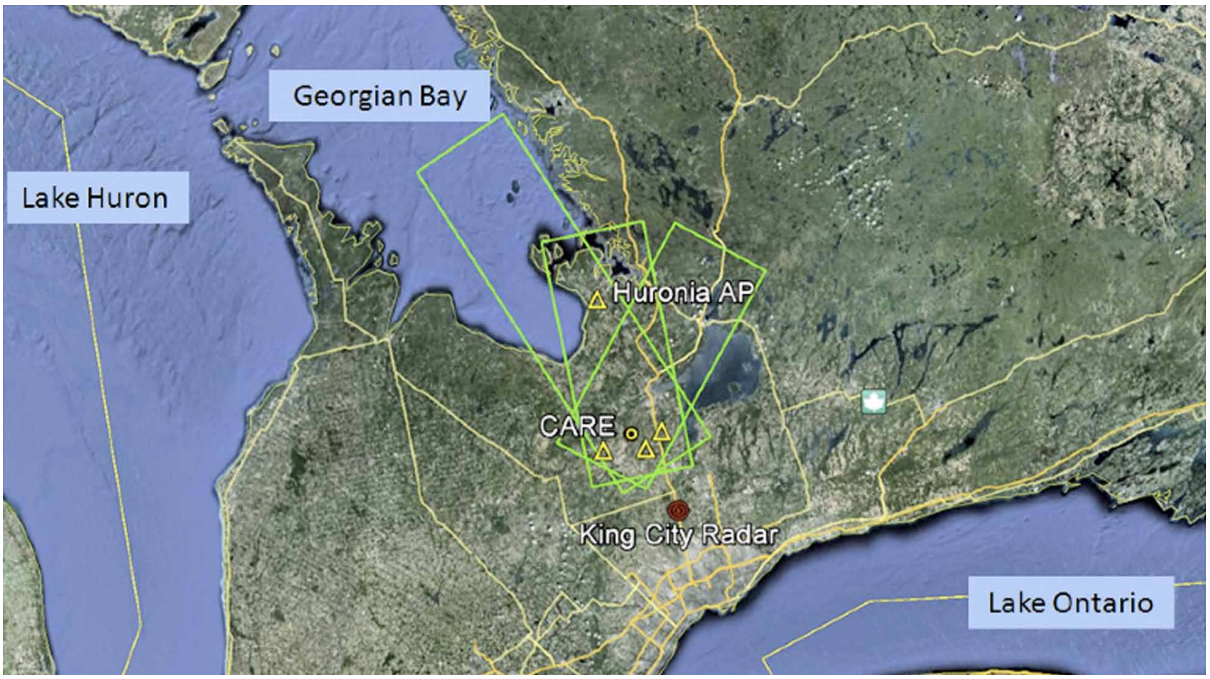

Figure 1. This diagram shows the experiment domain for the GCPEx campaign. The central CARE site with surrounding ground instrument cluster locations, the Huronia lake-effect snow site, and the King City radar are labeled. Green boxes indicate DC-8 operating areas.

[3] For more information on C3VP visit: *c3vp.org* or *pmm.nasa.gov/science/ground-validation/C3VP*.

provided a high-quality, physically consistent, and coherent dataset that supports the critical assumptions at the root of satellite retrieval algorithms well suited to the development and testing of GPM snowfall retrieval algorithm physics.

These objectives also helped address significant areas of weaknesses and/or knowledge gaps in the current GPM snowfall detection and estimation algorithms, including:

- a lack of realistic representation of snow particles, their bulk density, size and shape distributions, and their associated microwave radiative properties;
- a limited understanding of the behavior and mitigation of surface emission on satellite passive microwave (PMW) measurements over multiple temporal scales and surface types;
- a shortage of representative databases for simultaneous active and passive observations linked to a measurement reference;
- the low sensitivity to light-to-moderate snowfall events by passive sensors, and contaminating sensitivity to tropospheric water vapor profiles;
- the ambiguity in reflectivity—snowfall rate and T_B—ice water path (IWP) relationships;
- near-surface clutter contamination for radar observations; and
- the detection and influence of cloud water embedded in snow profiles.

GCPEx provided a high-quality, physically-consistent, and coherent dataset that supports the critical assumptions at the root of satellite retrieval algorithms well suited to the development and testing of GPM snowfall retrieval algorithm physics.

Field Experiment Strategy, Instruments, and Operations

As alluded to above, GCPEx employed a "ground-up/top-down" multiscale observing strategy to address the aforementioned science objectives—see **Figure 2**. The observational strategy involved deployment of the NASA DC-8 aircraft carrying the Conical Scanning Millimeter-wave Imaging Radiometer (CoSMIR) and the Airborne Second Generation Precipitation Radar (APR-2) dual-frequency radar—instruments detailed in **Table 1** (next page). Meanwhile, two *in situ* cloud microphysics aircraft—meaning that they fly at the same level and within the clouds and precipitation—surveyed the lower altitudes: the University of North Dakota's (UND's) Citation and the National Research Council of Canada's (NRC's) Convair-*580*. Instrumentation on each of these aircraft is listed in **Table 2** (next page).

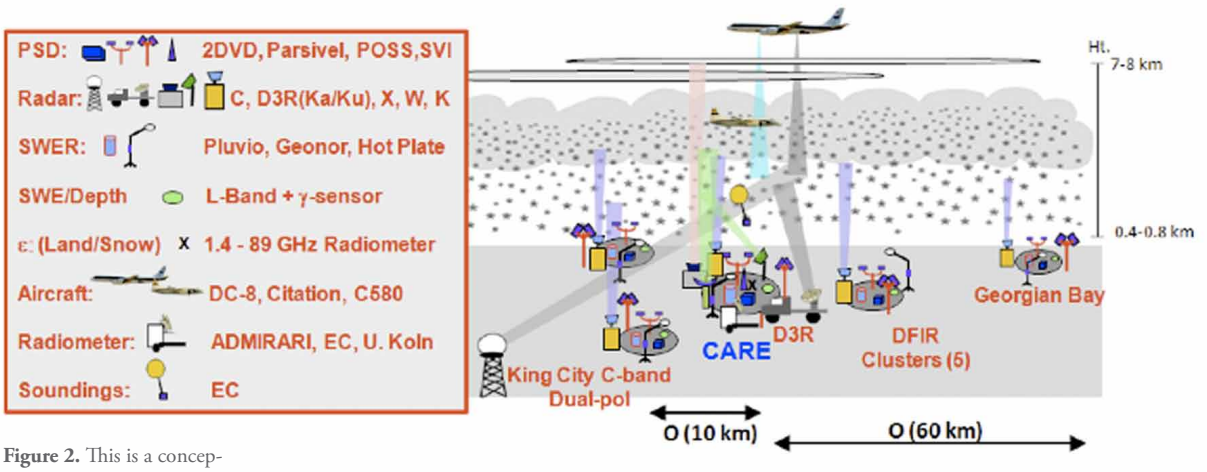

Figure 2. This is a conceptual model of the GCPEx observational strategy with approximate arrangement and approximate geometry of the double-fence international reference (DFIR) ground clusters, King City dual-polarimetric radar, and aircraft are indicated.

While the three aircraft were flying above, five ground-based precipitation *instrument clusters* were busy taking redundant measurements of snow water equivalent (SWE) accumulation/depth; snow particle size, shape, and concentration properties; and radar and radiometer measurements of precipitation vertical profile properties.

Table 1. This table provides details about the CoSMIR radiometer and the APR-2 dual-frequency radar satellite "simulator" instruments onboard the NASA DC-8.

CoSMIR *(Passive)* H+V polarizations	**Characteristics**
Frequencies	50, 52 89, 165.5, 183.3±1, 183.3±3, 183.3±7 GHz
Resolution at 20-km range	1.4-km footprint at nadir
APR-2 *(Active)*	**Characteristics**
Frequency (inner/outer beam)	13.4, 35.6 GHz (HH, HV)
Transmit peak power	200 W (K_u), 100 W (K_a)
3-dB beam width	3.8° K_u, 4.8° K_a
Minimum detectable signal (MDS) (dBZ_e, 6 dB pulse width of 60 m, 10-km range)	+5.0 / +5.0 dBZ_e
Range gate	30 m
Beam swath	±25°

Table 2. This table displays the *in situ* microphysics aircraft instrumentation on the UND Citation and Convair-*580*. Note that atmospheric state parameters—e.g., temperature (T), relative humidity (RH), and pressure (P)—were also collected by the aircraft.

UND Citation Instrument	**Measurement**
King Liquid Water Sensor	Cloud liquid water content (LWC)
Particle Measuring Systems' (PMS) two-dimensional (2D)-Cloud Imaging Probe (C/CIP)	Cloud and precipitation particle spectra
High-volume Precipitation Spectrometer (HVPS)-3	Precipitation particle spectra
Cloud Particle Imager (CPI)	Cloud particle images
Cloud Droplet Probe (CDP)	Cloud droplet spectra
Nevzorov Water Content Probe	Total water content
Rosemount Icing Detector	Supercooled liquid water
Condensation Nuclei (CN) Counter	Aerosol
NRC Convair-*580* Instrument	**Measurement**
King Liquid Water Sensor	Cloud LWC
PMS 2D-C/P	Cloud and precipitation particle spectra
Forward Scattering Spectrometer Probe (FSSP) – SN002/100	Cloud drops (3 – 45 mm)
Optical Array Probe (OAP)-2DG-P (150-um)	Precipitation spectra and shape
Cloud Combination Probe (CCP)	LWC, cloud particle spectra and shape
Cloud Particle Spectrometer with Depolarization (CPSD)	Particle diameter, depolarization, scattering ratio – inference of particle composition and shape
Nevzorov Water Content Probe	Total water content
Rosemount Icing Detector	Icing indicator
NRC Airborne W and X-band (NAWX) Radar (dual-polarimetric)	Cloud structure and dynamics

These clusters were situated within and adjacent to double-fence intercomparison reference[4] (DFIR) enclosures. The cluster instruments are listed in **Table 3**. All ground and airborne data collections were connected over the broader domain by a scanning C-band dual-polarimetric radar, referred to as the EC King City radar (Figure 1). The result of all these observations is a cross section of the atmospheric conditions over the study area, from top to bottom, obtained at a particular time.

Table 3: This table displays the ground instrumentation (# = number of instruments).

Instrument	#	Purpose [Site(s) Deployed]	Provider
C-band Dual Polarimetric Radar	1	Four-dimensional (4-D) precipitation [King City]	Environment Canada (EC)
Dual-Frequency Dual-Polarimetric Doppler Scanning Radar (D3R) K_a/K_u	1	4-D precipitation [CARE]	NASA
W-band vertically pointing radar	1	Cloud/hydrometeor profiles [CARE]	McGill University (U)
X-band vertically pointing radar	1	Hydrometeor profiles [CARE]	McGill U
Micro Rain Radar (MRR) (24.2 GHz)	5	Particle size distribution (PSD) and precipitation profile [1/site]	NASA/EC
Advanced Microwave Radiometer for Rain Identification (ADMIRARI) + MRR (19-37 GHz)	1	Cloud/liquid water retrievals [CARE]	U Bonn/Leicester
Ground-staring Radiometer (1.4, 19, 37, 89 GHz)	1	SWE snow pack [CARE]	EC
Dual Polarimetric Radiometer (89-150 GHz)	1	Scanning/profiling water content [CARE]	U Cologne
2D Video Disdrometer	5	PSD/precip rate/variability [1/site]	NASA
Parsivel Disdrometer	10	PSD/precip Rate/variability [2/site]	NASA
Precipitation Occurrence Sensor System (POSS)	2	PSD/precip rate [CARE, Huronia]	EC
Snow Video Imager	3	PSD/image [CARE, Huronia, Steamshow]	NASA
Snow Camera	1	High resolution imagery [CARE]	U Manitoba
Pluvio-2 Weighing Gauge (200, 400)	9	SWE accum/rate [~2/site]	NASA
TPS 3100 Hot Plate	5	SWE accum/rate [1/site]	NASA
Snow LWE system (L-band + sonic)	5	SWE accum/rate [~1/site]	NASA (Duke U)
Rawinsonde (soundings)	1	T/P/RH profiles [CARE[	EC
Profiling Lidar	1	Backscatter/water vapor [CARE]	EC
Surface Meteorology	5	T/RH/P/winds [1/site]	EC

The DC-8 flies at an altitude of 10 km (~6 mi), a vantage point that provides the closest approximation in this experiment to what the instruments on GPM will actually "see"—i.e., DC-8 instruments will provide a dataset consistent with the viewing angles and radar and radiometer measurements characteristic of the GPM Core Observatory. The DC-8 instruments thus serve as *proxy satellite observations* that can be compared to other measurements. These DC-8 observations of the

[4] An internationally recognized snow gauge sensor enclosure.

integrated column are physically related to the physical processes taking place in the underlying cloud columns—that were sampled by the UND and NRC aircraft—and are subsequently also related to measurements made on the ground via multiparameter radar and network gauge measurements. The ground instrument clusters were chosen to attempt capture of snowfall spatial and regime variability properties in the study area. Four of the five ground instrument clusters were positioned around the CARE site with a spatial separation of 10 km (~6 mi); the fifth site was located ~50 km (~31 mi) to the northwest of CARE, near Huronia and the Georgian Bay (see Figures 1 and 2) to accommodate sampling of more-frequent, heavy lake-effect snow events. The CARE site was also used as a sounding location for collecting tropospheric profiles of temperature, pressure, water vapor, and wind just prior to and after each airborne operation.

While the focus of DC-8 airborne operations was primarily oriented toward sampling falling snow, an effort was also made to collect measurements of land surface emission characteristics during cloud-free days of the experiment. In those *clear-air flights*, the focus was on collecting CoSMIR radiometer views of the land surface under the influence of varying snow and vegetation conditions, to understand—and possibly mitigate—the influence of land-surface emission properties on snowfall retrieval algorithms. In at least one case, clear-air and snowfall cases were sampled along the same flight line on two adjacent days. Accompanying observations from excavated snow pits and ground-based, downward-looking radiometer observations (Table 3) of the snow pack were conducted at the CARE site.

While the focus of DC-8 airborne operations was primarily oriented toward sampling falling snow, an effort was also made to collect measurements of land surface emission characteristics during cloud-free days of the experiment. In those clear-air flights, the focus was on collecting CoSMIR radiometer views of the land surface under the influence of varying snow and vegetation conditions, to understand—and possibly mitigate—the influence of land-surface emission properties on snowfall retrieval algorithms.

The Benefits of Joint Observations

Approximately 25 precipitation events were sampled during GCPEx[5]. The snowfall events ranged from those associated with widespread mid-latitude storm systems to more locally confined bands of light-to-heavy lake-effect snow. Additionally, two clear-air flights were conducted by the DC-8 to sample land surface emission characteristics. In contrast to the heavy snow observed in the area during the winter of 2010-11, during the winter of 2011-12 precipitation—and in particular, snowfall—was below normal in the GCPEx area. In fact, early in the project any significant precipitation amounts invariably involved either rain or mixed precipitation. The middle part of the experiment had generally light snowfall events or lake-effect events that missed the main measurement site at CARE. However, the latter part of the experiment saw a number of significant snowfall events, with liquid-equivalent rates of up to 5 mm/h (0.20 in/h).

A snow event sampled January 30-31, 2012, provides a good example the value of the joint airborne and ground-based observations conducted during GCPEx—see **Figure 3** (next page). A weak upper-level synoptic disturbance moved through the region during that time and caused light-to-moderate snowfall across the sampling domain.

Airborne sampling for this event began at approximately 2330 UTC on January 30, when the UND Citation arrived on station to begin spiral descents/ascents over CARE and its adjacent ground sites. The DC-8 arrived on station at 0000 UTC, at which time coordinated operations between the two aircraft began, and lasted until approximately 0200 UTC. During flight operations the DC-8 maintained its 10-km (~6-mi) altitude while completing both *race track*- and *dogbone*-shaped patterns over the top of the UND Citation, which in turn completed *in situ* profiling spiral descents and straight stepped-flight legs in the vicinity, extending northwest of the CARE site. Additional data were obtained by the D3R radar, which performed an alternating sequence of range-height indicator (RHI) scans along different ground site azimuths and along the aircraft flight legs. In addition, the King City radar completed low-level planned-position indicator (PPI), sector, and RHI scans over the sites. Concurrently, disdrometers, gauges, and profiling radars (W-, K-, and X-band) at the CARE and

[5] A detailed table describing each of these flights can be found at: *pmm.nasa.gov/GCPEx/data-collection-summary*.

surrounding sites collected particle size, type, and fall-speed information (Figure 3). SWE accumulations for this event were light at the CARE site [3.5 mm (0.14 in), liquid-equivalent], and slightly larger in surrounding regions.

Preliminary analysis of the microphysical data indicated the presence of a mixture of snow crystal types including bullets, columns (occasional capped), and branched crystals (plates, dendrites, stellar-dendrites) with occasional evidence of light riming on crystals observed in imagery collected both in cloud and at the ground.

This light-to-moderate snow event and several others like it will enable testing of lower detection thresholds for GPM falling snow retrieval algorithms. Note that only weak T_B depressions were detected in CoSMIR radiometer data (Figure 3).

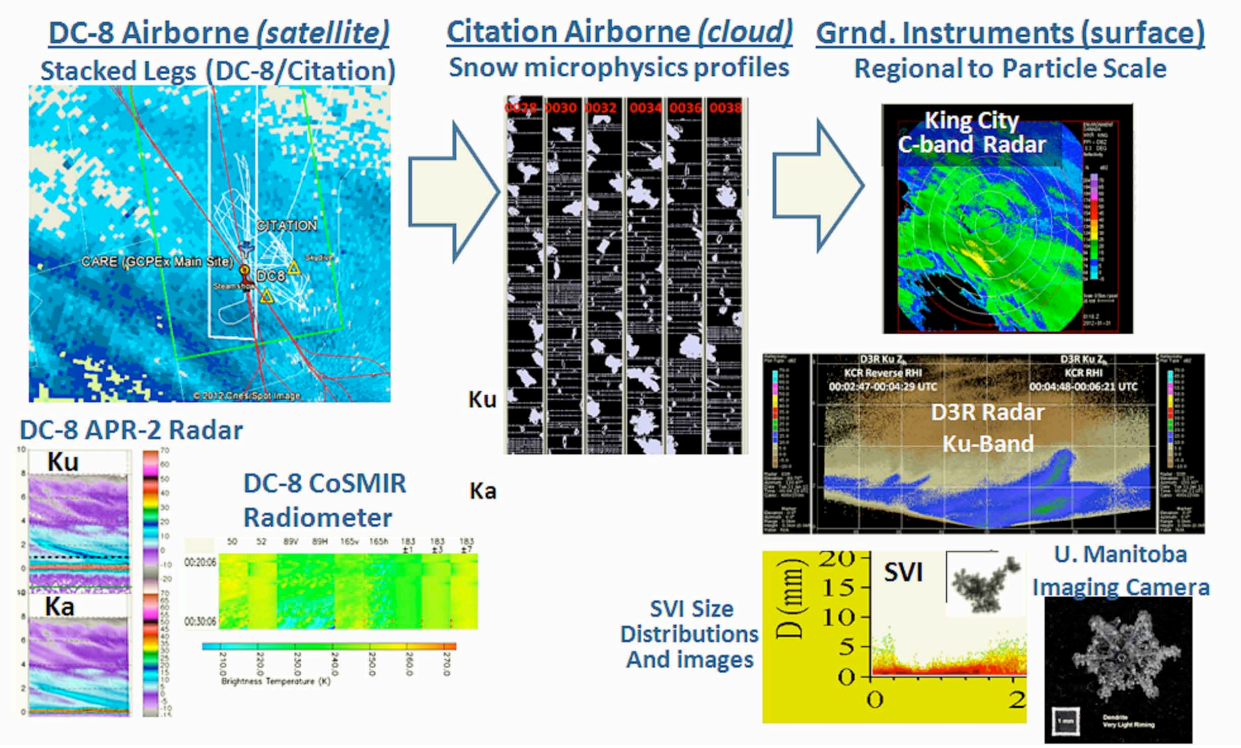

Figure 3. An example of data collection on January 30-31, 2012, illustrating the progression of domain-wide high-altitude and *in situ* sampling provided by aircraft. The images at left show tracks overlaid on radar reflectivity and data from instruments including the APR-2 radar (reflectivity, Z) and CoSMIR radiometer (T_B). The image in the center shows an example of microphysical profiles collected on six different stacked legs. The images on the right show ground-based measurements of C-band radar reflectivity, a cross section of K_u-band reflectivity from the D3R radar, and particle images provided by NASA Snow Video Imager and University of Manitoba Snow Camera.

In contrast to the January 30-31 event, a stronger, longer-duration event was observed on February 24, 2012. Sampling during this event ranged from multi-aircraft, *in situ,* microphysical data collections (two Citation missions, and a Convair-580 mission) coordinated with the DC-8 in light-to-heavy snow, to single-aircraft DC-8 sampling of both heavy snow and mixed-phase precipitation along, over, and to the north of Lake Ontario—see **Figure 4** (next page). Collectively, the February 24 event will provide a case study "bridge" relative to examining GPM algorithm detectability thresholds across a spectrum of snowfall intensities (i.e., light, moderate, and heavy snow events).

Future Analysis Directions

We anticipate that the GCPEx dataset will satisfy the majority of the GPM falling-snow retrieval algorithm validation objectives originally set forth for the experiment. These datasets will be suitable for conducting observational and model-based studies of bulk/particle-scale snow microphysical and scattering properties observed at the ground, through the atmospheric column, and at high altitudes, as observed from the vantage point of remote sensing instrumentation to be deployed on the GPM Core Observatory. A strong emphasis will be placed on characterizing GPM falling-snow algorithm detectability limits for both the GPM DPR and GMI instruments as related to cloud physical processes, intervening cloud environment parameters, and land surface properties.

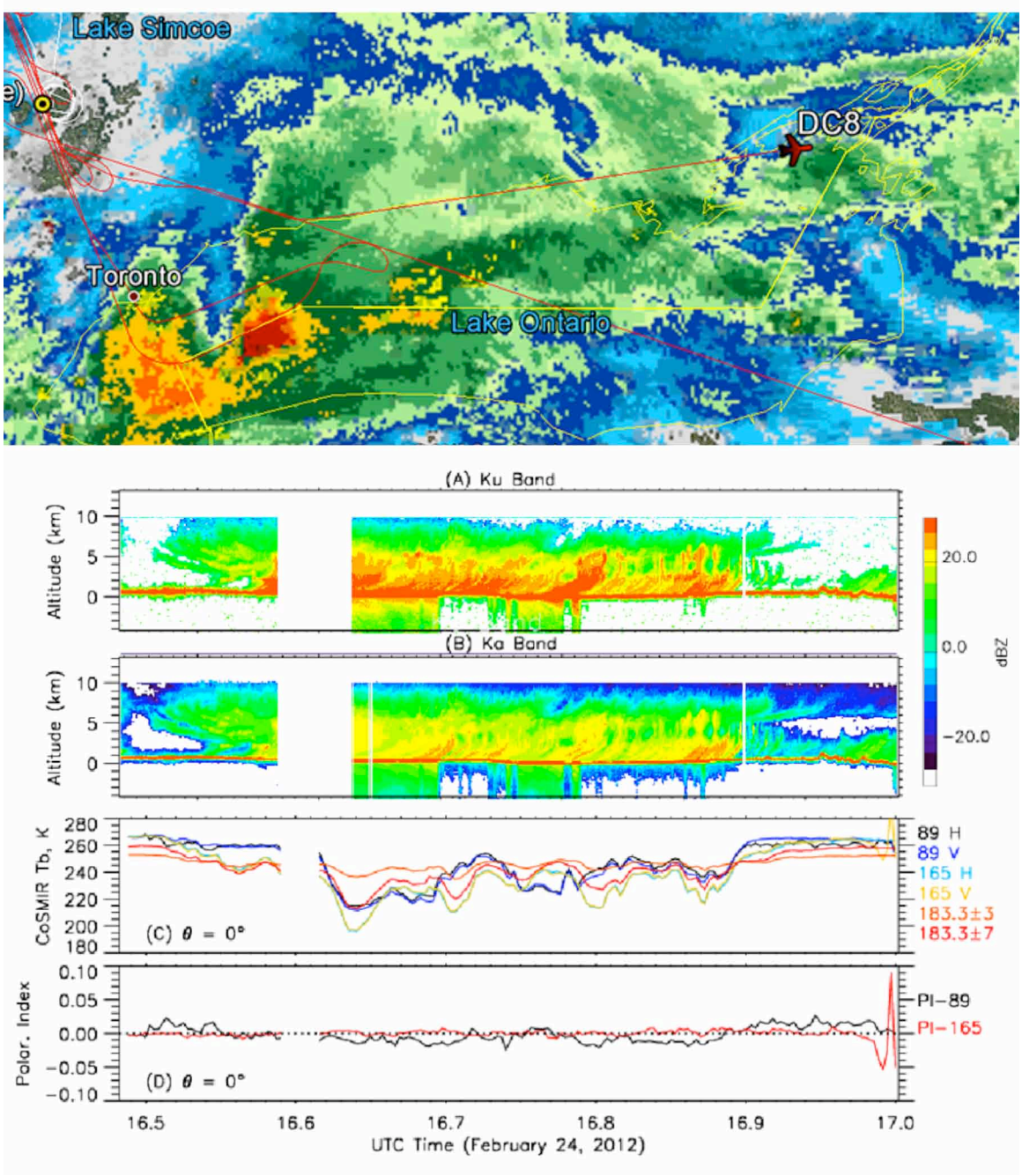

Data quality control and archiving of the complete GCPEx dataset is targeted for December 2012. For information regarding the datasets, please visit the GPM Ground Validation Data Portal for GCPEx at *gpm.nsstc.nasa.gov/gcpex/data.html*. For more information about the GPM Mission and Ground Validation activities please consult the GPM website at *gpm.nasa.gov*.

Acknowledgements: The GPM Flight Project funded airborne and ground based instrument deployments for the NASA component of GCPEx. Environment Canada is gratefully acknowledged for its funding support of Canadian ground-based platforms and its outstanding support for managing the deployment logistics for GCPEx. Funds for the Convair C-580 were provided by the Canadian Space Agency (CSA) and NRC. The CSA and NRC provided funds for the Convair C-580, with in-kind contributions from EC and NASA's Glenn Research Center. ■

Figure 4. Data collected during the February 24, 2012, event. [*Top image*] Plane view of DC-8 patterns and position at 1645 UTC overlaid on composite radar data. [*Bottom image*] The1630-1700 UTC radar reflectivity from the APR-2 radar (K_u and K_a bands), and CoSMIR T_B observations with Polarization Index (PI). The PI is sensitive to the orientation and size of hydrometeors, which impact observed scattering properties. Hence, PI measurements may improve the accuracy of retrieved hydrometeor parameters such as size, shape, and integrated water content.

feature articles

Eyes on the Bay: Using Near-real-time Satellite Data to Monitor the Chesapeake Bay

Diane Davies, Sigma Space/Trigg-Davies Consulting, diane.k.davies@nasa.gov

*In recent years, the health of the Bay has become a subject of great interest and concern, and has been closely monitored using **in situ** sampling methods and modeling.*

The Chesapeake Bay is the largest estuary in the U.S. Its drainage basin covers 64,000 mi^2 (165,759 km^2) of habitat in six states (New York, Pennsylvania, Delaware, Maryland, Virginia, and West Virginia). Over 17 million people live in the Bay's watershed, and the ever-increasing population has had adverse impacts on the health of the land and water[1]. More people generally means more nutrients going to septic systems or wastewater treatment plants; more runoff from roads, driveways, rooftops, and other impervious surfaces; more intensive farming; and more air pollution as people drive farther—and all these "pollution sources" eventually make their way toward the Chesapeake. In recent years, the health of the Bay has become a subject of great interest and concern, and has been closely monitored using *in situ* sampling methods and modeling[2]. Increasingly, satellite data—including near-real-time (NRT) data from the Moderate Resolution Imaging Spectroradiometer (MODIS) on the Terra and Aqua platforms—are being added to the palate of tools that researchers have at their disposal to help them keep tabs on the health of this irreplaceable natural resource.

Mark Trice [Maryland Department of Natural Resources (DNR) Resource Assessment Service] has a keen interest in using satellites to improve monitoring efforts for the Chesapeake Bay. According to Trice, funding cuts are starting to put a squeeze on *in situ* sampling at a time when information from satellites could play an increasingly important monitoring role. He notes that while satellites are not yet officially being used for regulatory decisions (e.g., the Chesapeake Bay TMDL[3]), they do serve as a helpful tool to communicate the geographic distribution of algal blooms and the delivery of sediment to the Bay to a wide audience.

Imagery and data from MODIS are already proving useful at providing the "big picture" of water quality in the Bay. Daily MODIS true-color images, provided by NASA's Land Atmosphere Near-real-time Capability for EOS (LANCE) Rapid Response, and MODIS-derived turbidity, chlorophyll, and suspended matter data products, processed by the National Oceanic and Atmospheric Administration (NOAA) Coast Watch, are routinely posted and accessed by resource managers and the general public through the *Eyes on the Bay* website—*www.eyesonthebay.net*.

According to Trice, "Satellite data provide everyone with the same picture," which is particularly useful when communicating with a broad audience, and especially after large events, such as tropical storms and hurricanes.

In September 2011 the combined effects of Hurricane Irene and Tropical Storm Lee caused large amounts of debris, garbage, sewage, farm runoff, and mud to wash into the Bay. The impact could be clearly seen in the time-series of MODIS true-color images—see **Figure**, next page. Such remote monitoring is useful in the aftermath of storms as it allows a rapid assessment of which areas of the Bay will most likely require intervention. It can also provide information on areas that are too dangerous for boat travel due to the risk of significant floating debris.

[1] According to the *Chesapeake Bay Journal*, impact from watershed's population growth may overtake gains in Bay cleanup. The article can be found at *www.bayjournal.com/article/impact_from_watersheds_population_growth_may_overtake_gains_in_bay_cleanup*.

[2] The September–October 2012 issue of *The Earth Observer* [**Volume 24**, **Issue 4**, pp. 26-32] describes a symposium that took place recently that focused on how modeling efforts are helping to inform assessment and regulatory efforts in the Chesapeake Bay watershed, with particular emphasis on the TMDL implementation described in Footnote 3 below.

[3] The Total Maximum Daily Load (TMDL) prescribes a "pollution diet" for the Chesapeake Bay that seeks to reduce concentrations of nitrogen, phosphorous, and sediment in the watershed by the year 2025—the goal is to achieve 25%, 24%, and 20% reductions, respectively, from their 2010 levels.

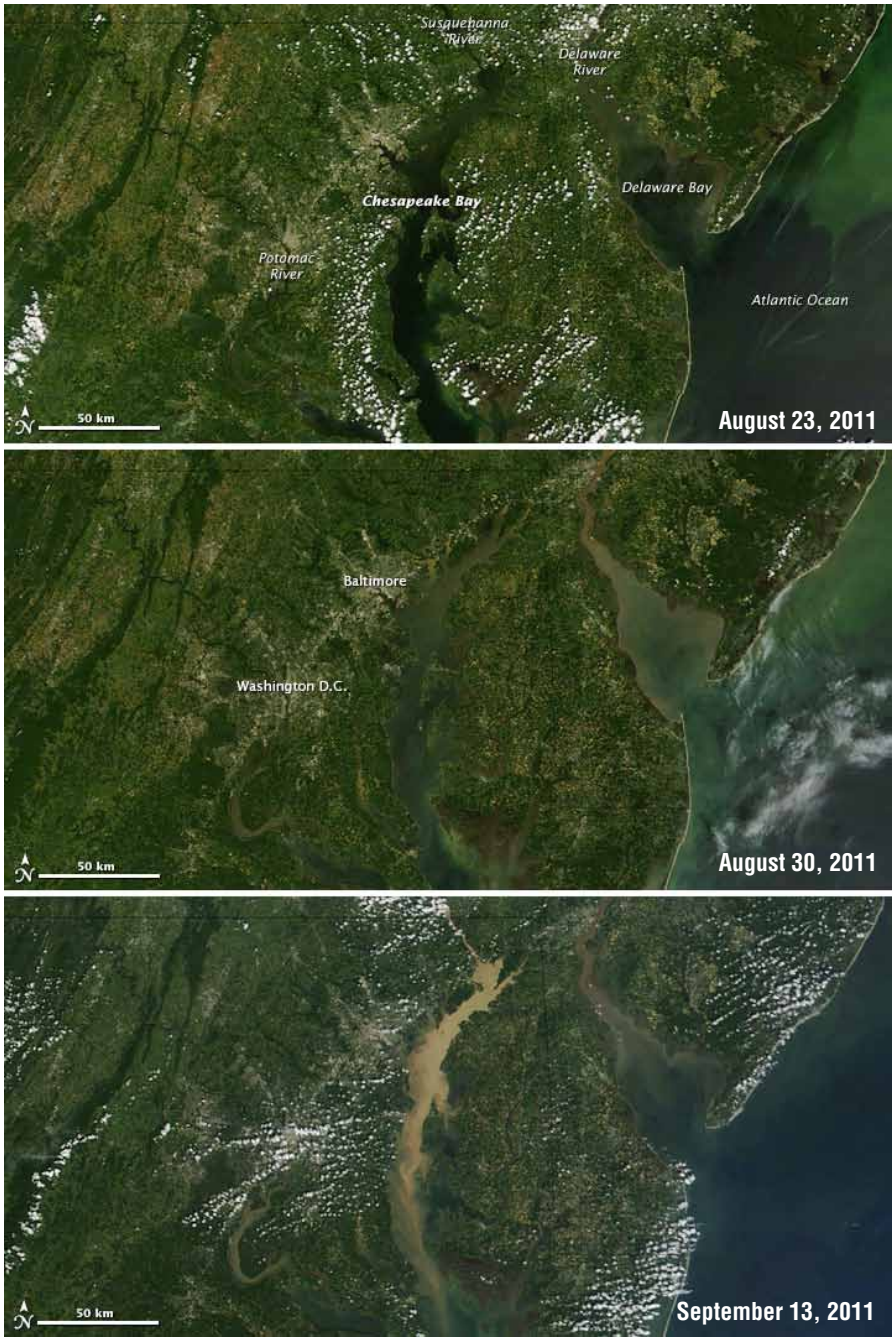

Figure: The images shown here illustrate how water in the Bay turned from dark blue on August 23, 2011 [*top*]—the normal color of the Chesapeake Bay in true-color images—to a turbid mix of blue and shades of brown on August 30, 2011 [*center*] in the wake of Hurricane Irene, and to a muddy tan on September 13, 2011 [*bottom*], in the aftermath of Tropical Storm Lee. The change in color is indicative of the large amounts of surface runoff (sediment) that moved into the Bay during these two events. DNR managers use such images, along with other satellite data, to help determine the extent of runoff events. **Image credit:** NASA's MODIS Rapid Response Team

On October 29-30, 2012, Superstorm Sandy[4] impacted the Bay watershed area; Trice and his team plan to use satellite images to track the sediment impact that almost certainly will follow. In anticipation of these images, officials from the Calvert Cliff Nuclear Power Plant (located on the southern Bay) have already been in contact with the team to find out when the *debris field* created in the aftermath of Sandy should make it downstream from the Susquehanna River. Experience (from Irene, Lee, and other similar events) tells the team to expect to see it two-to-three weeks after the storm. Satellite images will help them pinpoint if and when plant operators need to take further action in order to mitigate damage to plant infrastructure caused by excessive sediment and other debris clogging the plant's water intakes.

continued on page 40

[4] This storm is referred to as a *superstorm* because it was a rare hybrid storm that formed when the core of Hurricane Sandy interacted with upper level dynamics to create a *Nor'easter* that had devastating impact on the U.S. East Coast—including parts of the Chesapeake Watershed. The article on **page 18** of this issue presents a visual chronology of the storm's progress as viewed by NASA's Earth-observing satellites.

meeting/workshop summaries

Summary of the 2012 Quadrennial Ozone Symposium

Ernest Hilsenrath, NASA (retired); University of Maryland Baltimore County, Joint Center for Earth Systems Technology; ADNET Systems, Inc., hilsenrath@umbc.edu

The Quadrennial Ozone Symposium (QOS) took place August 27-31, 2012 in Toronto, Canada with 311 attendees from 31 countries. The 2012 symposium focused on the following themes, which provide an overall scope for the meeting:

- Polar ozone: troposphere and stratosphere;
- tropospheric ozone chemistry and air quality—e.g., trends and long-range transport;
- model calculations and predictions—e.g., dynamics and chemistry coupling;
- ozone-climate interactions;
- detecting ozone; and
- ozone and related constituents: observation accuracies from ground and space.

The highlights from this meeting will be summarized in this article. However the introduction begins with a historical perspective on this quadrennial event as a context for the highlights from the 2012 Symposium that follow.

A Historical Perspective

The first Ozone Symposium was held in 1948, when the International Ozone Commission became part of the International Union of Geodesy and Geophysics (IUGG). The Commission has met every four years since then[1]. At each symposium new findings on stratospheric ozone chemistry and variability have been reported and discussed, based on the most recent model calculations and observations. Along with these topics, attendees engaged in intense discussions aimed at improving ground-based ozone observations, which were coordinated by the World Meteorological Organization (WMO).

At the 1972 QOS in Arosa, Switzerland, historic breakthroughs in atmospheric science began to emerge. These included the first measurements of trace gases involved in ozone chemistry, initial results from the first backscatter ultraviolet (BUV) measurement of ozone from space (measured by NASA's Nimbus-4 satellite), and improved models of ozone photochemistry that included catalytic chains that result in net ozone destruction. These new theories on ozone chemistry led to three Nobel prizes in 1995[2].

It became clear in the early 1970s that Earth's stratospheric ozone layer would be threatened by *anthropogenic* (i.e., human-caused) emissions. Initial concerns were focused on the proposed fleet of commercial supersonic transport (SST) aircraft. The fear was that oxides of nitrogen (NO_x) in the exhaust from these planes would result in ozone depletion in sufficient amounts to be harmful to life on Earth.

In the mid-1980s, both ground-based and NASA satellite measurements detected the Antarctic ozone hole. The consensus from the 1988 QOS, held in Gottinghen, Germany—with 500 attendees from 34 countries—was that "Ozone decline was established as a global phenomenon[1]." By this time, the *WMO/NASA International Ozone Trends Panel Report: 1988*[3] had also released its indisputable evidence that stratospheric ozone was decreasing, resulting from activation of chlorine originating in manufactured CFCs. These findings provided scientific support for strengthening the Montreal Protocol[4] that had been signed just one year earlier. Subsequent reports [e.g., *WMO/United Nations Environment Programme (UNEP) Scientific Assessment of Ozone Depletion: 1989, 1994, 1998, 2002, 2006, 2010*[3]] continued to update knowledge of stratospheric ozone chemistry, based on scientific efforts reported at the QOS and other international forums. The detection and explanation of ozone depletion and subsequent regulation of ozone-depleting substances is acknowledged as an environmental protection triumph. This success was due to cooperative efforts by the international scientific community, policy makers, and industry that developed CFC substitutes.

Subsequent QOS meetings have continued to provide the catalyst for developing more sophisticated chemical-dynamical-climate models for improving observations from the ground and satellites, and for expanding research to examine the impact of ozone in

[1]A summary of Commission activities has been written: *International Ozone Commission: History and Activities*, compiled by **R.D. Bojkov**, International Association of Meteorology and Atmospheric Sciences, 2012, Publication Series No. 2.

[2]The Nobel Prize in Chemistry 1995 was awarded jointly to **Paul J. Crutzen**, **Mario J. Molina**, and **F. Sherwood Rowland** "…for their work in atmospheric chemistry, particularly concerning the formation and decomposition of ozone." For more information, visit: *www.nobelprize.org/nobel_prizes/chemistry/laureates/1995.*

[3]For more information on how to find this report, visit: *www.wmo.int/pages/prog/arep/gaw/ozone_reports.html.*

[4]The original Montreal Protocol, signed in 1987, was the first step in international efforts to protect stratospheric ozone. Since that time, the Montreal Protocol has been repeatedly strengthened by both controlling additional ozone-depleting substances (ODS) as well as by moving up the date by which already-controlled substances must be phased out.

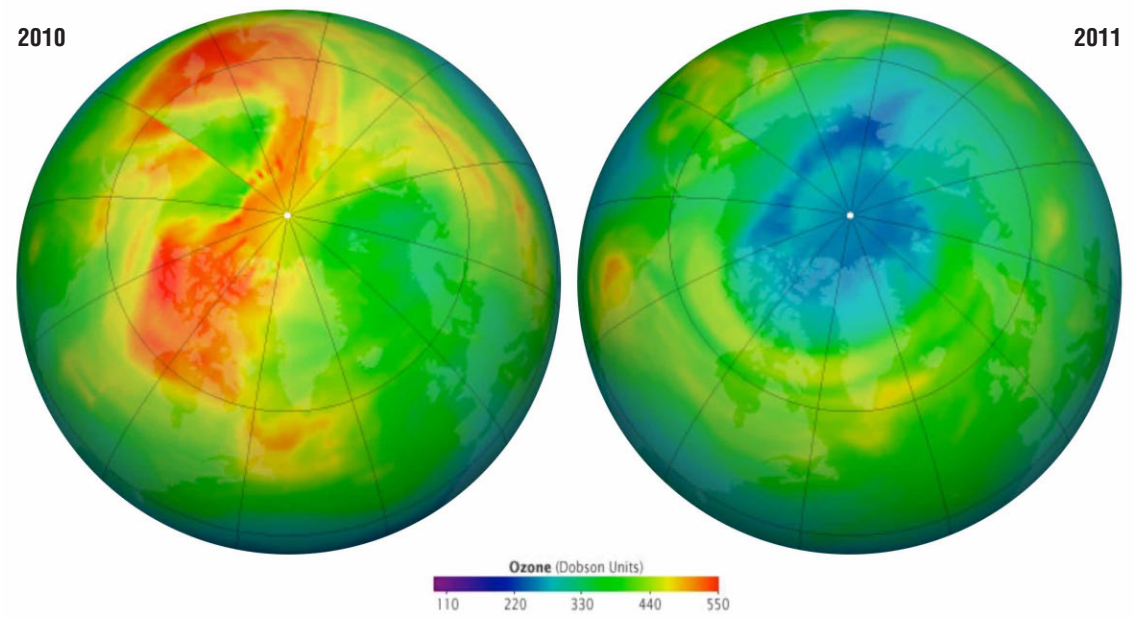

Figure 1. This figure shows the deep ozone depletion (purples and blues) that occurred over the Arctic during the 2011 Northern Hemisphere winter/spring seasons [*right*] compared to the same period in 2010 [*left*]. The colors indicate the column ozone levels from near the surface to the top of the atmosphere. The 2010 ozone levels are typical for the Arctic for this time of year. **Image credit**: NASA's Earth Observatory

the troposphere, including the *planetary boundary layer* (PBL)[5], where air quality is a concern since ozone is the foremost pollutant in this layer. In addition, ozone has a strong climate connection, in that it is also a greenhouse gas in both the troposphere and stratosphere, and thus affects the Earth's radiative balance throughout the atmosphere.

Present Findings and Topics

Given limited space for this report, only a few examples of key findings from the 2012 Symposium can be summarized here, but those chosen encompass the themes outlined in the article's introduction. The oral and poster programs, abstracts, and presentations can be found on the symposium website at *www.cmos.ca/QOS2012*. Click on *Scientific Program* under *Conference Information* on the left.

The 2011 Arctic Ozone Depletion Event and the Antarctic Ozone Hole

During Northern Hemisphere's 2011 early spring, ground, balloon, and satellite measurements detected a surprising stratospheric ozone loss over the Arctic. Losses of similar magnitude occur every year in the Antarctic, resulting in formation of the now-familiar "ozone hole" during the Southern Hemisphere spring. However, owing to differences in meteorological conditions, the ozone depletion that occurs in the Arctic is not as regular or as prominent as that which takes place in the Antarctic.

The 2011 winter was unusually cold in the Arctic stratosphere. While the temperatures were not as cold as those observed in the Antarctic, the abnormally cold conditions persisted for longer than normal, which allowed polar stratospheric clouds (PSCs) to form for longer than they typically do. These upper-level clouds are known to play a key role in facilitating the chemical reactions that destroy ozone, as halogens (primarily chlorine), which arise at ground level and travel throughout the stratosphere, can more easily become activated in the presence of PSCs.

The magnitude of the 2011 ozone depletion event was the largest ever observed for the Arctic. Activated chlorine in the Arctic catalytically destroyed ozone in amounts comparable to Antarctic ozone hole events. Ozone depletion, from the low temperatures, was further exacerbated by reduction of *meridional*—south to north—transport of ozone that normally occurs in Northern Hemisphere winter/spring, while lacking in the Southern Hemisphere. The tendency in the Arctic for lower and persistent temperature in the stratosphere is also one of the signatures of "global warming."

Shown in **Figure 1** is a comparison of the Arctic ozone loss in 2011 to that observed in 2010. The measured ozone loss in the Arctic in 2011, as reported by several authors using ground and satellite data, was on the order of 50%—a slightly smaller percentage than that which occurs in the Antarctic. Measurements of ozone profiles showed losses to be concentrated in a narrow range in the middle stratosphere—an altitude similar

[5]The *planetary boundary layer (*PBL) is the lowest region of the atmosphere, whose thickness from the Earth's surface is a few hundred meters (several hundred feet,) and which is directly influenced by the Earth surface. The top of the PBL is often accompanied by a temperature inversion.

to that for Antarctic ozone hole events. Chemistry-dynamic model calculations, using March 2011 meteorology conditions, found Arctic ozone column loss ranging from 40–50%. Some authors found a connection of this event with solar-cycle activity and with the state of that year's El Niño/Southern Oscillation (ENSO) phenomena. The ozone-depleted stratospheric air reached densely populated areas in central Siberia and Asia. Ground level ultraviolet radiation resulting from reduced ozone reached amounts typical of summer, when seasonal ozone levels are at their lowest.

The Arctic stratospheric winters have been getting colder over the past decades, increasing the chances of PSC formation. This raises concerns that Arctic ozone depletion may further intensify over the coming decades if the climate continues to warm near the surface and consequent stratospheric cooling continues. Model simulations of the 2011-2012 winter presented at the symposium showed that cooling of the Arctic lower stratosphere could offset the reductions in halogen loading that result from adherence to the Montreal Protocol, thereby inhibiting ozone recovery in polar regions[6].

Tracking the Hole at the Other Pole…

Although the 2011 Arctic event was a featured topic of the symposium, the annual Antarctic ozone hole also received considerable attention. Most importantly was the refinement of chemical and dynamic factors used for model predictions and the "watch out" for turnaround—i.e., the beginnings of predicted ozone recovery. Model predictions continue to show recovery occurring well beyond 2060, depending on the impact of climate changes. No clear signs of an Antarctic ozone hole recovery have yet occurred, although the "hole" is not increasing in size.

Tropospheric Ozone and Air Quality

While ozone in the stratosphere shields us from harmful effects of ultraviolet radiation, in the PBL, ozone is a pollutant in the lower atmosphere, and has a direct impact on air quality. In the upper troposphere, ozone is a greenhouse gas and an indicator of the transport between the troposphere and stratosphere—where most of the Earth's ozone layer resides. Therefore, tracking ozone in the troposphere is important to both air quality and climate. Space observations of ozone and associated photochemically active gases continue to be a challenge because of their small quantities (ranging from parts per billion (ppb) to a few parts per million (ppm) and the spectroscopic complexity introduced by the surface, other absorbing gases, and the solar spectrum.

Although satellite data in the troposphere are difficult to interpret, there is a growing ability to track air quality on city and regional scales. An attention-grabbing example of satellite-measured air quality appeared in a poster paper that summarized several aspects of tropospheric chemistry, and showed the change in the amount and distribution of nitrogen dioxide (NO_2) over the I-95 corridor from Washington, DC, to New York City, NY, decreasing over the period from 2005 to 2010—see **Figure 2** (next page). NO_2 is an ozone *precursor*—meaning it is one of the atmospheric species linked to photochemical ozone production. The image also depicts other ozone "hotspots," such as Atlanta, GA, Pittsburgh, PA, Buffalo, NY, Boston, MA, and others, that also show decreasing amounts of pollution. These data have been qualitatively confirmed by observations from local ground-based instruments and the European Envisat satellite. While several papers confirmed decreasing pollution in the U.S. and parts of Europe, others provided reports of increasing pollution over industrial areas in Asia.

Another highly relevant and timely example of ground-based air quality measurements was a paper dealing with ozone pollution in Wyoming, resulting from *fracking*[7] to extract natural gas. Ozone is produced by complex chemical reactions of natural gas and other hydrocarbons released from the rock during fracking in the presence of sunlight. In this case, the site was snow covered, which may have further triggered the photochemical process from the reflected sunlight. The amount of ozone pollution was measured to be 166 ppb—which exceeds the 2008 EPA noncompliance levels by more than a factor of two. It is noteworthy that this occurrence was in a pristine location, away from any urban pollution sources.

Global Ozone Trends

The 1987 Montreal Protocol and its subsequent amendments placed limits on CFCs; subsequent production was phased out. Since then, CFC levels have been monitored from the ground, while halogens and other compounds active in ozone chemistry are being

[6]Further discussion of the Arctic ozone depletion event can be found on the NASA/Jet Propulsion Laboratory news site at *www.jpl.nasa.gov/news/news.php?release=2011-308* and the NASA Earth Observatory website at *earthobservatory.nasa.gov/IOTD/view.php?id=49874*.

[7] The term *fracking* comes from *hydraulic fracturing*, which is a method to release oil and gas from rocks deep beneath the surface with high-pressure liquids, using mostly water with various unspecified fluids. Once the rock layer is fractured, the released natural gas is captured and then collected and added to existing pipelines.

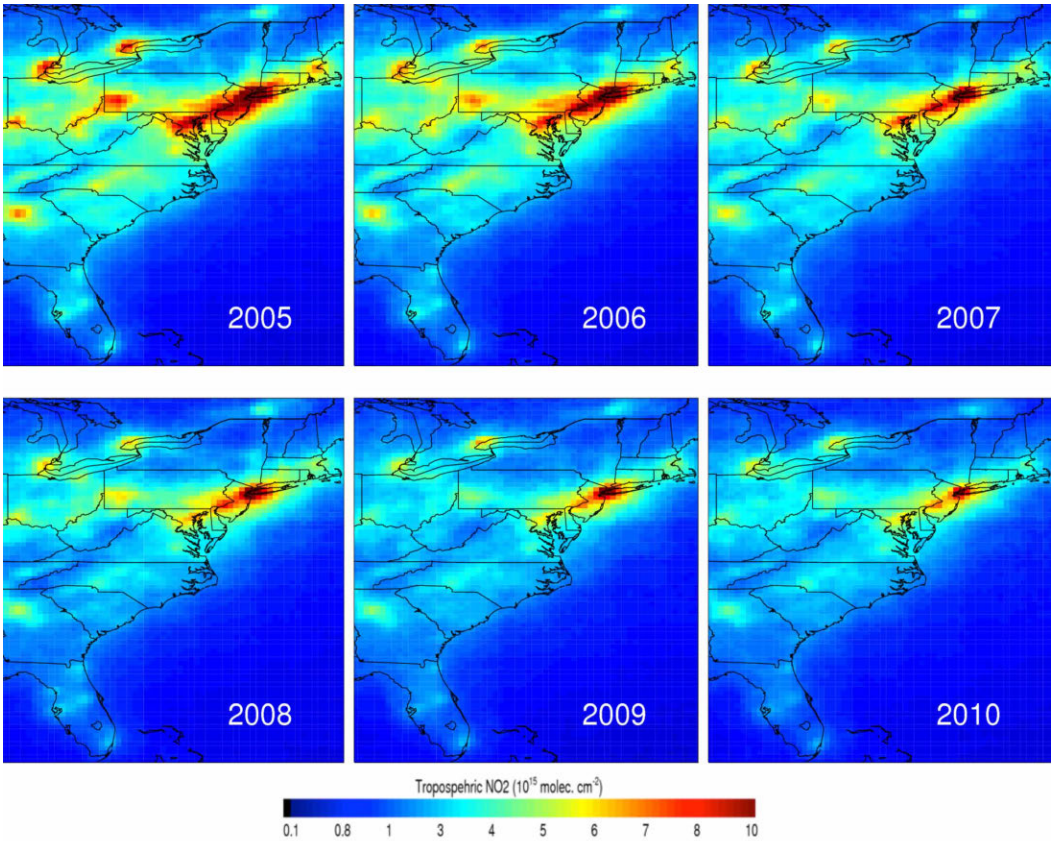

Figure 2. This figure shows data derived from the Ozone Monitoring Instrument onboard the Aura satellite, which has been mapping ozone since 2004. The instrument is also capable of measuring certain species related to air quality in the troposphere. The sequence of observations shows column amounts of nitrogen dioxide (NO_2) in the lower troposphere from 2005 to 2010. NO_2 is a precursor to tropospheric ozone, with levels that range from a few parts per billion (ppb) to over 100 ppb, depending on the pollution source, time of day, and meteorological conditions. The image shows a clear decrease in the amount of pollution over the time period for the I-95 corridor and cities in the Northeastern United States. **Image credit**: Presented by **Ross Salawitch** [University of Maryland College Park Earth System Science Interdisciplinary Center] at the 2012 QOS; **Lok Nath Lamsal** [USRA] created the image.

monitored by satellites and some ground stations. These measurements have shown a steady decline in CFCs at the ground and in the stratosphere, while models predict ozone recovery to pre-1980 levels by about the middle of the twenty-first century. However, the meticulous development of accurate ozone datasets to monitor ozone recovery has recently revealed surprising results. Two papers using satellite data have shown that global average ozone may have already recovered to near pre-1980 levels when the 11-year solar cycle component of ozone production and loss is accounted for—see **Figure 3** as an example. Careful analysis of ground-based data also shows similar signs of ozone recovery, beginning about 2000. Recovery appears differently in the Northern and Southern Hemispheres because of different transport mechanisms in the two hemispheres. Chemistry-climate model calculations are beginning to predict earlier recovery because of more-accurate description of climate change (e.g., tropospheric heating with stratospheric cooling), which in turn affects planetary-scale atmospheric circulation, and therefore the rate of ozone recovery.

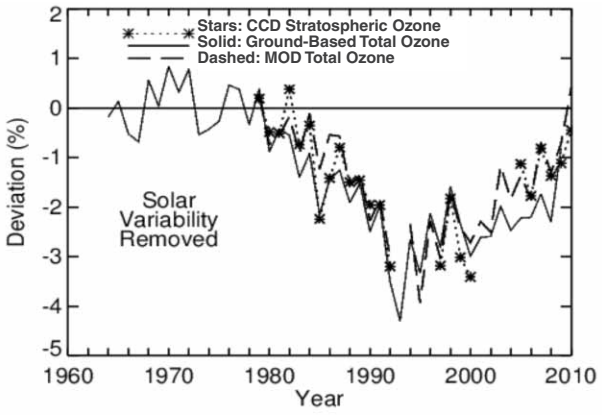

Figure 3. Deviations from a 1970–1980 baseline column ozone from 60° S to 60° N latitude; annual mean time series of Total Ozone Mapping Spectrometer (TOMS) + Ozone Monitoring Instrument (OMI) Convective Cloud Differential (CCD) stratospheric column amounts (stars and dashed line), time series from selected ground-based stations (solid line), and annual mean time series of total column ozone from the GSFC Merged Ozone Dataset (dashed line). The 11-year solar cycle signal has been removed by linear regression. A three-year running average was applied to both time series for smoothing. **Image credit**: Presented by **Jerry Ziemke** [GESTAR] at the 2012 QOS.

A New and Improved Standard for Ozone Measurements

New spectroscopic data for ozone ultraviolet cross sections have now been nearly universally accepted by the ozone science community. The Absorption Cross Sections of Ozone (ACSO)[1] effort was guided by the WMO with an overall result of better internal measurement consistency and improved intercomparability amongst all the NASA, NOAA, and European Space Agency satellite instruments, as well as comparability with ground-based measurements. Nearly all ozone instruments employing ultraviolet absorption, on the ground and in space, have been reprocessed using these new data.

[1] For more information about ACSO, visit: *igaco-o3.fmi.fi/ACSO/index.html*.

Space and Ground Observations

Until now, space-based observations have reasonably characterized the composition of Earth's atmosphere. In addition to NASA's Aura mission and several National Oceanic and Atmospheric Administration (NOAA) satellites, Europe and Canada have been providing collaborative data with their own missions. But some of these missions have either ended (e.g., Envisat) or have well exceeded their lifetimes. Potential gaps are looming, but the good news is that a few highly anticipated instruments were recently launched into orbit. Some of the initial results from these missions were presented at the QOS.

The newest instruments reported on were the:

- Ozone Mapper Profiler Suite (OMPS) on the Suomi National Polar-orbiting Partnership (NPP) satellite (launched in 2011);
- Superconducting Submillimeter-Wave Limb-Emission Sounder (SMILES), a Japanese instrument on the International Space Station (launched in 2009, but no longer operating); and
- Total Ozone Unit and Solar Backscatter Ultraviolet Sounder (TOU/SBUS) instruments on the Chinese FY-3 meteorological satellite (launched in 2008).

Each of these instruments are being subjected to extensive validation processes by means of calibration checks and comparison with data from heritage satellite and ground-based instruments. Several oral presentations and poster papers detailed these validation efforts and confirmed that these instruments were providing accurate and consistent data that are expected to continue the long-term ozone record collected to date. ■

Eyes on the Bay: Using Near-real-time Satellite Data to Monitor the Chesapeake Bay

continued from page 35

Knowing the extent of runoff is important for understanding the health of the Bay, as mud and debris can smother marine life (such as oysters) and damage submerged aquatic vegetation that provides prime habitats for the many fish and shellfish that make their home on or near the Bay floor[5]. Along with sediment, floodwaters carry dissolved nutrients that can cause phytoplankton blooms. When the blooms die, the decomposition process uses up oxygen in the water column, which can lead to fish kills, with concomitant effects on ecosystems and fishing.

One such fish kill in 2005 stumped resource managers, who noted the dead fish; but when boats went out the next day, they found nothing unusual that could explain the cause. Satellite data helped solve their mystery: MODIS images that mapped chlorophyll concentration revealed higher-than-average readings over the impacted region, indicating the likely cause as an algal bloom die-off, with subsequent reduction in oxygen in the water column.

The present assessments are interpolations based on monthly, or bimonthly observations. However, Trice would like to see more research to validate *in situ* and satellite measurements, so that researchers could use data from instruments aboard NASA satellites to monitor water quality and algal blooms almost daily. Earlier this year, Trice joined NASA's LANCE User Working Group to help steer future developments in NASA's LANCE program to provide such capability.

Maps, satellite imagery, and other data that track cleanup efforts can be found at the Eyes on The Bay website, provided earlier in this article. ■

[5] To illustrate this, according to *chesapeakebay.noaa.gov/submerged-aquatic-vegetation/submerged-aquatic-vegetation-as-fisheries-habitat-*, juvenile blue crabs can be 30 times more abundant in submerged aquatic vegetation (SAV) beds than in adjacent un-vegetated areas. Furthermore, many other species of fish and shellfish use SAV for shelter and as a place to find food. They eat the plants as well as the many small animals that live on and around the plants.

Aura Science Team Meeting

Anne Douglass, NASA's Goddard Space Flight Center, anne.r.douglass@nasa.gov
Joanna Joiner, NASA's Goddard Space Flight Center, joanna.joiner-1@nasa.gov

The annual Aura Science Team Meeting took place October 1-3, 2012, at the Pasadena Convention Center in Pasadena, CA. The Microwave Limb Sounder (MLS) and Tropospheric Emission Spectrometer (TES) teams—both located at the NASA/Jet Propulsion Laboratory (JPL) in Pasadena—hosted the meeting. More than 100 abstracts were submitted, as Aura data continue to be used broadly for atmospheric research related to composition and climate phenomena in the stratosphere and troposphere. The agenda included contributed and invited science talks and a large poster session.

The presentations covered a broad range of topics using observations from all four of Aura's instruments: the High Resolution Dynamics Limb Sounder (HIRDLS), the Ozone Monitoring Instrument (OMI), MLS, and TES. Aura has celebrated eight years of observations, and ongoing improvements to retrieval algorithms and validation of Aura products continue to expand the possible quantitative uses of its instruments' measurements. For example, higher-quality retrievals of OMI nitrogen dioxide (NO_2) and formaldehyde (HCOH) columns are useful to improve emissions inventories from polluting sources and to understand the impact of changes in emissions on tropospheric ozone (O_3).

This year's meeting included several invited presentations concerning air quality. **Daniel Jacob** [Harvard University] gave an overview of the activities of the NASA Air Quality Applied Sciences Team (AQAST)—a team of NASA atmospheric scientists working in partnership with US air quality managers to facilitate the use of NASA satellite data to address air quality issues. **Chris McLinden** [Environment Canada] presented OMI observations related to air quality over the Canadian Oil Sands in Alberta—see **Figure** (next page). Recent improvements in the retrieval make it possible to quantify increased emissions of NO_2 and sulfur dioxide (SO_2) associated with this activity. **Meiyun Lin** [Princeton University] discussed intrusions of stratospheric air deep into the atmosphere (lower troposphere) that could affect the number of times that ground-level O_3 exceeded current air quality standards at a particular location.

Other invited speakers included **Richard van Engelen** [European Centre for Medium-Range Weather Forecasts] who focused on operational use of Aura-based observations. **Jean Francois Lamarque** [National Center for Atmospheric Research, Earth System Laboratory] discussed recent use of Aura data for model evaluation specifically related to the Atmospheric Chemistry and Climate Model Intercomparison Project (ACCMIP). Aura data investigators continue to develop the most informative ways to use models in conjunction with observations, including understanding how differences between models and observations contribute to uncertainty in the responses of models to specified changes in composition.

This year's meeting also included several presentations that described new products. **Michelle Santee** [JPL—*MLS Science Team*] provided an overview of the first global climatology of methyl chloride (CH_3Cl), the largest natural source of stratospheric chlorine. **Deijun Fu** [JPL] presented results for retrieval of tropospheric O_3, combining information in the infrared spectral region from TES with ultraviolet and visible information from OMI. **Brad Fisher** [Science Systems and Applications, Inc.] discussed efforts to produce a new cloud product that combined information from OMI with that from the Moderate Resolution Imaging Spectroradiometer (MODIS) on Aqua—demonstrating synergy among instruments on A-Train[1] platforms.

This year marks the end of the HIRDLS mission. An instrument anomaly, caused by a stalled chopper wheel, occurred in 2008; despite continuous efforts to restart the chopper, HIRDLS is unable to obtain any additional science data. The HIRDLS team also faced challenges caused by blanketing that obstructed the scan mirror at launch, eliminating data acquisition from most of the possible scan directions, and adding an unwanted signal from the blanketing to the atmospheric radiance.

[1] Called the Afternoon Constellation, or the A-Train for short, NASA and its international partners operate several Earth-observing satellites that cross the equator at about 1:30 PM local time, within seconds to minutes of each other, which allows near-simultaneous observations.

John Gille [NCAR—*U.S. HIRDLS Principal Investigator*] presented information about the last set of algorithm improvements that correct for the obstruction and thereby make it possible to produce HIRDLS high-vertical-resolution profiles for a suite of observations. The Aura community appreciates the successful efforts of Gille and the entire HIRDLS team to account for the obstruction and to produce a unique set of observations.

The next Aura Science Team Meeting, to be held in 2014 in Greenbelt, MD, will be a celebration of ten years of operations. More details will follow as they become available. ■

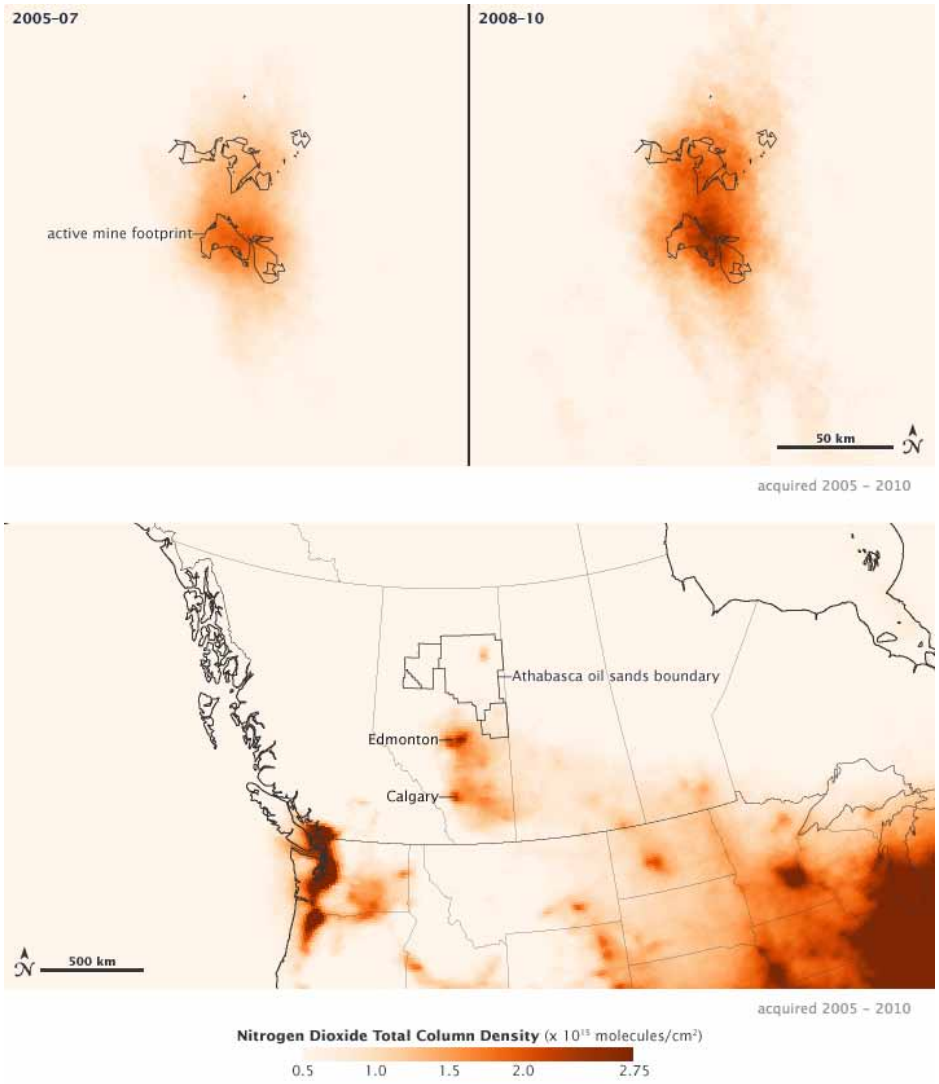

Figure. Using data from a NASA satellite, researchers have found that the emission of pollutants from *oil sands* mining operations in Canada's Alberta Province are comparable to the emissions from a large power plant or a moderately sized city.

Oil sands (a.k.a., *tar sands*) are actually *bitumen*—a very thick and heavy form of oil that coats grains of sand and other minerals. The asphalt-like oil must be extracted from the sand, and then partially refined so that it can be transported through pipelines to other refining facilities. About 1.8 million barrels of oil were produced daily in 2010 from the Canadian oil sands.

The top two maps above depict the concentration of nitrogen dioxide (NO_2) in the air above the main oil sands mining operation along the Athabasca River, as observed from 2005 to 2007 [*left*] and 2008 to 2010 [*right*]. The lower map shows those emissions in the broader context of the western provinces of Canada and the northern United States from 2005 to 2010. The Ozone Monitoring Instrument (OMI) on NASA's Aura satellite acquired all the data shown here.

A research team led by **Chris McLinden** [Environment Canada] examined a 30 x 50-km (19 x 31-mi) area around the mines, and found elevated levels of pollutants. NO_2 concentrations over two of the largest mining operations reached 2.5×10^{15} mol/cm^2 by 2010. The emissions had increased about 10% per year between 2005 and 2010—roughly the same rate as the growth of the oil sands industry. Sulfur dioxide concentrations (not shown above) peaked at 1.2×10^{16} mol/cm^2—also comparable to the levels measured around a large power plant.

SORCE Science Team Meeting

Jerald Harder, Laboratory for Atmospheric and Space Physics, University of Colorado, Jerry.Harder@lasp.colorado.edu
Martin Snow, Laboratory for Atmospheric and Space Physics, University of Colorado, Marty.Snow@lasp.colorado.edu
Tom Woods, Laboratory for Atmospheric and Space Physics, University of Colorado, Tom.Woods@lasp.colorado.edu

The SOlar Radiation and Climate Experiment (SORCE) Science Team (ST) continued its series of meetings in Annapolis, MD, September 18-19, 2012. The title of this year's meeting was *Solar Spectral Irradiance Variability: Origins in the Solar Atmosphere and Impacts on Earth's Atmosphere*. The two-day meeting had two sessions each day: one on observations, and one on models. A poster session addressed all topics of the meeting.

This year's SORCE ST Meeting revolved around key scientific questions that span issues related to our ability to understand the origins of spectral irradiance in the solar atmosphere, and how these variations impact Earth's atmosphere and climate. Many interesting—perhaps even conflicting—perspectives were presented at this meeting, demonstrating that our knowledge of the role of solar variability in understanding climate change remains 'low,' as stated in the Intergovernmental Panel on Climate Change's (IPCC) Fourth Assessment Report (AR4). The SORCE meetings provide an effective forum for addressing these outstanding and important climate sensitivity issues, and provide inspiration for future studies.

2012 SORCE Meeting Focus Questions:

1. *How will the development of three-dimensional (3-D) models of the solar atmosphere (which is rapidly progressing) further our understanding of the radiative properties of the solar atmosphere relative to static, 1-D models of the solar radiation?*

2. *Do changes in small-scale processes on the Sun give rise to irradiance variability, and do they give a reasonable explanation of changes that can occur on decadal or centennial scales that relate to climate change?*

3. *Does incorporating solar spectral irradiance (SSI) data into general circulation models (GCMs) improve the prediction skills of these models, and do different models produce similar results with the same solar input?*

4. *For both solar models and GCMs, how well do model predictions agree with observations over decadal time scales?*

The first session, *Modeling of the Solar Atmosphere with Emphasis on Spectral Irradiance*, featured talks on state-of-the-art solar models. **Han Uitenbroek** [National Solar Observatory] gave the first presentation, showing that 1-D-model-derived radiance is expected to be lower than that from the 3-D model due to the different ways that temperature is averaged. **Regner Trampedach** [University of Colorado (CU)] presented modeling results showing that small-scale magnetic elements in active regions heat in a lateral direction and show brightness variations with viewing angle. This result provides a better understanding of the cause of center-to-limb variability in active regions. **Juan Fontenla** [NorthWest Research Associates; Laboratory for Atmospheric and Space Physics (LASP)/CU] discussed the continued importance of 1-D modeling in light of the fact that the physical mechanisms of chromospheric and coronal heating are not yet fully understood. Even with recent advances in computing power and algorithms, it is currently not practical to use full, 3-D solar models for irradiance studies.

Judith Lean [Naval Research Laboratory (NRL)] gave the second keynote presentation in Session 1, discussing the development of the NRL solar spectral irradiance (SSI) model. Lean described the model's ability to reproduce total solar irradiance (TSI) trends, and noted that a new version of the model will reflect the change in TSI level observed by SORCE's Total Irradiance Monitor (TIM). She also demonstrated that the NRL SSI model predictions, SORCE Spectral Irradiance Monitor (SIM), and Solar Stellar Irradiance Comparison Experiment (SOLSTICE) observations are very similar in their ability to reproduce the 27-day

solar-rotation variation—see **Figure 1**—but they disagree at some wavelengths on longer-term trends that appear over the course of the 11-year solar cycle. The largest disagreements occur at wavelengths longer than 250 nm, where solar variability is small compared to the uncertainty in the corrections for instrument degradation trends. The session concluded with presentations on other SSI models from researchers in Europe and at NASA.

The second session, *Modeling of the Solar Influence on Earth Climate*, focused on the North Atlantic Oscillation (NAO), which may have little impact on global temperatures, but plays an important role in regional climate phenomena. The NAO is a topic of great interest, particularly in Northern Europe, due to the need for long-term weather forecasting.

The session began with keynote speaker **Sarah Ineson** [British Meteorology Office, U.K.], who spoke about the NAO and potential links to solar variability. Ineson and her colleagues have studied the effects of enhanced solar ultraviolet (UV) variability forcing a positive NAO, which then explains the extra heating in Europe during solar maximum conditions. How the Earth responds to changes in UV SSI is shown in **Figure 2** (next page). Although uncertainties in NAO measurements are about as large as the forcing from SSI, the signal appears to be large enough to play a useful role in seasonal-to-decadal climate predictions for Europe.

Concluding the session, **William Ball** [Imperial College, U.K.] and **William Swartz** [Johns Hopkins University] showed results from model-based sensitivity studies that provide insights into predicting ozone changes in the stratosphere arising from solar variability. **Charles Jackman** [NASA's Goddard Space Flight Center (GSFC)] and **Cora Randall** [LASP/CU] discussed in detail the mechanisms of energetic proton and electron impacts on polar total reactive oxidized nitrogen chemistry, with influences felt over several months.

The third session, *Observations of Solar Spectral Irradiance Variability,* concentrated on the measurements of SSI. The main focus was on comparisons between observations from SORCE and other solar irradiance instruments, both orbiting and ground-based. **Tom Woods** [LASP/CU—*SORCE Principal Investigator*] summarized the comparisons nicely, with an analysis of all existing UV datasets compiled over the past three solar-cycle minima. Except for the 250–400-nm spectral region, the majority of the published datasets are in fairly good agreement with each other. Woods' conclusion was that the long-term record supports the higher UV variability as measured by SORCE. However, his method has an uncertainty of about 20% in variability, which is close to the measurement uncertainty in many cases.

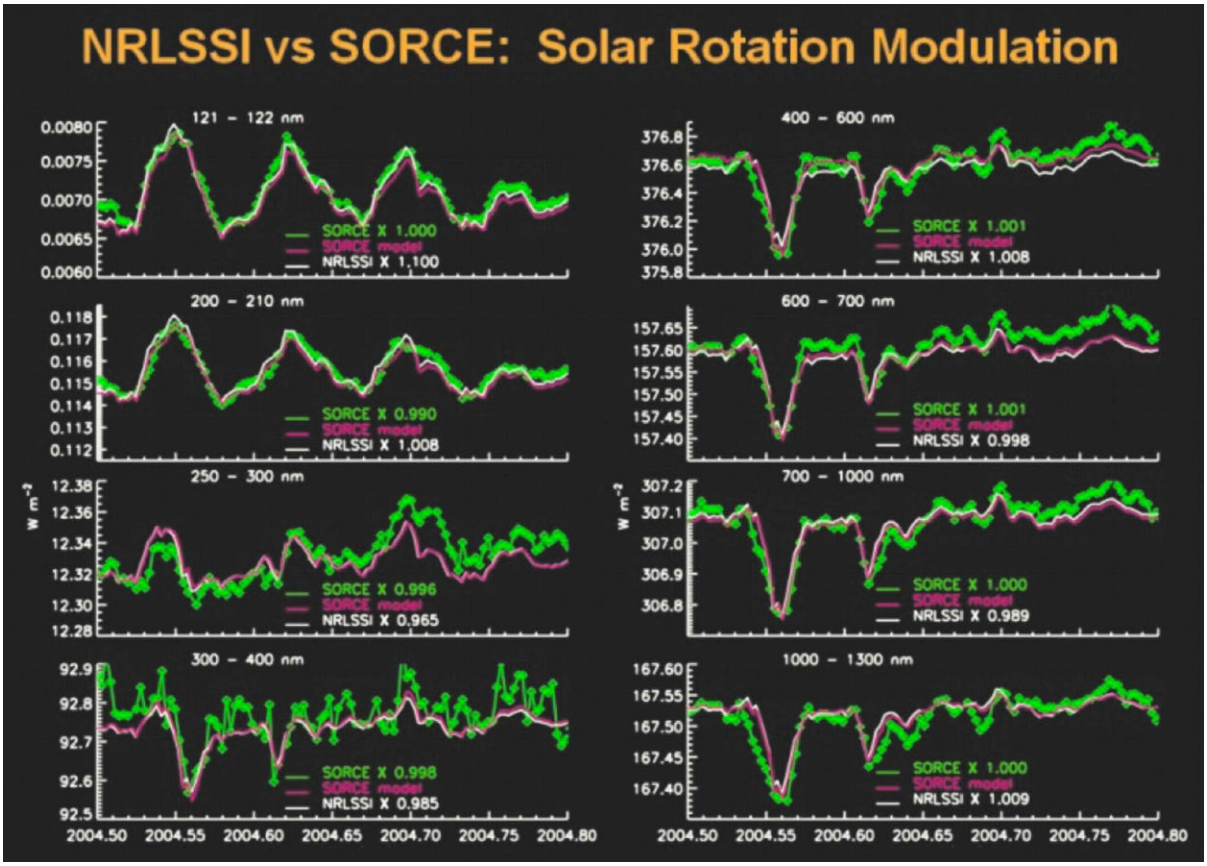

Figure 1. These graphs show a comparison of SSI calculations from the Naval Research Laboratory's Solar Spectral Irradiance (NRL SSI) model with observations from SORCE. The short-term solar variations, related mostly to the 27-day solar rotation, are in very good agreement.
Image credit: Judith Lean

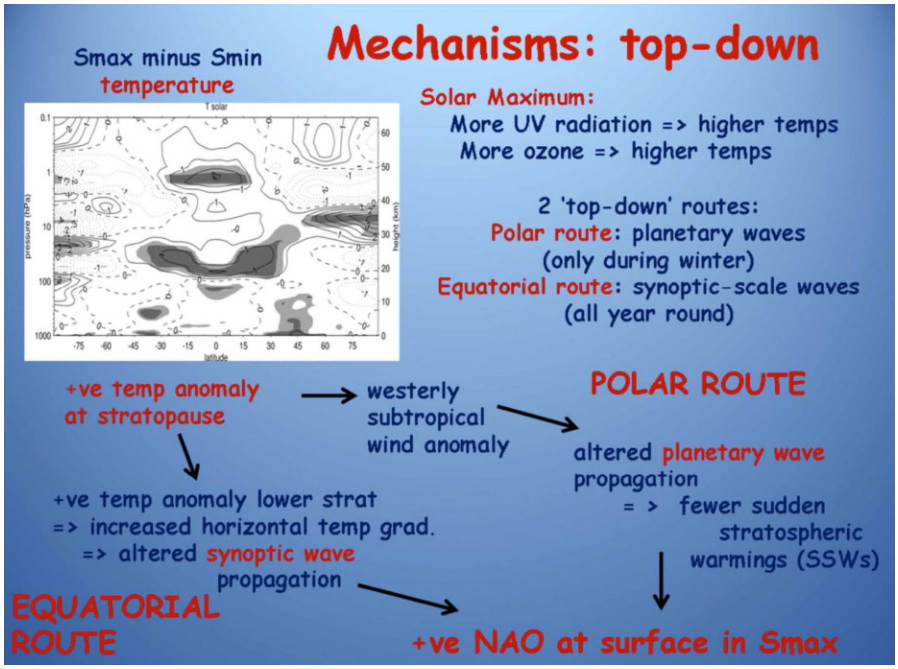

Figure 2. This diagram explains a top-down mechanism for how solar-cycle variability in stratospheric ozone and heating can induce planetary wave propagation through two routes to produce a positive NAO response (labeled "+ve" in the figure). **Image credit: Sarah Ineson**, courtesy of **Lesley Gray**, University of Oxford

There were also a wide variety of presentations on observations of SSI in the visible and near-infrared (NIR) spectral bands. Of particular interest was that the SORCE SIM results indicate that some wavelengths in the visible and NIR regions are out of phase with the solar cycle, i.e., there is more irradiance at solar minimum. One of the more unusual datasets discussed was that from the Solar and Heliospheric Observatory (SOHO) satellite's Large Angle and Spectrometric Coronagraph (LASCO). **Russell Howard** [NRL] discussed a unique measurement of solar variability at visible wavelengths using scattered light from the solar corona that gave results consistent with TSI variations measured by SORCE TIM. Howard's scattered-light measurements indicate that SSI variations are in-phase with the solar cycle in the visible spectral band.

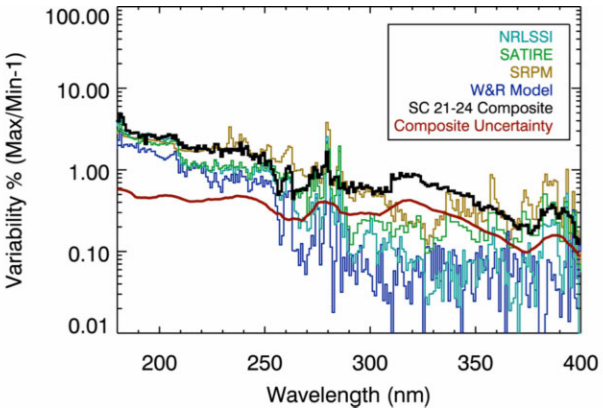

Figure 3. This plot shows a comparison of several solar irradiance models with a LASP Solar Cycle 21-24 composite middle-ultraviolet (MUV) spectrum constructed from several instruments.[1] The composite is generally higher than the models in the 290–350-nm range. This composite construction indicates lower UV variability than presented in Harder, J., *et al., Geophysical Research Letters*, 36, L07801, 2009. **Image credit: Tom Woods**

Dora Preminger [San Fernando Observatory (SFO); University of California, Northridge] presented ground-based solar-image analysis that shows out-of-phase solar-cycle variations in the visible range, but with smaller magnitude than was observed by SORCE SIM. **Mark Rast** [LASP/CU] gave a presentation that could provide insight into resolving the contradictory results for the visible spectral band. He discussed *plage*[2] observations from the Mauna Loa Observatory, suggesting that some plages can appear "dark" relative to the quiet Sun, and the fraction of *faculae*[3] showing such negative continuum contrast varies with the solar cycle, decreasing into solar minimum, and increasing again coming out of it. Exactly how this darkening would manifest itself in the SFO and SOHO records could be the answer to how some wavelengths in the visible could be out of phase with the solar cycle in one dataset and not in the other.

The session closed with a broader perspective on the solar cycle. **Ken Tapping** [National Research Council, Canada] updated his study of the 65-year record of the 10.7-cm radio flux (F10.7) coronal measurement relative to the sunspot record. His results show that F10.7 and sunspot number continue to diverge in interesting ways,

[1] These include the Solar Mesosphere Explorer (SME), Upper Atmosphere Research Satellite (UARS) SOLSTICE, UARS Solar Ultraviolet Spectral Irradiance Monitor (SUSIM), SORCE SIM, and SORCE SOLSTICE.

[2] A *plage* is a bright cloud-like region in the Sun's chromosphere around a sunspot. They are also linked with the occurrence of smaller-scale *faculae* (see Footnote 3 for a definition of a *facula)*.

[3] A *facula* is literally a "bright spot" on the Sun's photosphere that burns hotter than the surrounding area that often, but not always, occurs in proximity to dark (cooler) regions known as *sunspots*.

meeting/workshop summaries

Workshop Summary: Understanding Trends in Solar Spectral Irradiance

Martin Snow, Laboratory for Atmospheric and Space Physics, University of Colorado, Marty.Snow@lasp.colorado.edu

Just prior to the September 2012 SOlar Radiation and Climate Experiment (SORCE) Science Team Meeting, experts from around the world who measure solar spectral irradiance (SSI) met on September 17, 2012, in Annapolis, MD, to discuss recent SSI observations. The primary topic of interest is that SORCE measurements show larger solar variability in the descending phase of Solar Cycle 23 (i.e., from mid-2003 to the end of 2008) than most other previous instruments in Solar Cycle 22. This workshop was the sequel to a workshop held at the National Institute of Standards and Technology (NIST) in February 2012[1]. The ultimate goal of these SSI workshops is to understand the uncertainties in the comparisons to previous and overlapping datasets, and to validate SORCE measurements.

SSI Trends Workshop participants. [*Front row, left to right*] Martin Snow, Odele Coddington, Guoyong Wen, Don McMullin, William Ball, Jae Lee; [*Second row, left to right*] Tom Woods, Gerard Thuillier, Matt DeLand, William McClintock, Jerry Harder, Stéphane Beland, Linton Floyd; [*Third row, left to right*] Doug Lindholm, Peter Pilewskie, Judith Lean, Erik Richard, Dong Wu, Bob Cahalan, Tom Sparn, Gary Rottman, Alexander Shapiro, Dave Harber, and Jeff Morrill. **Photo Credit: Vanessa George**.

The primary source of uncertainty in any long-term SSI dataset is in the correction for instrument degradation. The morning session featured presentations by **Martin Snow**, **Jerald Harder**, and **Stéphane Beland** [all from LASP/CU] on improvements to the current SORCE degradation functions for the Solar-Stellar Irradiance Comparison Experiment (SOLSTICE) and the Solar Irradiance Monitor (SIM). There was also a presentation by **Odele Coddington** [LASP/CU] describing an alternative algorithm for determining the SIM degradation function that folds in an estimate of the radiation dose seen by the instrument as a function of time. This dose-model approach was inspired by discussions held at the February 2012 workshop.

A discussion of the general approach that should be used in operating an instrument with multiple channels rounded out the morning session. **Erik Richard** [LASP/CU] showed test results from the Total and Spectral Irradiance Sensor (TSIS), which is currently under development at LASP/CU, and is planned to be a component of the Joint Polar Satellite System, currently scheduled for first-satellite launch in 2017. **Linton Floyd** [Interferometrics, Inc.] shared some valuable insight, based on degradation measurements from the Solar Ultraviolet Spectral Irradiance Monitor (SUSIM) on the Upper Atmosphere Research Satellite (UARS).

The afternoon session was devoted to comparison of measurements from SORCE to other instruments. **Alexander Shapiro** [Physikalisch-Metorologisches Observatorium Davos (PMOD), Switzerland] showed comparisons to broadband photometers on the Solar and Heliospheric Observatory (SOHO), PICARD[2], and PROject for Onboard Autonomy 2 (PROBA2) satellites. **Gerard Thuillier** [Laboratoire Atmosphères, Milieux, Observations Spatiales (LATMOS-CNRS), France] calculated ratios using data from the SOLar SPECtrum (SOLSPEC) instrument on the International Space Station (ISS); **Linton Floyd** compared SOLSTICE and SIM to the UARS SUSIM data taken during 2003 and 2005. **Jae Lee** [GSFC] presented an analytical statistical analysis of measurements and models. The workshop ended with **Tom Woods** [LASP/CU] giving a re-analysis of trends across multiple solar cycles.

One of the workshop's conclusions is that differences in solar-cycle variability among the different instruments appear to be within the uncertainty of instrument degradation trends for many of the wavelengths—and especially at wavelengths longer than 250 nm.

[1] This meeting was described in the July–August 2012 issue of *The Earth Observer* [**Volume 24**, **Issue 4**, pp. 17-20].
[2] PICARD is not an acronym, but rather named after the French astronomer Jean Picard (1620-1682), who achieved the first accurate measurements of the solar diameter.

first starting in Solar Cycle 23 (1996–2008) and perhaps continuing into (the current) Solar Cycle 24. This divergence in variability relationships might be an indicator of secular solar variations. One interesting conclusion is that Solar Cycle 24 may have already peaked as of November 2011, in contrast to the NASA–National Oceanic and Atmospheric Administration Solar Cycle Panel prediction that Cycle 24 might reach its maximum in mid-2013.

The fourth and final session of the meeting, addressing *Observations of the Solar Influence on Earth Climate,* tackled observations and models of Earth's atmosphere as related to solar-cycle variations. One important topic discussed was comparison of 2-D and 3-D atmospheric models. There appears to be good consistency in the results between different models, suggesting that the chemistry and dynamics in these models are well-represented in both. Several model comparisons, using either the NRL SSI model or SORCE SIM measurements, indicate that the UV variability observed by SIM should produce a larger stratosphere-mesosphere change of ozone (O_3) and hydroxide (OH^-) than results using NRL SSI. Different atmospheric measurements can provide diverse—and seemingly conflicting—conclusions about which solar variability inputs to the models produce results that best agree with the atmospheric observations. One critical component in such comparisons is how O_3 data are analyzed. For example, **Aimee Merkel** [LASP/CU] showed observations where daytime and nighttime data can be separated to show out-of-phase solar-cycle changes in the lower mesosphere. Therefore, O_3 datasets derived entirely from occultation measurements, which are always taken under dawn or dusk conditions, could mask the true solar-forcing effects on a global scale.

Many of the 2012 SORCE Meeting presentations are available online at *lasp.colorado.edu/sorce/news/2012ScienceMeeting/agenda.html.*

The final topic of discussion focused on determining the theme of the next SORCE ST Meeting. It was generally agreed that rather than a 10-year anniversary meeting, there should be an 11-year celebration in honor of SORCE's observations over the full 11-year solar cycle. The next SORCE ST Meeting will likely take place in early 2014, with a focus on topics that address the key results obtained during the SORCE mission. ■

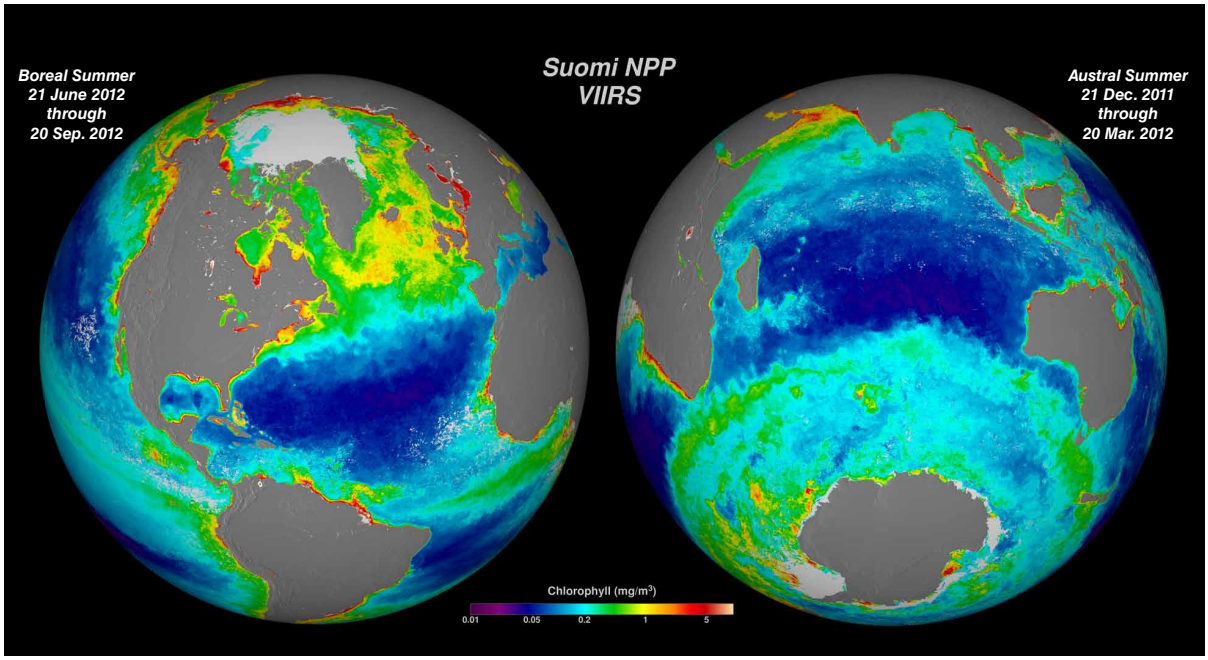

On October 28, 2011, the Suomi National Polar-orbiting Partnership (NPP) satellite launched into orbit. For over a year, Suomi NPP has been returning images and data that provide critical weather and climate measurements of the complex Earth system. These two images for example, are season-long composites of ocean chlorophyll concentrations derived from visible radiometric measurements made by the Visible Infrared Image Radiometer Suite (VIIRS). Purple and blue shades represent lower chlorophyll concentrations indicating lesser phytoplankton biomass, while orange and red shades represent higher chlorophyll concentrations indicating greater amounts of phytoplankton. Data from Suomi NPP will help improve computer models that predict future environmental conditions. **Credit:** NASA/Suomi NPP/**Norman Kuring**

in the news

NASA C-20A Completes Radar Study of Pacific Rim Volcanoes

Beth Hagenauer, Public Affairs, NASA's Dryden Flight Research Center, beth.hagenauer-1@nasa.gov

NASA's Airborne Science C-20A aircraft, carrying a specialized synthetic aperture radar, recently completed a mission to study active volcanoes in Alaska, the Aleutian Islands, and Japan in early October.

The aircraft, a modified version of the Gulfstream III business jet, made 10 flights totaling more than 50 hours during the eight-day campaign. The Uninhabited Aerial Vehicle Synthetic Aperture Radar (UAVSAR), developed and operated by NASA's Jet Propulsion Laboratory, collected 60 of 61 planned data lines.

UAVSAR provides a measurement system that complements satellite-based observations by providing rapid revisits and imaging of active volcanoes to better understand their deformation prior to, during, or after an eruption.

The flight path took the aircraft north from California, imaging the volcanoes of the Western U. S., en route to an overnight stay at Joint Base Elmendorf-Richardson near Anchorage, AK.

After departing Elmendorf, the NASA aircraft imaged volcanoes in Alaska and the Aleutian Islands before arriving at Yokota Air Base near Tokyo, Japan. Yokota was the staging location for science missions that collected data about volcanoes that pose a hazard to nearby populations on several islands in Japan.

Working closely with the Japan Aerospace Exploration Agency (JAXA), three volcano-imaging flights were flown from Yokota over various volcano and disaster monitoring sites throughout Japan from October 5–8.

NASA's Airborne Science C-20A made a refueling stop at Eareckson Air Station on Shemya Island, AK, during a mission to image volcanoes in Alaska and the Aleutian Islands. The aircraft crew and mission scientists, led by **John McGrath** [NASA's Dryden Flight Research Center—*C-20A Project Manager*], kneeling at left, paused for a group photo by the air station sign before boarding the aircraft and continuing onto Japan for UAVSAR imaging of active volcanoes. **Image credit:** NASA/**John McGrath**

The aircraft repeated the outbound routing during the return flight to its home base at the Dryden Aircraft Operations Facility in Palmdale, CA.

John McGrath [NASA's Dryden Flight Research Center—*C-20A Project Manager*] said a mission of this complexity faced numerous challenges.

"Preparation has been ongoing since May," McGrath commented. "We had tremendous support from both Elmendorf and Yokota air bases and our colleagues at JAXA." ■

NASA's modified Airborne Science C-20A is seen on the parking ramp at Yokota Air Force Base near Tokyo, Japan. The aircraft, carrying the UAVSAR mounted in an undercarriage pod, was deployed to conduct a radar imaging mission of Japan's active volcanoes. **Image credit:** NASA/**John McGrath**

New Data Release

SSM/I and SSMIS Version 7 Ocean Product Suite

The Global Hydrology Resource Center (GHRC)[1], a data center that is part of NASA's Earth Observing System Data and Information System (EOSDIS), is pleased to announce the release of the *version 7* Ocean Product Suite, comprised of data from the Special Sensor Microwave/Imager (SSM/I) on Defense Meteorological Satellite Program (DMSP) satellites F08, F10, F11, F13, and F14, and the Special Sensor Microwave Imager Sounder (SSMIS) on DMSP satellites F15, F16, and F17. All data are processed by Remote Sensing Systems (RSS). These data—in netCDF[2] (v4) format—are generated by the Distributed Information Services for Climate and Ocean Products and Visualizations for Earth Research (DISCOVER) Project (Frank Wentz, Principal Investigator), as part of NASA's Making Earth Science Data Records for Use in Research Environments (MEaSUREs) Program.

The RSS Ocean Product Suite includes the following data products:

- RSS SSM/I Ocean Products Grids, Daily;
- RSS SSM/I Ocean Products Grids, 3-Day Average;
- RSS SSM/I Ocean Products Grids, Weekly Average; and
- RSS SSM/I Ocean Products Grids, Monthly Average.

These datasets can be ordered from the GHRC using the Hydrologic Data search, Retrieval, and Order system (HyDRO) at *ghrc.nsstc.nasa.gov/hydro* and NASA's Reverb at *reverb.echo.nasa.gov*.

Detailed information for these datasets is available in the SSMI and SSMIS netCDF Data Products document found at *ftp://ghrc.nsstc.nasa.gov/pub/doc/ssmi_netcdf/ssmi_ssmis_dataset.html*.

NASA's Marshall Space Flight Center and the University of Alabama in Huntsville jointly manage the GHRC.

OPeNDAP

The GHRC would like to also announce the availability of Open-source Project for a Network Data Access Protocol (OPeNDAP)[3] for the entire RSS Ocean Product Suite, as referenced above. OPeNDAP is a data transport architecture and protocol widely used by Earth system scientists to access remotely distributed data. OPeNDAP includes standards for encapsulating structured data, annotating the data with attributes, and adding semantics that describe the data. Data and metadata hosted through OPeNDAP are available for both interactive, browser-based access by users, or through programmatic interfaces that allow applications to access distributed data resources. Access is enhanced by the interface options to easily subsample, subset, aggregate, and reformat data. Several existing client applications (e.g., ncBrowse, IDV, Panoply) and software libraries (e.g., netCDF) readily support OPeNDAP data access.

The GHRC OPeNDAP server is available at *ghrc.nsstc.nasa.gov/opendap*.

Please contact our User Services Office at *ghrcdaac@itsc.uah.edu* for more information.

[1]For more information about GHRC, visit: *ghrc.msfc.nasa.gov*.
[2] NetCDF stands for Network Common Data Form. For more information, visit: *www.unidata.ucar.edu/software/netcdf*.
[3] For more information about OPeNDAP, visit: *www.opendap.org*.

in the news

2012 Antarctic Ozone Hole the Second Smallest in 20 Years

Steve Cole, NASA Headquarters, stephen.e.cole@nasa.gov
Katy Human, National Oceanic and Atmospheric Administration, Office of Communications and External Affairs, katy.g.human@noaa.gov

The average area covered by the Antarctic ozone hole this year was the second smallest in the last 20 years, according to data from NASA and National Oceanic and Atmospheric Administration (NOAA) satellites—see **Figure 1**. Scientists attribute the event to warmer temperatures in the Antarctic lower stratosphere.

The size of the ozone hole reached its maximum on September 22, covering 8.2 million mi^2 (21.2 million km^2)—or the approximate area of the U.S., Canada, and Mexico combined. The average size of the 2012 ozone hole was 6.9 million mi^2 (17.9 million km^2). For comparison, the largest ozone hole on record occurred on September 6, 2006, and measured 11.5 million mi^2 (29.8 million km^2).

"The ozone hole mainly is caused by chlorine from human-produced chemicals, and these chlorine levels are still sizable in the Antarctic stratosphere," said NASA atmospheric scientist **Paul Newman** [NASA's Goddard Space Flight Center (GSFC)]. "Natural fluctuations in weather patterns resulted in warmer stratospheric temperatures this year. These temperatures led to a smaller ozone hole."

The ozone layer acts as Earth's natural shield against ultraviolet radiation, which can cause skin cancer. The yearly ozone hole phenomenon—a cyclical diminution of stratospheric ozone—began making a yearly appearance in the early 1980s. The Antarctic ozone layer likely will not return to its early 1980s state until about 2065, Newman said—see **Figure 2**. The lengthy recovery is because of the long lifetimes of ozone-depleting substances in the atmosphere. This means that even though the harmful substances are no longer being added to the atmosphere[1], and overall ozone levels are no longer declining, the damage to the ozone layer will take a long time to fully recover.

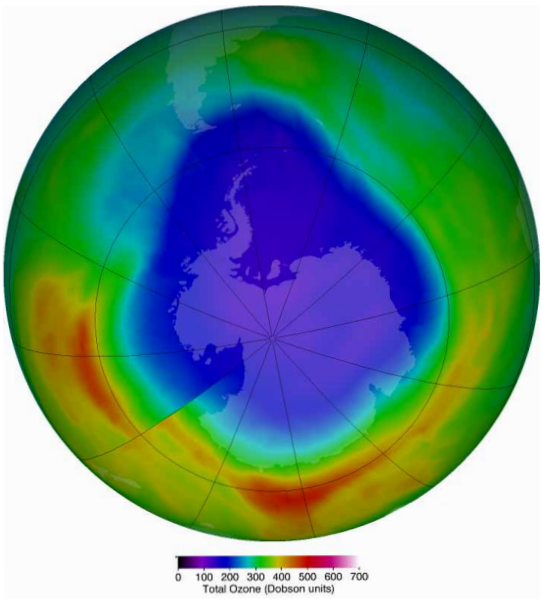

Figure 1. ***The 2012 Antarctic Ozone Minimum.*** This image shows the Antarctic ozone hole for September 22, 2012, as measured by OMPS on Suomi NPP.

[1] The Montreal Protocol, enacted in 1987 and strengthened in subsequent years was an international agreement to phase out the production of ozone-destroying chlorofluorocarbons (CFCs.)

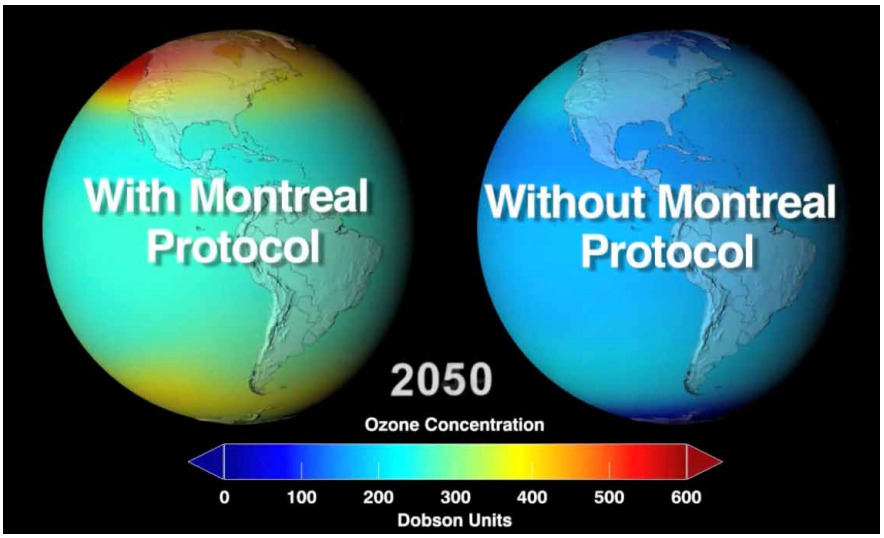

Figure 2. ***The world that was averted...*** After realizing the serious threat that CFCs posed to Earth's delicate ozone layer, the nations of the world enacted the Montreal Protocol in 1987. By 1989, 193 countries had signed the treaty, and as of 2011 every nation on Earth is a signatory. This is widely regarded as a shining example of the possibility of international cooperation to address global environmental issues. The image shown here compares projected ozone concentrations for the year 2050, with [*left*] and without [*right*] enactment of the Montreal Protocol.

This year also marked a change in the concentration of ozone over the Antarctic over previous years—see **Figure 3**. The minimum value of total ozone, measured in Dobson units (DU), was the second highest in two decades reaching 124 DU on October 1; NOAA ground-based measurements at the South Pole recorded 136 DU on October 5. When the ozone hole is not present, total ozone typically ranges between 240 and 500 DU.

Another first for this year was that the ozone hole was observed by an ozone-monitoring instrument on the Suomi National Polar-orbiting Partnership (NPP) satellite—a bridging mission leading to the next-generation polar-orbiting environmental satellites called the Joint Polar Satellite System—which will extend ozone monitoring into the 2030s. The Suomi NPP instrument, called the Ozone Mapping Profiler Suite (OMPS), is based on heritage instruments, such as the Total Ozone Mapping Spectrometer (TOMS) and the Solar Backscatter Ultraviolet (SBUV/2) instrument, continuing a satellite record dating back to the early 1970s.

In addition to observing the annual formation and extent of the ozone hole, scientists hope OMPS will help them better understand ozone destruction in the middle and upper stratosphere with its Nadir Profiler; ozone variations in the lower stratosphere will be measured with its Limb Profiler.

"OMPS Limb [Profiler] looks sideways, and it can measure ozone as a function of height," said **Pawan "P. K." Bhartia** [GSFC], a NASA atmospheric physicist and OMPS Limb Profiler instrument lead. "This OMPS instrument allows us to more closely see the vertical development of Antarctic ozone depletion in the lower stratosphere where the ozone hole occurs."

NASA and NOAA have been monitoring the ozone layer with instruments on the ground and on satellites, aircraft, and balloons since the 1970s. Long-term ozone monitoring instruments have included TOMS, SBUV/2, the Stratospheric Aerosol and Gas Experiment (SAGE) series of instruments, the Microwave Limb Sounder, the Ozone Monitoring Instrument both on Aura, and the OMPS instrument on Suomi NPP.

NASA and NOAA have a mandate under the Clean Air Act to monitor ozone-depleting gases and stratospheric depletion of ozone. The NOAA Earth System Research Laboratory performs ground-based monitoring; the Climate Prediction Center performs satellite monitoring.

To monitor the state of the ozone layer above Antarctica, visit: *ozonewatch.gsfc.nasa.gov.*

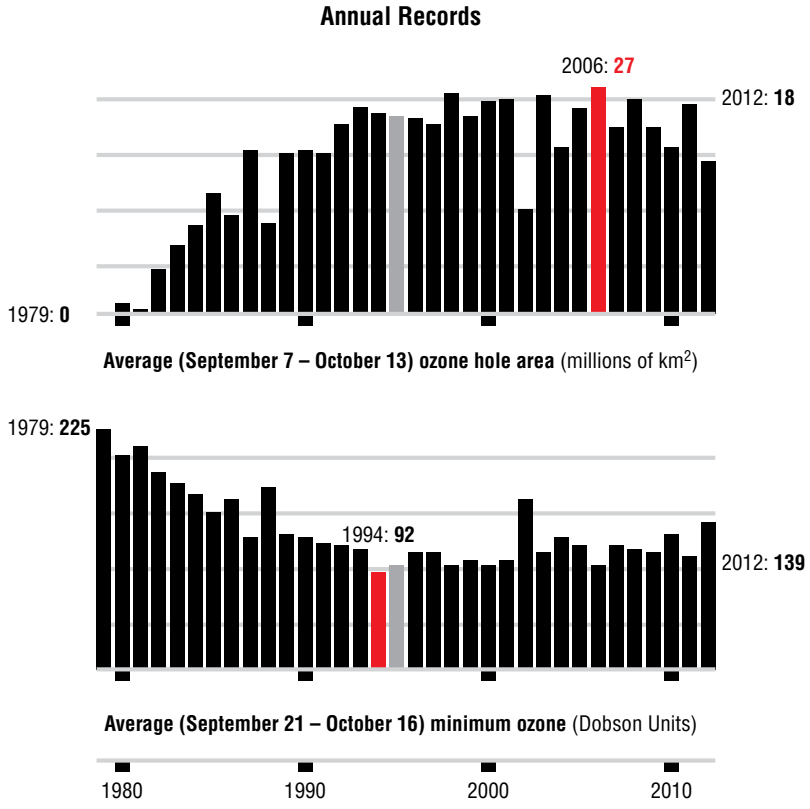

Figure 3. These graphs show the variations of ozone from 1979 to 2012. The red bars indicate the largest area and the lowest minimum value. The year-to-year fluctuations are superimposed on a trend extending over the last three decades. Note that the average minimum value for 2012 [bottom graph] is the second-highest it has been in two decades. **Credit:** NASA Ozone Watch

NASA Earth Science in the News

Patrick Lynch, NASA's Earth Science News Team, patrick.lynch@nasa.gov

Mapping Underground Faults and Fractures in Surprise Valley, September 4; *Scientific American.* A team of scientists and engineers, led by the U.S. Geological Survey and funded by NASA, collected magnetic data using ground surveys and an aircraft that can fly without a pilot or crew onboard—an uninhabited aerial vehicle (UAV)—to map the geophysics below the surface of Surprise Valley in Northeastern California. The corrugated Surprise Valley Fault snakes 85 km (~53 mi) along the Warner Mountain Range. The landscape is pocked with smaller surface scars called *fault scarps* that indicate movement along faults, and hot springs that billow steam—proof that the area is anything but seismically quiet. While some surface faults and fractures are visible, some remain completely hidden underground. The group will produce a three-dimensional map that will provide geophysical data on Surprise Valley at a level of detail as yet not achieved for the area.

Mysterious Changes in Ocean Salt Spur NASA Expedition, September 5; *Yahoo! News.* Over the past 50 years the salty regions of the oceans have become saltier, the fresher regions have become even fresher, and the degree of these changes is greater than scientists can yet explain. Understanding such phenomena is important because oceans are at the heart of the planet's water cycle, with 86% of global evaporation and 78% of global precipitation occurring over oceans, according to NASA—the lead entity behind the project, called Salinity Processes in the Upper Ocean Regional Study (SPURS). Researchers are heading out into the middle of the North Atlantic Ocean—a particularly salty region—to acquire data in hope of better understanding what drives variations in salinity in the upper ocean.

Arctic Sea Ice Extent Reaches Record-shattering Minimum, September 19; *The Washington Post.* The 2012 sea ice extent had already dropped below the 2007 record on August 26, three weeks before the mid-September minimum. "Climate models have predicted a retreat of the Arctic sea ice, but the actual retreat has proven to be much more rapid than the predictions," said **Claire Parkinson** [NASA's Goddard Space Flight Center (GSFC)—*Climate Change Senior Scientist*]. A large Arctic storm in early August played a role in the

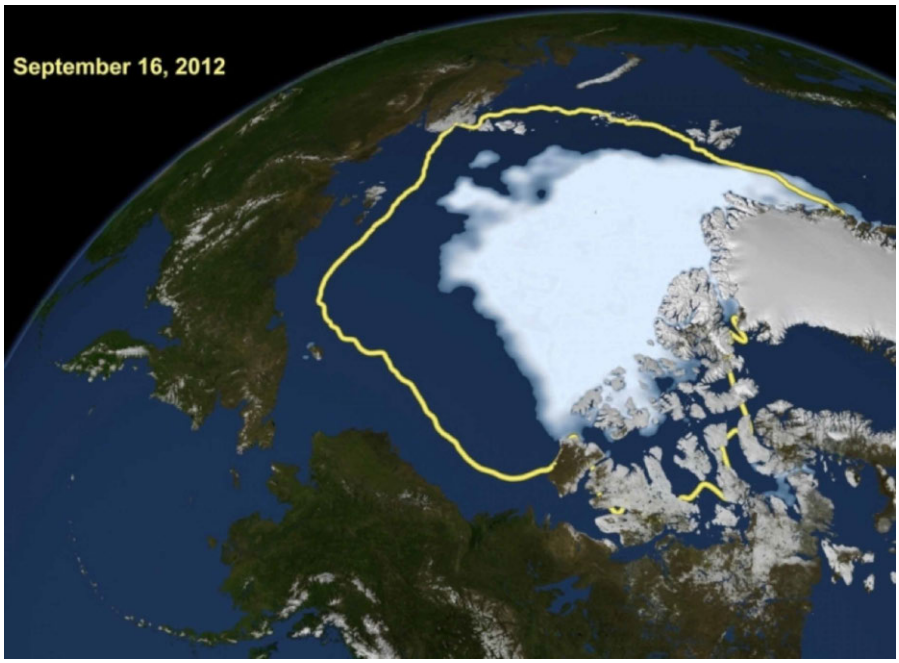

This image shows Arctic sea ice on September 16, 2012, the day the NASA-supported National Snow and Ice Data Center (NSIDC) declared the 2012 Arctic sea ice minimum. This year marked the smallest sea ice extent and area in the satellite record, which dates to 1979. The white line marks the average minimum extent during the past 30 years. **Image credit**: NASA Scientific Visualization Studio/GSFC

record low extent. "The storm cut off a large section of sea ice north of the Chukchi Sea and pushed it south to warmer waters that made it melt entirely. It also broke vast extensions of ice into smaller pieces more likely to melt[1]."

Research Buzz: Unmanned Aircraft Venture into Hurricanes, October 1; *The Baltimore Sun.* NASA's Hurricane Severe Storm Sentinel Mission (HS3), is exploring the massive tropical systems from high altitudes via two unmanned Global Hawk aircraft. Instruments onboard the planes will collect data that researchers and meteorologists plan to use to better understand how tropical storms and hurricanes form and strengthen. The first of what will be a three-year-long series of flights was launched September 7, 2012, to explore what was then Hurricane Leslie for 10 hours from an altitude of ~18,288 m (60,000 ft). Measurements of winds, temperature, water vapor, precipitation, and aerosols could help explain "… the interaction of tropical disturbances and cyclones with the hot, dry, and dusty air that moves westward off the Saharan Desert," said **Scott Braun** [GSFC—*Research Meteorologist*].

Warming Lakes: Barometers of Climate Change?, and **Warming Lakes: Effects of Climate Change Seen on Lake Tahoe**, October 5; *NationalGeographic.com.* Following the 2010 publication of a study that showed widespread water temperature increases in lakes, **Simon Hook** [NASA/Jet Propulsion Laboratory (JPL)] began collaborating with other scientists in the Global Lake Temperature Collaboration (GLTC). A special supplement to the *Bulletin of the American Meteorological Society*, published this past summer, compared the results of the JPL study and one by a group called ARC-Lake[2], and found that both sets of data were "…consistent in identifying relatively rapid warming in lakes of both North America and Europe." The GLTC has since grown to comprise over 50 investigators studying lakes all over the world, including the Great Lakes and Lake Tahoe in North America, Lake Baikal in Russia, and Lake Tanganyika in East Africa. The group held its first meeting in June at the University of Nebraska-Lincoln, and began pooling data and expertise to better understand global changes in lake temperatures.

Increasing Demand for Palm Oil Resulting in "Massive Carbon Dioxide Emissions," October 8; *FoodNavigator.com.* According to a new study funded by NASA's Land Cover Land Use Change Program and led by **Lisa Curran** [Stanford University], growing demand for *palm oil*—a common ingredient in processed foods and confectionery products—is driving the destruction of carbon-rich tropical forests in Borneo, leading to huge releases of carbon dioxide into the atmosphere.

***Antarctic Ozone Hole is the Second Smallest It's Been in 20 Years**, October 25; *The Huffington Post.* The ozone hole above the Antarctic has hit its maximum extent for the year on September 22 but—due to warm temperatures—the opening in the protective atmospheric layer was the second smallest it has been for 20 years. Stretching to 21.2 million km^2 (8.2 million mi^2), an area roughly the size of North America. The largest hole recorded to date encompassed some 30 million km^2 (~11.5 million mi^2) in 2006. Although the production of ozone-depleting chemicals has been regulated for the past 25 years, scientists say it could be another decade before we start seeing clear signs of Antarctic ozone layer recovery. **Paul Newman** [GSFC—*Atmospheric Chemist*] has estimated that the ozone layer above Antarctica likely will not return to its early 1980s state until about 2060.

*See news story in this issue for more details.

*Interested in getting your research out to the general public, educators, and the scientific community? Please contact **Patrick Lynch** on NASA's Earth Science News Team at **patrick.lynch@nasa.gov** and let him know of your upcoming journal articles, new satellite images, or conference presentations that you think would be of interest to the readership of The Earth Observer.* ■

[1] See news story in the September–October 2011 issue of *The Earth Observer* [**Volume 24**, **Issue 4**, p. 47].

[2] ARC-Lake stands for ATSR Reprocessing for Climate: Lake Surface Water Temperature and Ice Cover. ARC-Lake is a European Space Agency funded project that aims uses observations from Along Track Scanning Radiometers (ATSRs) to derive observations of lake surface water temperature and lake ice cover for major lakes globally, from 1991 to 2010. It is also designed to demonstrate the usefulness of these observations for climate science, generally. For more information, visit: *www.geos.ed.ac.uk/arclake*.

NASA Science Mission Directorate – Science Education and Public Outreach Update

Theresa Schwerin, Institute for Global Environmental Strategies, theresa_schwerin@strategies.org
Morgan Woroner, Institute for Global Environmental Strategies, morgan_woroner@strategies.org

NASA Earth and Space Science Fellowship Program for Graduate Students

New applicants apply by February 1; renewal applicants, by March 15

NASA announces a call for graduate fellowship proposals to the NASA Earth and Space Science Fellowship (NESSF) program for the 2013-2014 academic year. This call for proposals solicits applications from accredited U.S. universities on behalf of individuals pursuing master of science or doctoral degrees in the Earth and space sciences, or related disciplines. The purpose of NESSF is to ensure continued training of a highly qualified workforce in disciplines needed to achieve NASA's scientific goals. Awards resulting from the competitive selection will be made in the form of training grants to the respective universities.

The NESSF call for proposals and submission instructions are located at the NESSF solicitation index page at *nspires.nasaprs.com*. Click on "Solicitations" and select "Open Solicitations." Then select the "NESSF 13" announcement. Please also refer to "Proposal Submission Instructions" and "Frequently Asked Questions" listed under the "Other Documents" menu on the NESSF 13 solicitation index page.

For further information, please contact **Claire Macaulay** [NESSF Earth Science Research—*Program Administrator*] at (202) 358-0151, or **Dolores Holland** [NESSF Heliophysics Research, Planetary Science Research, and Astrophysics Research—*Program Administrator*] at (202) 358-0734.

Tri-Agency Climate Education Catalog

The NASA, National Oceanic and Atmospheric Administration (NOAA), and National Science Foundation (NSF) tri-agency climate education collaboration is pleased to announce the public release of the Tri-Agency Climate Education (TrACE) Catalog of educational products and resources. This is a tool for the climate education community that helps educators leverage existing resources, minimize duplication of efforts, and benefit from the expertise represented in a broad range of products. The catalog contains over 200 educational resources, representing more than 80 tri-agency-funded projects, categorized by audience and resource type. To search and browse the catalog, visit: *1.usa.gov/TKI5GY*.

GPM Precipitation Education Website

The international Global Precipitation Measurement (GPM) mission will use multiple Earth-orbiting satellites to collect global rain, snow, and other precipitation data every three hours. The Precipitation Education website is filled with activities, videos, and other educational resources that will educate audiences on precipitation and the GPM mission. To visit the site, go to: *1.usa.gov/RRaxYZ*.

NASA's Earth Science Week Websites

Earth Science Week, celebrated from October 14-20, 2012, may be over, but the celebratory website created by NASA can be used year round! The site is filled with useful resources, videos, blog entries, and recordings of live events, all exploring the numerous Earth science careers available to young Earth scientists. To explore NASA's Earth Science Week website, visit: *climate.nasa.gov/eswSite*.

This year, NASA also has translated the website for Spanish-speaking audiences. To view the site, visit: *1.usa.gov/VtrwRe*.

NASA Wavelength is Here!

NASA Wavelength is a new online resource for educators and students that helps to bring Earth, the Solar System, and the Universe into the classroom. It features hundreds of resources organized by topic and audience level—from elementary to college and out-of-school programs—that span the scope of science at NASA. Educators at all levels can easily locate resources through information on educational standards, subjects, keywords, and other relevant details, such as the learning time required to complete a lesson or activity, cost of materials, and more. All resources featured on the site have been peer-reviewed by both scientists and educators. Please stop by to check out this valuable new resource at *nasawavelength.org*.

CAMEL Climate Change Continuing Education Online Symposium

Upcoming Webinar: December 4

Climate Adaptation Mitigation E-Learning (CAMEL) is offering a free online Climate Change Continuing Education Symposium, comprised of a series of weekly webinars. Each presenter will discuss a teaching resource and how to use it. The resources are designed for upper-level education, but many can be modified for other levels or incorporated into hybrid teaching modalities. For more information and to view previously recorded webinars, visit: *bit.ly/VtC5UB*. ■

EOS Science Calendar

April 2–4, 2013
2013 Spring Land-Cover/Land-Use Change Science Team Meeting, Rockville, Maryland. URL: *lcluc.umd.edu/meetings.php?mid=40*

April 30–May 2, 2013
Terrestrial Ecology Meeting, San Diego, CA.
URL: *cce.nasa.gov/cce/meetings.htm*

May 7–9, 2013
CERES Science Team Meeting, Hampton, VA.
URL: *ceres.larc.nasa.gov/ceres_meetings.php*

October 23–25, 2013
GRACE Science Team Meeting, Austin, TX.
URL: *www.csr.utexas.edu/grace/GSTM*

Global Change Calendar

January 1–14, 2013
Land-Cover and Land-Use Change Dynamics and its Impacts in South Asia, Karunya University, Coimbatore, India. URL: *lcluc.umd.edu/meetings.php?mid=40*

January 6–10, 2013
Americal Meteorological Society, Austin, TX.
URL: *annual.ametsoc.org/2013/?CFID=599140&CFTOKEN=30157218*

January 15–17, 2013
National Conference on Science Policy and the Environment, Washington, DC. URL: *www.environmentaldisasters.net*

March 24–28, 2013
American Society of Photogrammetry and Remote Sensing, Baltimore, MD. URL: *www.asprs.org/Conferences/Baltimore-2013/blog*

April 15–17, 2013
Joint Aquarius–SMOS Workshop, Brest, France
URL: *congrexprojects.com/13c07/announcement*

June 24–28, 2013
AGU Chapman Conference - Crossing the Boundaries in Planetary Atmospheres: From Earth to Exoplanets
URL: *chapman.agu.org/planetaryatmospheres/*

Code 610
National Aeronautics and Space Administration

Goddard Space Flight Center
Greenbelt, MD 20771

PRSRT STD
Postage and Fees Paid
National Aeronautics and Space Administration
Permit 396

Official Business
Penalty for Private Use: $300

(affix mailing label here)

eos.nasa.gov

The Earth Observer

The Earth Observer is published by the EOS Project Science Office, Code 610, NASA Goddard Space Flight Center, Greenbelt, Maryland 20771, telephone (301) 614-5561, FAX (301) 614-6530, and is available in color on the World Wide Web at *eospso.gsfc.nasa.gov/eos_homepage/for_scientists/earth_observer.php*. Black and white hard copies can be obtained by writing to the above address.

Articles, contributions to the meeting calendar, and suggestions are welcomed. Contributions to the calendars should contain location, person to contact, telephone number, and e-mail address. Newsletter content is due on the weekday closest to the 15th of the month preceding the publication—e.g., December 15 for the January–February issue; February 15 for March–April, and so on.

To subscribe to *The Earth Observer*, or to change your mailing address, please call Cindy Trapp at (301) 614-5559, or send a message to *Cynthia.trapp-1@nasa.gov*, or write to the address above. If you would like to stop receiving a hard copy and be notified via email when future issues of *The Earth Observer* are available for download as a PDF, please send an email with the subject **"Go Green"** to *Cynthia.trapp-1@nasa.gov*. Your name and email address will then be added to an electronic distribution list and you will receive a bi-monthly email indicating that the next issue is available for download. If you change your mind, the email notification will provide an option for returning to the printed version.

The Earth Observer Staff

Executive Editor:	Alan B. Ward (alan.b.ward@nasa.gov)
Assistant/Technical Editors:	Heather H. Hanson (heather.h.hanson@nasa.gov) Mitchell K. Hobish (mkh@sciential.com)
Technical Editor:	Ernest Hilsenrath (hilsenrath@umbc.edu)
Design, Production:	Deborah McLean (deborah.f.mclean@nasa.gov)

Printed on Recycled Paper

NP-2012-7-313-GSFC